

เยื่ออิเล็กทรอนิกส์ของจีนที่เดิมสารให้สีสำหรับการวิเคราะห์ไอออน



นางสาวอมรรัตน์ สายทองดี

จุฬาลงกรณ์มหาวิทยาลัย

CHULALONGKORN UNIVERSITY

บทคัดย่อและแฟ้มข้อมูลฉบับเต็มของวิทยานิพนธ์ตั้งแต่ปีการศึกษา 2554 ที่ให้บริการในคลังปัญญาจุฬาฯ (CUIR)

เป็นแฟ้มข้อมูลของนิสิตเจ้าของวิทยานิพนธ์ ที่ส่งผ่านทางบัณฑิตวิทยาลัย

The abstract and full text of theses from the academic year 2011 in Chulalongkorn University Intellectual Repository (CUIR) are the thesis authors' files submitted through the University Graduate School.

วิทยานิพนธ์นี้เป็นส่วนหนึ่งของการศึกษาตามหลักสูตรปริญญาวิทยาศาสตรดุษฎีบัณฑิต

สาขาวิชาปิโตรเคมี

คณะวิทยาศาสตร์ จุฬาลงกรณ์มหาวิทยาลัย

ปีการศึกษา 2557

ลิขสิทธิ์ของจุฬาลงกรณ์มหาวิทยาลัย

ELECTROSPUN COLORING AGENT-LOADED ZEIN MEMBRANE FOR ANALYSIS OF IONS

Miss Amornrat Saithongdee



A Dissertation Submitted in Partial Fulfillment of the Requirements
for the Degree of Doctor of Philosophy Program in Petrochemistry

Faculty of Science

Chulalongkorn University

Academic Year 2014

Copyright of Chulalongkorn University

Thesis Title	ELECTROSPUN COLORING AGENT-LOADED ZEIN MEMBRANE FOR ANALYSIS OF IONS
By	Miss Amornrat Saithongdee
Field of Study	Petrochemistry
Thesis Advisor	Assistant Professor Apichat Imyim, Ph.D.

Accepted by the Faculty of Science, Chulalongkorn University in Partial
Fulfillment of the Requirements for the Doctoral Degree

.....Dean of the Faculty of Science
(Professor Supot Hannongbua, Dr.rer.nat.)

THESIS COMMITTEE

.....Chairman
(Assistant Professor Warinthorn Chavasiri, Ph.D.)

.....Thesis Advisor
(Assistant Professor Apichat Imyim, Ph.D.)

.....Examiner
(Associate Professor Mongkol Sukwattanasinitt, Ph.D.)

.....Examiner
(Associate Professor Wimonrat Trakarnpruk, Ph.D.)

.....External Examiner
(Assistant Professor Thammasit Vongsetskul, D.Phil.)

อมรรัตน์ สายทองดี : เยื่ออิเล็กโทรสปันของซินที่เติมสารให้สีสำหรับการวิเคราะห์ไอออน (ELECTROSPUN COLORING AGENT-LOADED ZEIN MEMBRANE FOR ANALYSIS OF IONS) อ.ที่
 ปรักษาวิทยานิพนธ์หลัก: ผศ. ดร.อภิชาติ อิ่มยิ้ม, 101 หน้า.

สังเคราะห์ไดฟลูออโรเคอร์คูมิน ($\text{BF}_2\text{-CurOH}$) และ 3,5-ได(4-เอทีนิล-เอ็น,เอ็น-ไดเมทิลอะนิลีน)-2-ไฮดรอกซีเบนซัลดีไฮด์ (F_3) พิสูจน์เอกลักษณ์เคอร์คูมิน, $\text{BF}_2\text{-CurOH}$ และ F_3 ซึ่งใช้เป็นสารที่ทำให้เกิดสีด้วยเทคนิคอินฟราเรดสเปกโทรสโกปีและนิวเคลียร์แมกเนติกเรโซแนนซ์สเปกโทรสโกปี เตรียมแผ่นเส้นใยจากซิน ซึ่งเป็นพอลิเมอร์ธรรมชาติที่ใช้เป็นตัวรองรับผสมกับสารให้สีด้วยกระบวนการปั่นเส้นใยด้วยไฟฟ้าแล้วตามด้วยปฏิกิริยาการเชื่อมขวางโดยใช้กรดซัลฟิวริกเป็นตัวเชื่อมขวางที่ไม่มีพิษ เตรียมแผ่นเส้นใย 5 เปอร์เซ็นต์โดยน้ำหนักต่อน้ำหนัก (เคอร์คูมิน/ซิน), แผ่นเส้นใย 0.25 เปอร์เซ็นต์โดยน้ำหนักต่อน้ำหนัก ($\text{BF}_2\text{-CurOH}$ /ซิน) และแผ่นเส้นใย 0.1 เปอร์เซ็นต์โดยน้ำหนักต่อน้ำหนัก (F_3 /ซิน) สำหรับการวิเคราะห์ พิสูจน์เอกลักษณ์แผ่นเส้นใยด้วยกล้องจุลทรรศน์อิเล็กตรอนแบบส่องกราด, อินฟราเรดสเปกโทรสโกปี และดีฟิวส์รีเฟลกแทนส์อัลตราไวโอเลต-วิสิเบิลสเปกโทรสโกปี ได้เส้นใยที่มีขนาดเส้นผ่านศูนย์กลางอยู่ในช่วง 394 ถึง 586 นาโนเมตรและไม่มีเม็ดปม จากนั้นทดสอบความสามารถการตรวจวัดของแผ่นเส้นใยด้วยตาเปล่า พบว่าแผ่นเส้นใยซินที่เติมเคอร์คูมินเปลี่ยนสีจากเหลืองเป็นน้ำตาลในสารละลายที่มีไอออนของเหล็ก(III) มีภาวะที่เหมาะสมในการตรวจวัดคือสารละลายที่พีเอช 2 โดยไม่มีการรบกวนของไอออนโลหะ 17 ชนิด (Ag^+ , As^{5+} , Ba^{2+} , Ca^{2+} , Cd^{2+} , Co^{2+} , Cr^{3+} , Cu^{2+} , Fe^{2+} , Hg^{2+} , K^+ , Mn^{2+} , Na^+ , Ni^{2+} , Pb^{2+} , Zn^{2+} และ Mg^{2+}) มีขีดจำกัดต่ำสุดของการตรวจวัดด้วยตาเปล่าคือ 0.4 มิลลิกรัมต่อลิตร และเป็นวิธีที่สามารถวิเคราะห์ไอออนของเหล็ก(III) ในตัวอย่างน้ำดื่มและน้ำผิวดินที่ให้ความถูกต้องดีโดยเทียบผลกับวิธีอ้างอิงด้วยเครื่องอินดักทีฟลิคัปเปิลพลาสมาออปติคัลอิมิสชันสเปกโทรมิเตอร์ แผ่นเส้นใยซินที่เติม $\text{BF}_2\text{-CurOH}$ เปลี่ยนสีจากสีส้มเป็นสีเขียวหลังจากสัมผัสกับแอมโมเนีย โดยความเข้มข้นจะเพิ่มขึ้นเมื่อความเข้มข้นของแอมโมเนียสูงขึ้น จึงเป็นวิธีที่สามารถนำไปประยุกต์ใช้สำหรับการตรวจวัดแอมโมเนียด้วยตาเปล่าได้ ภายใต้แสงหลอดยูวีแผ่นเส้นใยซินที่เติม F_3 เปลี่ยนระดับสีจากสีเขียวอ่อนเรืองแสงเป็นมืดในสารละลายที่มีไอออนของเหล็ก(III) มีภาวะในการตรวจวัดที่เหมาะสมคือสารละลายที่พีเอช 2 โดยไม่มีผลการรบกวนของไอออนโลหะทั้ง 17 ชนิดตามด้านบน ให้ขีดจำกัดต่ำสุดของการตรวจวัดด้วยตาเปล่าเป็น 10 มิลลิกรัมต่อลิตร หาค่าเฉลี่ยระดับสีเทาจากภาพถ่ายของแผ่นเส้นใยด้วยโปรแกรมอิมเมจ เจ สำหรับการตรวจวัดปริมาณ พบว่าค่าเฉลี่ยระดับสีเทาตกลงเมื่อความเข้มข้นของสารละลายไอออนของเหล็ก(III) เพิ่มขึ้น กราฟระหว่างค่าเฉลี่ยระดับสีเทากับความเข้มข้นของไอออนของเหล็ก(III) ในช่วง 20 ถึง 50 มิลลิกรัมต่อลิตร มีความเป็นเส้นตรง ($R^2 = 0.989$) ซึ่งใช้เป็นกราฟมาตรฐาน จึงเป็นวิธีที่สามารถใช้วิเคราะห์หาความเข้มข้นไอออนของเหล็ก(III) ในตัวอย่างน้ำดื่ม, น้ำผิวดินและน้ำใต้ดินที่ให้ความถูกต้องปานกลางโดยเทียบผลกับวิธีการตรวจวัดด้วยเครื่องไอซีพี-โออีเอส นอกจากนี้แผ่นเส้นใยให้ประสิทธิภาพการตรวจวัดที่ดีกว่าแผ่นฟิล์มแบบหล่อ โดยสรุปได้ออปติคัลเซ็นเซอร์ชนิดใหม่สำหรับการวิเคราะห์ไอออน ซึ่งเป็นเทคนิควิธีที่ง่าย ราคาถูก และเป็นมิตรต่อสิ่งแวดล้อม

สาขาวิชา ปีโตรเคมี

ปีการศึกษา 2557

ลายมือชื่อนิสิต

ลายมือชื่อ อ.ที่ปรึกษาหลัก

5373920023 : MAJOR PETROCHEMISTRY

KEYWORDS: ZEIN MEMBRANE / NANOFIBER MAT / ELECTROSPINNING / NAKED-EYE SENSOR / CURCUMIN / DIFLUOROBORON CURCUMIN

AMORN RAT SAITHONGDEE: ELECTROSPUN COLORING AGENT-LOADED ZEIN MEMBRANE FOR ANALYSIS OF IONS. ADVISOR: ASST. PROF. APICHAT IMYIM, Ph.D., 101 pp.

Difluoroboron curcumin ($\text{BF}_2\text{-CurOH}$) and 3,5-di(4-ethynyl-*N,N*-dimethylanilyl)-2-hydroxybenzaldehyde (F_3) were synthesized. Curcumin, $\text{BF}_2\text{-CurOH}$ and F_3 as coloring agents were characterized by Fourier transform infrared spectroscopy (FT-IR) and nuclear magnetic resonance spectroscopy (NMR). Zein as a supporting natural polymer blending with coloring agents fiber mats were fabricated by electrospinning, followed by a crosslinking reaction using citric acid as a non-toxic crosslinker. 5%wt/wt (curcumin/zein) fiber mat, 0.25%wt/wt ($\text{BF}_2\text{-CurOH}$ /zein) fiber mat and 0.1%wt/wt (F_3 /zein) fiber mat were prepared for analytical purpose. The fiber mats were characterized by scanning electron microscopy (SEM), Fourier transform infrared spectroscopy (FT-IR) and diffuse reflectance ultraviolet-visible spectroscopy (DRUV-Vis). The fiber diameters ranged from 394 to 586 nm without node. Then fiber mat sensing ability was examined by naked-eye. The color of curcumin-loaded zein fiber mat changed from yellow to brown in the presence of Fe^{3+} . The optimal sensing condition was at pH 2 without any effect of 17 interfering metal ions (Ag^+ , As^{5+} , Ba^{2+} , Ca^{2+} , Cd^{2+} , Co^{2+} , Cr^{3+} , Cu^{2+} , Fe^{2+} , Hg^{2+} , K^+ , Mn^{2+} , Na^+ , Ni^{2+} , Pb^{2+} , Zn^{2+} and Mg^{2+}). The visual detection limit was 0.4 mg/L. This method could be employed for the analysis of Fe^{3+} in potable water and surface water samples with a good accuracy comparing with the reference method by inductive coupled plasma optical emission spectrometer (ICP-OES). The color of $\text{BF}_2\text{-CurOH}$ -loaded zein fiber mat changed from orange to green after being exposed to ammonia gas. The degree of color change of the fiber mat increased proportionally with the increasing concentration of ammonia gas. This method could be applied for ammonia gas sensing by naked-eye. The shade colors of F_3 -loaded zein fiber mat changed from weak green fluorescence to dark in the presence of Fe^{3+} under UV lamp. The optimal sensing condition was at pH 2 without any effect of the same 17 interfering metal ions stated above. Its optical detection limit was 10 mg/L. For quantitative detection, the mean gray value was evaluated from the photograph of fiber mat using image J software. The mean gray value decreased with increasing concentrations of Fe^{3+} . The graph between the mean gray value and the concentration of Fe^{3+} in the range of 20-50 mg/L as the calibration graph for Fe^{3+} sensing was linear ($R^2 = 0.989$). This method was applied for the determination of concentration Fe^{3+} in potable water, surface water and ground water samples with moderate accuracy comparing with the result from ICP-OES detection. Moreover, the fiber mat sensing efficiency was higher than the cast film. In conclusion, new optical sensors for analysis of ions were obtained. This technique is easy to use, low cost and falls in environmental friendly technique.

Field of Study: Petrochemistry

Academic Year: 2014

Student's Signature

Advisor's Signature

ACKNOWLEDGEMENTS

I would like to express my greatest appreciation to my reverent advisor, Assistant Professor Dr. Apichat Imyim, for assistance, suggestion, constructive criticism, inspiration and encouragement during my research. Furthermore, I would like to thank my thesis committees, Assistant Professor Dr. Warinthorn Chavasiri, Associate Professor Dr. Mongkol Sukwattanasinitt, Associate Professor Dr. Wimonrat Trakarnpruk and Assistant Professor Dr. Thammasit Vongsetskul for their precious suggestions and comments.

This thesis could not be completed without the kindness, help and support of many people. I would like to thank Assistant Professor Dr. Wanlapa Aeungmaitrepirom and Assistant Professor Dr. Fuangfa Unob for their advices and suggestions. Furthermore, I would like to thank all members in the Environmental Analysis Research Unit (EARU) for their lovely friendship and encouragement. I also would like to thank Ms. Warangkhana Khaodee, Mr. Apiwat Promchat and Mr. Anusak Chaicham for suggestion about experimental techniques and recommendation. This thesis was financially supported by Overseas Research Experience Scholarship for Graduate Student, Support for the Overseas Presentations of Graduate Level Academic Thesis and National Center of Excellence for Petroleum, Petrochemicals, and Advanced Materials (NCE-PPAM).

Finally, I would like to express my gratitude to my family for their love and care at all time.

CONTENTS

	Page
THAI ABSTRACT	iv
ENGLISH ABSTRACT	v
ACKNOWLEDGEMENTS	vi
CONTENTS	vii
LIST OF TABLES	xii
LIST OF SCHEMES	xiii
LIST OF FIGURES	xiv
LIST OF ABBRIVIATIONS.....	xix
CHAPTER I INTRODUCTION	1
1.1 Statement of the Problem.....	1
1.2 Objectives	2
1.3 Scope of the Research.....	3
1.4 The Benefits of This Research	3
CHAPTER II THEORY AND LITERATURE REVIEW	4
2.1 Colorimetric Sensor	4
2.1.1 Liquid-phase Colorimetric Sensor.....	4
2.1.2 Solid-phase Colorimetric Sensor.....	4
2.2 Electrospinning.....	6
2.2.1 Basic and Feature	6
2.2.2 Applications.....	11
2.3 Zein	11
2.3.1 Chemical and Physical Properties	11

	Page
2.3.2 Fabricability and Crosslinking	13
2.4 Coloring Agents	15
2.4.1 Curcumin	15
2.4.2 Difluoroboron Curcumin (BF ₂ -CurOH)	16
2.4.3 3,5-di(4-ethynyl- <i>N,N</i> -dimethylanily)-2-hydroxybenzaldehyde (F ₃)	17
2.5 Literature Review	19
CHAPTER III EXPERIMENTAL SECTIONS	22
3.1 Apparatus	22
3.2 Chemicals	23
3.2.1 Preparation of solution	24
3.3 Synthesis of Coloring Agents	26
3.3.1 Synthesis of Difluoroboron Curcumin (BF ₂ -CurOH)	26
3.3.2 Synthesis of 3,5-di(4-ethynyl- <i>N,N</i> -dimethylanily)-2- hydroxylbenzaldehyde (F ₃)	26
3.4 Characterization of Coloring Agents	27
3.4.1 Fourier Transform Infrared Spectrometer (FT-IR)	27
3.4.2 Nuclear Magnetic Resonance Spectrometer (NMR)	27
3.5 Preliminary Study of the Amount Coloring Agent on Zein Fiber Mats for Analysis of Ions	28
3.6 Preparation of Zein Blending with Coloring Agents Fiber Mats	29
3.6.1 Preparation of Zein Blending with Curcumin Fiber Mat	29
3.6.2 Preparation of Zein Blending with Difluoroboron Curcumin (BF ₂ - CurOH) Fiber Mat	30

3.6.3 Preparation of Zein Blending with 3,5-di(4-ethynyl- <i>N,N</i> -dimethylanily)-2-hydroxybenzaldehyde (F ₃) Fiber Mat.....	30
3.7 Fiber Mats Characterization.....	31
3.7.1 Fourier Transform Infrared Spectrometer (FT-IR)	31
3.7.2 Diffuse Reflectance Ultraviolet-visible Spectrophotometer (DR-UV-Vis)...	31
3.7.3 Scanning Electron Microscope (SEM).....	32
3.8 Fiber Mat Sensing Ability.....	32
3.8.1 Influence of pH	32
3.8.2 Effect of Interferences	33
3.8.3 Limit of Detection (LOD) and Method Validation	33
3.9 Applications.....	34
3.9.1 Curcumin Fiber Mat for the Determination of Iron(III) Ions	34
3.9.2 Difluoroboron Curcumin (BF ₂ -CurOH) Fiber Mat for Ammonia Sensing.....	35
3.9.3 3,5-di(4-ethynyl- <i>N,N</i> -dimethylanily)-2-hydroxybenzaldehyde (F ₃) Fiber Mat for the Determination of Iron (III) Ions	35
3.10 Preparation of Film Sensing for Comparison with Fiber Mat	36
CHAPTER IV RESULTS AND DISCUSSION.....	37
4.1 Synthesis of Coloring Agents.....	37
4.1.1 Synthesis of Difluoroboron Curcumin (BF ₂ -CurOH).....	37
4.1.2 Synthesis of 3,5-di(4-ethynyl- <i>N,N</i> -dimethylanily)-2-hydroxybenzaldehyde (F ₃).....	38
4.2 Characterization of Coloring Agents	40
4.2.1 Curcumin	40
4.2.1.1 Fourier Transform Infrared Spectroscopy (FT-IR)	40

	Page
4.2.1.2 Nuclear Magnetic Resonance Spectroscopy (NMR)	41
4.2.2 Difluoroboron Curcumin (BF ₂ -CurOH)	42
4.2.2.1 Fourier Transform Infrared Spectroscopy (FT-IR)	42
4.2.2.2 Nuclear Magnetic Resonance Spectroscopy (NMR)	43
4.2.3 3,5-di(4-ethynyl- <i>N,N</i> -dimethylanily)-2-hydroxybenzaldehyde (F ₃)	44
4.2.3.1 Fourier Transform Infrared Spectroscopy (FT-IR)	44
4.2.3.2 Nuclear Magnetic Resonance Spectroscopy (NMR)	45
4.3 Preliminary Study of the Amount of Coloring Agent on Zein Fiber Mats for Analysis of Ions	46
4.4 Electrospun Zein Blending with Curcumin Fiber Mats	48
4.4.1 Morphology of Curcumin-loaded Zein Fiber Mat	48
4.4.2 FT-IR Characterization of Curcumin-loaded Zein Fiber Mat	50
4.4.3 DR-UV-Vis Characterization of Curcumin-loaded Zein Fiber Mat	53
4.4.4 Naked-eye Sensing for Iron(III) Ions	54
4.4.5 Analysis of Real Water Samples	60
4.5 Electrospun Zein Blending with Difluoroboron Curcumin	62
4.5.1 Morphology of BF ₂ -CurOH-loaded Zein Fiber Mat	62
4.5.2 FT-IR Characterization of BF ₂ -CurOH-loaded Zein Fiber Mat	63
4.5.3 DR-UV-Vis Characterization of BF ₂ -CurOH-loaded Zein Fiber Mat	64
4.5.4 Applicability of Borax Sensing	66
4.5.5 Applicability of Ammonia Sensing	67
4.6 Electrospun Zein Blending with 3,5-di(4-ethynyl- <i>N,N</i> -dimethylanily)-2- hydroxybenzaldehyde (F ₃)	70
4.6.1 Morphology of F ₃ -loaded Zein Fiber Mat	70

	Page
4.6.2 FT-IR Characterization of F ₃ -loaded Zein Fiber Mat	71
4.6.3 DR-UV-Vis Characterization of F ₃ -loaded Zein Fiber Mat.....	72
4.6.4 Naked-eye Sensing for Iron(III) Ions	74
4.6.5 Analysis of Real Water Samples	80
4.7 Comparison of Fiber Mat and Film Sensing Efficiency	82
CHAPTER V CONCLUSION AND SUGGESTIONS	85
5.1 Conclusion	85
5.2 Suggestions for Future Work.....	87
REFERENCES	88
VITA.....	101



LIST OF TABLES

	Page
Table 2.1 Electrospinning factors and their effects on fiber morphology.....	10
Table 3.1 Apparatus list	22
Table 3.2 Chemical list.....	23
Table 3.3 The ICP-OES operating conditions for Fe evaluation.....	34



LIST OF SCHEMES

	Page
Scheme 4.1 Synthesis of difluoroboron curcumin (BF ₂ -CurOH)	38
Scheme 4.2 The synthesis of 3,5-di(4-ethynyl- <i>N,N</i> -dimethylanily)-2-hydroxybenzaldehyde (F ₃).....	39
Scheme 4.3 The complex formation of curcumin and iron(III) ion	56
Scheme 4.4 The ICT process of BF ₂ -CurOH + NH ₃	69
Scheme 4.5 The proposed quenching mechanism of F ₃ + Fe ³⁺	76



LIST OF FIGURES

	Page
Figure 2.1 The common electrospinning setup	6
Figure 2.2 The photograph of spinning jet	8
Figure 2.3 The structure and physical/chemical properties of zein	12
Figure 2.4 The structure and physical/chemical properties of curcumin	16
Figure 2.5 The structure and physical/chemical properties of difluoroboron curcumin (BF ₂ -CurOH)	17
Figure 2.6 The structure and physical/chemical properties of 3,5-di(4-ethynyl- <i>N,N</i> -dimethylanily)-2-hydroxybenzaldehyde (F ₃).....	18
Figure 4.1 FT-IR spectrum of curcumin	40
Figure 4.2 ¹ H-NMR spectrum of curcumin in DMSO- <i>d</i> ₆	41
Figure 4.3 FT-IR spectrum of difluoroboron curcumin (BF ₂ -CurOH)	42
Figure 4.4 ¹ H-NMR spectrum of difluoroboron curcumin (BF ₂ -CurOH) in DMSO- <i>d</i> ₆	43
Figure 4.5 FT-IR spectrum of 3,5-di(4-ethynyl- <i>N,N</i> -dimethylanily)-2-hydroxybenzaldehyde (F ₃).....	44
Figure 4.6 ¹ H-NMR spectrum of 3,5-di(4-ethynyl- <i>N,N</i> -dimethylanily)-2-hydroxybenzaldehyde (F ₃) in CDCl ₃	45
Figure 4.7 Photographs of curcumin-loaded zein fiber mats with varying amount of curcumin immersed in DI water and different concentrations of Fe ³⁺	47
Figure 4.8 SEM images (5,000x magnification) of (a) dry and (b) wet curcumin-loaded zein fiber mats before and after immersing in DI water at room temperature for 3 hours. Inset: SEM image (750x magnification) and the photographs of curcumin-loaded zein fiber mats (upper right corner).	49

Figure 4.9 SEM images (5,000x magnification) of (a) dry and (b) wet zein fiber mats before and after immersing in DI water at room temperature for 3 hours. Inset: SEM image (750x magnification) and the photographs of zein fiber mats (upper right corner).	49
Figure 4.10 FT-IR spectrum of curcumin-loaded zein fiber mat	51
Figure 4.11 FT-IR spectrum of zein fiber mat	52
Figure 4.12 FT-IR spectrum of zein powder	52
Figure 4.13 DRUV-Vis spectrum of curcumin-loaded zein fiber mat (Inset shows the photograph of curcumin-loaded zein fiber mat.).....	53
Figure 4.14 DRUV-Vis spectrum of zein fiber mat (Inset shows the photograph of zein fiber mat.).....	54
Figure 4.15 Photographs of curcumin-loaded zein fiber mats immersed in DI water and Fe^{3+} solution at different pHs (sample volume = 1 mL, time = 3 hours, room temperature).....	55
Figure 4.16 Photographs of the curcumin-loaded zein fiber mats after immersing into various metal ion solutions (concentrations= 200 μM , pH = 2, sample volume= 1 mL, time= 3 hours)	57
Figure 4.17 The photographs of the curcumin-loaded zein fiber mats after immersing into solutions at different concentration of Fe^{3+} for qualitative. (yes/no response) and quantitative testing (1: positive response, o: null response).....	58
Figure 4.18 DR-UV-Vis spectra of curcumin-loaded zein fiber mats after immersing for 3 hours in different concentrations of Fe^{3+} at pH 2.....	59
Figure 4.19 Photographs of the curcumin fiber mat after immersing in real water samples (left) and the color calibration chart (right)	61

Figure 4.20 SEM images (5,000x magnification) of (a) dry and (b) wet difluoroboron curcumin (BF ₂ -CurOH)-loaded zein fiber mats before and after immersing in DI water at room temperature for 3 hours. Inset: SEM image (750x magnification) and the photograph of BF ₂ -CurOH-loaded zein fiber mats (upper right corner).....	63
Figure 4.21 FT-IR spectrum of difluoroboron curcumin (BF ₂ -CurOH)-loaded zein fiber mat.....	64
Figure 4.22 DR-UV-Vis spectrum of difluoroboron curcumin (BF ₂ -CurOH)-loaded zein fiber mat (Inset shows the photograph of BF ₂ -CurOH-loaded zein fiber mat.).....	65
Figure 4.23 DRUV-Vis spectrum of difluoroboron curcumin (BF ₂ -CurOH) powder (Inset shows the photograph of BF ₂ -CurOH powder.).....	65
Figure 4.24 DR-UV-Vis spectrum of zein fiber mat (Inset shows the photograph of zein fiber mat.).....	66
Figure 4.25 Photographs of difluoroboron curcumin (BF ₂ -CurOH)-loaded zein fiber mat immersed in DI water and B ₄ O ₇ ²⁻ solution at different pHs (sample volume = 1 mL, time = 3 hours).....	67
Figure 4.26 The photographs of BF ₂ -CurOH fiber mat after exposing to ammonia gas at different concentrations (time = 30 min, in a boiling water bath).....	68
Figure 4.27 SEM images (5,000x magnification) of (a) dry and (b) wet 3,5-di(4-ethynyl- <i>N,N</i> -dimethylanily)-2-hydroxybenzaldehyde (F ₃)-loaded zein fiber mats before and after immersing in DI water at room temperature for 3 hours (Inset: SEM image (750x magnification))	71
Figure 4.28 FT-IR spectrum of 3,5-di(4-ethynyl- <i>N,N</i> -dimethylanily)-2-hydroxybenzaldehyde (F ₃)-loaded zein fiber mat.....	72
Figure 4.29 DR-UV-Vis spectrum of 3,5-di(4-ethynyl- <i>N,N</i> -dimethylanily)-2-hydroxybenzaldehyde (F ₃)-loaded zein fiber mat.....	73

- Figure 4.30** The photographs of (a) zein fiber mat and (b) 3,5-di(4-ethynyl-*N,N*-dimethylanily)-2-hydroxybenzaldehyde (F_3)-loaded zein fiber mat under fluorescent lamp (Top) and 20W black light lamp (bottom)..... 73
- Figure 4.31** The mean color intensity at various pH values (sample volume = 1 mL, 3 hours, under 20 W black light)..... 75
- Figure 4.32** Photographs of 3,5-di(4-ethynyl-*N,N*-dimethylanily)-2-hydroxybenzaldehyde (F_3)-loaded zein fiber mats immersed in DI water and Fe^{3+} solution at pH 2 (sample volume = 1 mL, 3 hours, under 20 W black light)..... 75
- Figure 4.33** Photographs of F_3 fiber mats after immersing into various solutions (concentration = 200 μ M, pH = 2, sample volume = 1 mL, 3 hours, under 20 W black light)..... 77
- Figure 4.34** The mean color intensity with various metal ion solutions (concentration = 200 μ M, pH = 2, sample volume = 1 mL, 3 hours, under 20 W black light)..... 77
- Figure 4.35** The photographs of the F_3 -loaded zein fiber mats after immersing into solutions at different concentration (pH = 2, sample volume = 1 mL, 3 hours, under 20 W black light) 78
- Figure 4.36** The mean color intensity and concentration of Fe^{3+} in various concentrations (pH = 2, sample volume = 1 mL, 3 hours, under 20 W black light).... 79
- Figure 4.37** The calibration graph for Fe^{3+} sensing (pH = 2, sample volume = 1 mL, 3 hours, under 20 W black light)..... 79
- Figure 4.38** The comparative results of Fe(III) ion concentration determined by naked-eye, Image J software and ICP-OES 81
- Figure 4.39** SEM images (5,000x magnification) of (a) dry and (b) wet curcumin-loaded zein film (c) dry and (d) wet zein film before and after immersing in DI water at room temperature for 3 hours (Inset: the photographs of films (upper right corner)) 83

Figure 4.40 The photographs of curcumin-loaded zein (a) fiber mat and (b) film before (top) and after (bottom) immersed into 10 mg/L of Fe^{3+} solution (sample volume = 3 mL, time = 3 hours, room temperature)..... 84

Figure 4.41 The photographs of curcumin-loaded zein film before (a) and after (b) immersed in 10 mg/L of Fe^{3+} solution for 24 hours (sample volume = 3 mL, room temperature)..... 84



LIST OF ABBRIVIATIONS

%	Percent
°C	Degree Celsius
μL	Microlitre
μM	Micromolar
BF ₂ -CurOH	Difluoroboron curcumin
cm	Centimeter
F ₃	3,5-di(4-ethynyl- <i>N,N</i> -dimethylanily)-2-hydroxybenzaldehyde
g	Gram
kV	Kilovoltage
LOD	Limit of detection
M	Molar
mg/L	Milligrams per litre
mg/m ³	Milligram per cubic meter
mL	Millilitre
min	Minute
nm	Nanometer
ppm	Part per million
S.D.	Standard deviation
v/v	Volume by volume
wt/v	Weight by volume
wt/wt	Weight by weight

CHAPTER I

INTRODUCTION

1.1 Statement of the Problem

Colorimetric sensor is a sensing device that can alter its coloring character with small change in a chemical or physical property of samples. In recent years, many researches have paid attention to analyze color character by eye since it is easy to detect without specific instrument.

A coloring agent is a chemical that can be change its color under special conditions. Curcumin is a natural organic pigment from extraction of *Curcuma longa* L. It displays a yellow color under acidic conditions and changes to red under alkaline conditions. It is used as a pH indicator, food coloring agent and metal complex dyes [1-3]. Moreover, difluoroboron curcumin ($\text{BF}_2\text{-CurOH}$) is a derivative of curcumin that shows color changing from red in acidic solutions to blue in alkaline solutions. It was employed as a coloring agent in the solution system to detect cyanide ions [4]. Recently, 3,5-di(4-ethynyl-*N,N*-dimethylanily)-2-hydroxybenzaldehyde (F_3) shows a high sensitivity for cyanide detection. It exhibits turn-on fluorescent phenomenon in cyanide solutions [5].

Zein is a natural polymer extracted from corn. It is a low nutritive food since it contains mainly nonessential amino acids. Zein nanofiber mat has been used in many biomedical applications such as tissue engineering, drug delivery and food packaging [6-8]. Recently, the electrospun zein nanofiber mat was crosslinked using a non-toxic crosslinker [9]. It succeeded to improve their mechanical properties and water stability.

Electrospinning (electrostatic spinning) is a simple technique to fabricate a nanofiber mat or membrane which shows a very large surface area and porosity. The most prominent characteristic of nanofiber mat is a convenient handling and high response rate to external stimuli such as chemicals, pH, temperature and humidity.

Recently, researches on electrospun nanofiber mat in naked-eye sensing have been published [10, 11]. However, the process of mat fabrication is complexly involved and relatively high-priced. The use of synthetic polymeric nanofiber mat can cause an environmental pollution if unsuitable disposed.

Therefore, this research aimed to prepare zein blending with coloring agents (curcumin, difluoroboron curcumin ($\text{BF}_2\text{-CurOH}$) and 3,5-di(4-ethyl-*N,N*-dimethylanily)-2-hydroxybenzaldehyde (F_3)) fiber mats using electrospinning, followed by a crosslinking reaction. The fiber mats consist of zein as a supporting natural polymer, citric acid as a non-toxic crosslinker and curcumin, $\text{BF}_2\text{-CurOH}$ and F_3 as coloring agents. The green sensor fiber mats were obtained and characterized. Then fiber mat sensing ability was investigated by naked-eye. A curcumin-loaded zein fiber mat for the determination of iron(III) ions, a $\text{BF}_2\text{-CurOH}$ -loaded zein fiber mat for ammonia sensing and a F_3 -loaded zein fiber mat for the determination of iron(III) ions were tested. In addition, fiber mat and film sensing efficiency were investigated and compared.

1.2 Objectives

- To prepare of zein blending with coloring agents (curcumin, difluoroboron curcumin ($\text{BF}_2\text{-CurOH}$) and 3,5-di(4-ethynyl-*N,N*-dimethylanily)-2-hydroxybenzaldehyde (F_3)) fiber mats by electrospinning

- To investigate optimum conditions for qualitative and quantitative determination of iron(III) ions using curcumin-loaded zein fiber mat, ammonia sensing using $\text{BF}_2\text{-CurOH}$ -loaded zein fiber mat and iron(III) ions sensing by F_3 -loaded zein fiber mat.

1.3 Scope of the Research

The scope of this research includes:

- Synthesis of difluoroboron curcumin ($\text{BF}_2\text{-CurOH}$) and 3,5-di(4-ethynyl-*N,N*-dimethylanily)-2-hydroxybenzaldehyde (F_3) and characterization of coloring agents (curcumin, $\text{BF}_2\text{-CurOH}$ and F_3) by Fourier transform infrared spectroscopy (FT-IR) and nuclear magnetic resonance spectroscopy (NMR)

- Preliminary study of the amount of coloring agent on zein fiber mats for analysis of ions. Finding the suitable color change of fiber mats by naked-eye which could be apparently distinguished from their original color when being a sensor

- Preparation of zein blending with curcumin fiber mat zein blending with $\text{BF}_2\text{-CurOH}$ fiber mat and zein blending with F_3 fiber mat by electrospinning and a subsequent crosslinking reaction with citric acid as crosslinker

- Characterization of fiber mats by Fourier transform infrared spectroscopy (FT-IR), diffuse reflectance ultraviolet-visible spectroscopy (DR UV-Vis) and scanning electron microscopy (SEM)

- Investigation of suitable conditions for naked-eye qualitative and quantitative determination of iron(III) ions using a curcumin-loaded zein fiber mat, ammonia sensing by a $\text{BF}_2\text{-CurOH}$ -loaded zein fiber mat and iron(III) ions sensing by a F_3 -loaded zein fiber mat. The following parameters were studied: the influence of pH, the effect of interferences, the limit of detection (LOD) and method validation

- Study of the sensing efficiency of fiber mats by comparing with cast films

1.4 The Benefits of This Research

The electrospun coloring agent-loaded zein fiber mats for analytical application were achieved.

CHAPTER II

THEORY AND LITERATURE REVIEW

2.1 Colorimetric Sensor

Colorimetric sensor is a smart sensing device which exhibits its color change by chemical or physical stimuli. The color is the characteristics of light which can detect using instruments (spectrometer) or without instrument (image) [12, 13]. The most interesting detector is human eye. It is easy in detection, low cost, and user friendliness. Many researches on naked-eye sensor have been studied. It can be used in liquid-phase or solid-phase system.

2.1.1 Liquid-phase Colorimetric Sensor

Liquid-phase colorimetric sensor exhibits color change in a liquid system. They contain coloring agent(s) in a proper solvent. It must be homogeneously mixed with real sample. The mixture solution shows the different color when the coloring agent forms complex with analytes. The intensity of changing color is defined in qualitative and/or quantitative results [14-17]. Many coloring agents are organic dyes which dissolve in an organic solvent. It is hardly mixed to form a homogenous solution between the coloring agent and aqueous sample solutions. It is a big problem to develop this system.

2.1.2 Solid-phase Colorimetric Sensor

Solid-phase colorimetric sensors show color change in a solid system. The coloring agent is fixed on a solid support by grafting, blending or coating process. When the sensor is exposed to an analyte in a sample solution, the color of sensor is changed. The quantitative analysis is performed by comparing a color intensity between the sensor and calibration chart. Many researches have attended to approve the sensing detection limit and to develop a real-time sensing application.

The most common naked-eye sensor was developed for using in a real application for qualitative and quantitative analysis. In the solid-phase system, the naked-eye sensor exhibits dominant characteristics for on-site testing. It is comfortable and simple for sensing which lacks of complex operating procedure.

Many researchers studied to create the solid phase colorimetric sensors in various methods. Dutta *et al.* [18] reported a new method for the synthesis of conducting polyaniline in a filter paper for acting as an acid/base sensor. Its color changed from green to blue in an alkaline solution. Moreover, the use of sensor for ammonia sensing was possible. Pumtang *et al.* [19] grafted diacetylene lipids onto a filter paper using UV-irradiation and used for organic solvent type detection and identification. Zhou *et al.* [20] fabricated the crosslinked siloxane 3-aminopropyltriethoxysilane for H₂O₂ detection. The color of modified filter paper changed when it reacted with H₂O₂. Ozay *et al.* [21] synthesized rhodamine based reusable and colorimetric naked-eye hydrogel sensor. *N*-(Rhodamine-6G)lactam-*N'*-acryloyl-ethylenediamine (RH6GAC) as comonomer reacted with Fe³⁺ ions and formed a red complex on a hydrogel rod. Isaad *et al.* [22] prepared starch films containing quinolinium merocyanine dye by hand casting for low concentration detection of cyanide anions in water. The film could selectively detect sub-micromolar quantities of cyanide ion by a distinct color change. Poltue *et al.* [10] fabricated a sensor based on dimethylglyoxime blended poly(caprolactone) fiber mat by electrospinning for the detection of Ni²⁺. Moreover, Wang *et al.* [23] reported a film made by electrospinning which had higher sensitivities and adsorbent properties more than a film made by casting because the rate of sensing depends on a surface area effect. As mentioned above, the creative sensors were successfully innovated such as paper sensors, film sensors, rod sensors and fiber mat sensors for acting as the solid phase colorimetric sensor.

The important key for the most successful application of sensing is the good shape of colorimetric sensor. The good shape shall have a large surface area and can respond quickly to stimuli or analytes, and is easy to use. In addition, a method to create sensor with simple and quick response as well as low cost is desired.

2.2 Electrospinning

Electrospinning is a simple technique for a fabrication of nanofiber mat or membrane using electrostatic force [24-26]. It can be produce nanofiber with non-woven fabric or mat. It has a very large surface-to-volume, length-to-diameter ratios and high porosity. Therefore, it can be produce the good shape of sensor for sensing.

2.2.1 Basic and Feature

Three pieces of main equipment in laboratory are used. There are as follows: the high-voltage DC power supply, the spinneret as metallic needle and the collector. The common electrospinning setup is shown in Figure 2.1.

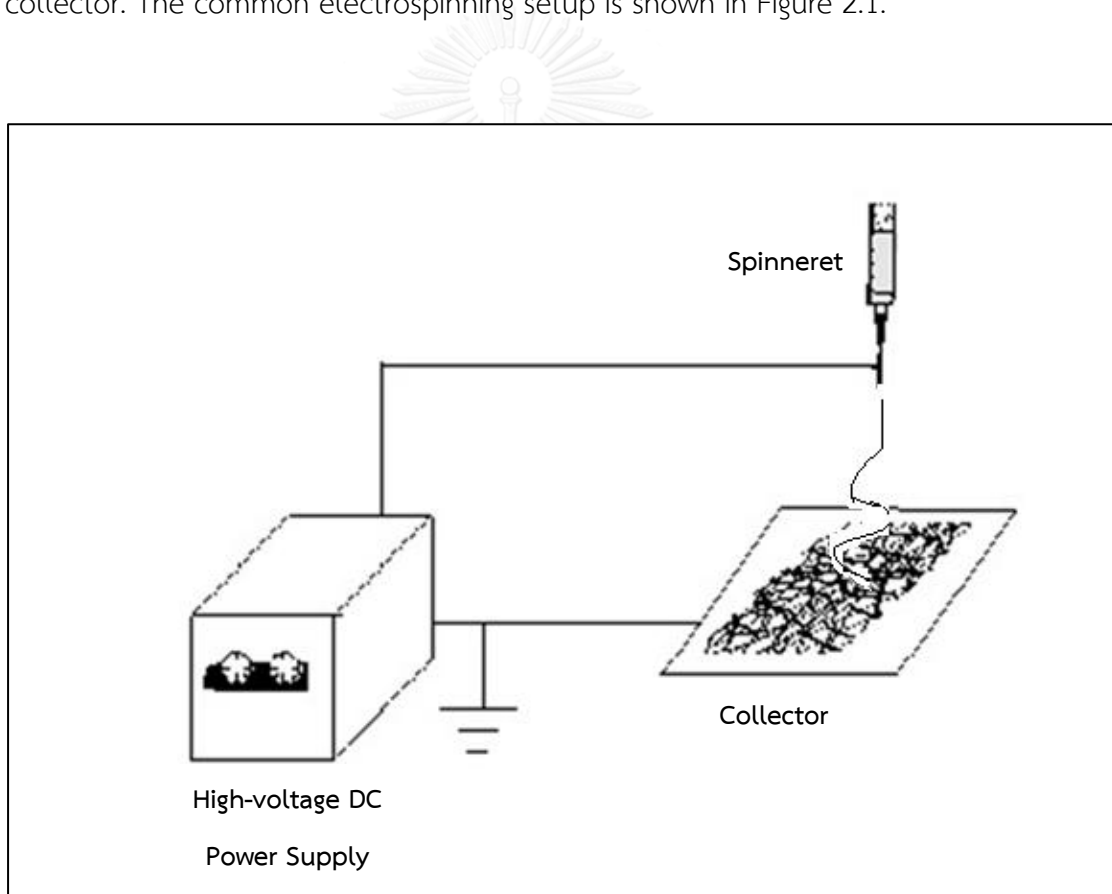


Figure 2.1 The common electrospinning setup

The electrostatic force at the spinneret is created by the high-voltage power supply. The electrically charged jet of polymer solution in the spinneret is generated. The jet is expelled from the needle tip when the electrostatic force on the surface of the polymer solution wins the surface tension of the polymer solution. The jet travels between the needle tip to the collector. The jet is pulled into small fibers. Then, it is dried by solvent evaporation. The fibers are continuously fabricated. Finally, the non-woven fabric or membrane is obtained on the surface of the collector.

Reneker *et al.* [27] divided the electrospinning into four steps: (1) creating of the jet, (2) elongation of straight region of jet, (3) whipping of instability region of jet and finally (4) solidification into fiber mat.

Creating of the jet. In an applied electric field, the charged droplet generates into ellipsoid at the end of the needle tip. Then, it is ejected into cone-like shape as known as the Taylor's cone at the critical voltage (V_c) applied to a droplet at the end of the tip of length (h) and radius (R) [28].

$$V_c^2 = \left(\frac{2L}{h}\right)^2 \left(\ln\left(\frac{2h}{R}\right) - 1.5\right) (0.117\pi RT).$$

When L = the distance between the needle and the collector

R = the internal radius of needle tip

This equation implies that the high-surface tension liquids require high electric field.

Elongation of straight region of jet. For launching of the jet, the coulombic repulsion will be insufficient to eject the jet. The slender fibril is initially created from cone in order to create additional surface area to accommodate surface charges. Jet initiation occurs instantaneously on application of a voltage exceeding V_c to the polymer solution. Then, the jet has an axial component with the coulombic repulsion of surface charges. The initially straight jet tapers down with extension in the region below the Taylor's cone. After that, the jet is elongated in its passage towards the collector. The photograph of spinning jet was shown in Figure 2.2. This figure was adapted from Shin *et al.* [29] and Li *et al* [30].

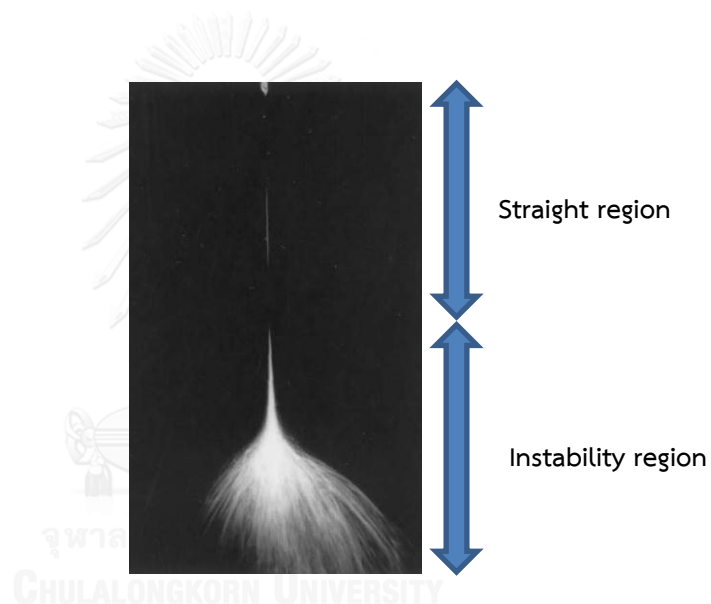


Figure 2.2 The photograph of spinning jet [29, 30]

Whipping of instability region of jet. The whipping instability region of jet may occur via different forces acting: gravitational force, electrostatic force, coulombic repulsion forces, viscoelastic force and surface tension force. Gravitational force (F_G) is dependent on density of solution (ρ). It moves jet in a vertically arranged collector. Electrostatic force (F_E) is determined by the applied electric field. It extends the jet and drives it towards the collector. Coulombic repulsion force (F_C) on the surface of the jet is dependent on the polymer solution. It introduces instability

and whipping motions. Viscoelastic force is dependent on the polymer solution. It works against elongation of the jet. Surface tension force is dependent on the polymer solution and additives. It works against the stretching of the jet.

Solidification into fiber mat. During the jet travel into the collector, the solvent is evaporated. The solidification rate is varied with many factors such as the polymer concentration, electrostatic field, gap distance, etc.

The fine fiber is circular cross-section, continuous and node free which is obtained under the best electrospinning conditions. There are several factors affecting the electrospinning process. These factors are mainly divided into three parts: (1) the solution parameters, (2) process parameters and (3) ambient parameters. The solution parameters include viscosity, polymer concentration, molecular weight of polymer and conductivity. The process parameters include applied voltage, tip to collector distance and flow rate. The ambient parameters include humidity and temperature. Table 2.1 shows the electrospinning factors and their effects on fiber morphology [25, 31]. The morphology and diameter of fibers are changed upon a several factors. For example, the polymer solution much has concentration high enough to continuous fiber formation. The viscosity of polymer solution is not over high to cause the difficulty of ejection of jets from the polymer solution. Moreover, the molecular weight of polymer shall be high enough to entangle with polymer chain in a solution. The jet is ejected from conductivity of the solution under enough applied voltage. The electrostatic repulsive force on the jet overcomes the viscosity and surface tension of the polymer solution. The jet is traveled from the tip to the collector. A minimum distance is required to evaporate solvent in time for dry fiber before reaching the collector.

Table 2.1 Electrospinning factors and their effects on fiber morphology [25, 31]

Parameters	Effect on fiber morphology	References
<i>Solution parameters</i>		
Viscosity	<ul style="list-style-type: none"> - Increase in fiber diameter with increase of viscosity - Decrease in the number of nodes on the fiber with decrease of viscosity 	[32-35]
Polymer concentration	<ul style="list-style-type: none"> - Increase in fiber diameter with increase of polymer concentration 	[36-38]
Molecular weight of polymer	<ul style="list-style-type: none"> - Decrease node generation on the fiber and droplets with increase of molecular weight of polymer 	[39-41]
Conductivity	<ul style="list-style-type: none"> - Decrease in fiber diameter with increase of conductivity 	[32, 38, 42]
<i>Processing parameters</i>		
Applied voltage	<ul style="list-style-type: none"> - Decrease in fiber diameter with increase of applied voltage 	[36, 38, 40]
Tip to collector distance	<ul style="list-style-type: none"> - Decrease in fiber diameter with increase of tip to collector distance 	[43-45]
Flow rate	<ul style="list-style-type: none"> - Decrease in fiber diameter with decrease of flow rate 	[35, 46, 47]
<i>Ambient parameters</i>		
Humidity	<ul style="list-style-type: none"> - Increase the number of circular pores on the fiber with increase of humidity 	[48]
Temperature	<ul style="list-style-type: none"> - Decrease in fiber diameter with increase of temperature 	[35]

2.2.2 Applications

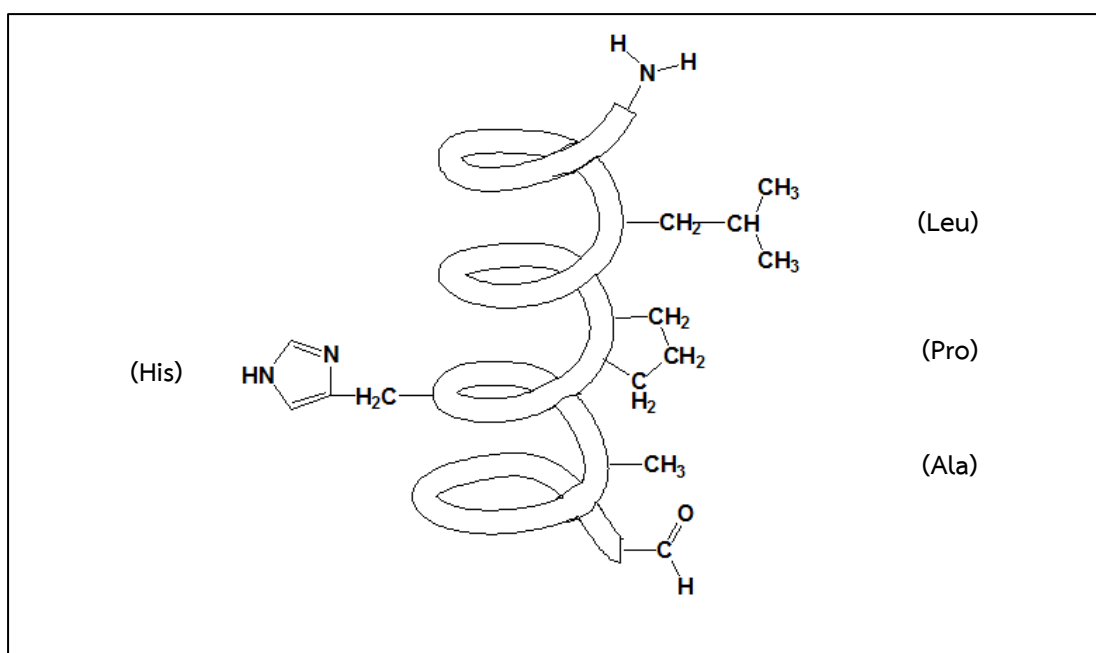
The electrospun fiber mat has several surprising characteristics such as a very large surface area that keeps a high chemical reaction rate and a suitable form that is satisfied in handling. The fiber mat composed of two or more substances that can be fabricated and improved its physical and chemical properties. The fiber mat displays outstanding properties for many application areas such as reinforced composites [31], filtration membrane [49], smart cloths [50], biomedical usage [51] and sensors [52].

Based on colorimetric sensor, the green sensor with using natural polymer is much attained. It falls environmentally friendly if inappropriately disposed.

2.3 Zein

2.3.1 Chemical and Physical Properties

Zein is a low-nutritive protein from corn. It contains mainly nonessential amino acids but it lacks some essential amino acids such as lysine and tryptophan [53-56]. The structure of zein is polypeptide helices that mainly contain nonpolar amino acids such as alanine, proline and leucine. The structure and physical/chemical properties of zein are presented in Figure 2.3.



Appearance: yellow powder

Molecular weight: 22,000 - 24,000 g/mol

Glass transition temperature: 165 °C

Thermal degradation point: 320 °C

Water solubility: Poor

Solubility: Aqueous alcohols

Figure 2.3 The structure and physical/chemical properties of zein

2.3.2 Fabricability and Crosslinking

Zein is a natural polymer with high molecular weight. Zein chains in solution can be entangled and easily continuously fabricated into fine fiber mats via electrospinning process. Many researchers studied to fabricate pure zein into nanofiber mats. Miyoshi *et al.* (2005) [57] produced an ultrafine fibrous zein mat by electrospinning of an 80%wt/wt ethanol aqueous solution. A polymer concentration and electric field affected its morphology. The fiber diameter was near 700 nm. Torres-Giner *et al.* (2008) [53] fabricated a white colored zein fiber mat with average fiber diameters below 100 nm. The polymer concentration, solvent content, flow-rate, applied voltage, needle tip-to-collector distance and pH were investigated in order to control the fiber size and morphology. Selling *et al.* (2007) [58] showed that zein fibers could be produced from a variety of lower alcohol/water solutions when spun under suitable conditions. Quality fibers could not be produced from *N,N*-dimethylformamide, acetone, acetic acid and NaOH aqueous solution as a solvent. As above researches, aqueous ethanol is the best solvent system for the electrospinning of zein. Moreover, it is a non-toxic and easily volatile solvent which allow the easy solidification of fibers.

Recently, there are continuously many reports on the electrospinning of blending zein. Blending of polymers is a very effective way to produce new multipurpose advanced materials. Yao *et al.* (2008) [59] produced zein/silk fiber mat with unique mechanical properties and excellent biocompatibility as biocomponent nanofibrous scaffolds for biomedical applications. Torres-Giner *et al.* (2009) [60] obtained novel antimicrobial ultrathin structures of zein/chitosan blends by electrospinning for an application in fields such as active and bioactive packaging, in antimicrobial food coatings and in biomedical purposes. Kayaci *et al.* (2012) [61] produced zein nanofibers containing cyclodextrins via electrospinning. The incorporation of cyclodextrin in zein improved the electrospinnability and node-free nanofibers at low zein concentrations. Cyclodextrins are cyclic oligosaccharides having a toroid-shaped molecular structure. Yang *et al.* (2013) [62] prepared ferulic acid drug-loaded zein composite fiber as drug carrier. Neo *et al.* (2013) [63] reported

the successful encapsulation of food grade antioxidant in natural biopolymer by electrospinning with zein/gallic acid blending as model for bioactive packaging. As stated above, many researches have attained to fabricate blending zein fiber mat for many applications such as food coating, food packaging especially in biomedical usage [7, 62, 64] because it is biocompatibility, renewable and biodegradable. However, the zein fiber mat dissolves in water and has poor mechanical properties. It is limited to use.

Recently, many researches have attained to improve these defects by employing a crosslinking of polymers. The crosslinking is the chemical reaction that produces the network in their structure by adding a crosslinker. It shows insoluble and swollen behavior in water. Yao *et al.* (2007) [65] studied the electrospinning and crosslinking of zein nanofiber mat. Hexamethylene diisocyanate as crosslinker was used to improve the flexibility and tensile strength of the nanofiber mat. Xu *et al.* (2008) [66] used citric acid as crosslinker and sodium hypophosphite monohydrate as catalyst in the electrospinning of zein solution. The crosslinked fiber mat showed a high wet strength and good water stability. Jiang *et al.* (2010) [9] reported the method of cytocompatible crosslinking zein fiber mat for tissue engineering and other medical applications. Citric acid as nontoxic crosslinker was used. The electrospun fiber mat was put in an oven at 150 °C for 2.5 hours for fully crosslinking reaction. The water stability of fiber mat was developed. Suwantong *et al.* (2011) [67] prepared crosslinked electrospun fiber mat by adding glyoxal as crosslinker for using in biomedical applications. The mechanical properties of fiber mat were improved. Moreover, the fiber mat form was preserved after immersion in water. As summarized by above researches, the crosslinking reaction is an important reaction to obtain a water stable fiber mat. In addition, a non-toxic crosslinker is needed to apply because it still represents the biocompatibility and sustainable development.

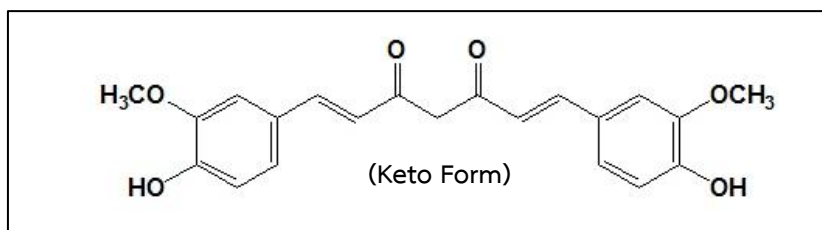
In conclusion, the crosslinked zein fiber mat blending with coloring agent can be possibly created for acting as a colorimetric sensor.

2.4 Coloring Agents

The coloring agents are mainly organic dyes that produce color. They can be attached on a supporting material. Coloring agents are regularly classified using their chemical structure such as azo, anthraquinone, thiazole, oxazine and xanthene [68, 69]. The coloring agents respond with a specific substance by intermolecular interaction. Thus, the position and/or intensity of the absorption and/or emission bands of coloring agents are changed resulting in color change. The coloring agent for sensing is variously applied.

2.4.1 Curcumin

Curcumin is a natural organic dye which is extracted from the root of *Curcuma longa* L. It contains phenolic compounds as major moieties. The structure of curcumin can alternate between keto and enol tautomeric forms in acid and base media, respectively [70, 71]. It shows a yellow color under acidic conditions and switch to red under alkaline conditions. The transition pH is in the range of 6.0-8.0. Curcumin has been used in many application areas such as food coloring agent [1], natural pH indicator, biomedical activities [72, 73], sensitizer [74] and metal-chelating agents [75-77]. The structure and physical/chemical properties of curcumin are presented in Figure 2.4.



Appearance: Bright yellow powder

Molecular weight: 368.38 g/mol

Melting point: 183°C

Water solubility: Insoluble

Solubility: Ethanol

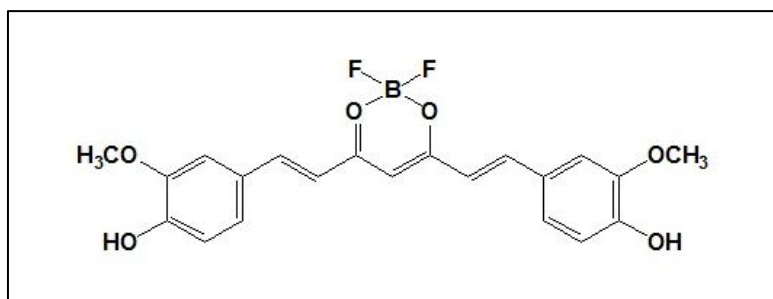
Absorption band: 408 - 430 nm

Emission band: 460 - 560 nm

Figure 2.4 The structure and physical/chemical properties of curcumin

2.4.2 Difluoroboron Curcumin (BF₂-CurOH)

Difluoroboron curcumin is prepared from curcumin by adding of BF₂ on the carbonyl groups of curcumin. The BF₂-CurOH inhibits keto- enol tautomerism. It can be improved the photophysical properties and stability of curcumin [4]. Moreover, difluoroboron curcumin (BF₂-CurOH) shows the color transition from red to blue in cyanide solution which could be observed by eye or UV-vis spectrometry. The BF₂-CurOH contains two methoxy phenol as the electron donor parts and difluoroboron enolate as the electron acceptor part which occur a strong intramolecular charge transfer (ICT) upon the binding of cyanide ions [78, 79]. In addition, BF₂-CurOH exhibits a red color under acidic conditions and turns to blue color under alkaline conditions. The structure and physical/chemical properties of difluoroboron curcumin (BF₂-CurOH) are presented in Figure 2.5.



Appearance: Red powder

Molecular weight: 443.26

Water solubility: Insoluble

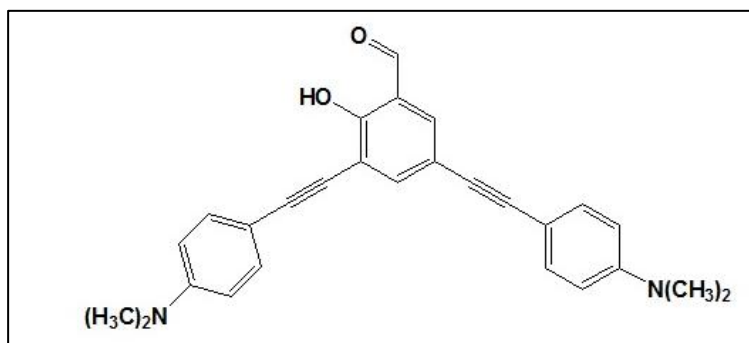
Absorption band: 465.1 – 513.0 nm

Emission band: 521.94 – 587.05 nm

Figure 2.5 The structure and physical/chemical properties of difluoroboron curcumin (BF₂-CurOH)

2.4.3 3,5-di(4-ethynyl-*N,N*-dimethylanily)-2-hydroxybenzaldehyde (F₃)

3,5-di(4-ethynyl-*N,N*-dimethylanily)-2-hydroxybenzaldehyde (F₃) is a fluorescent synthetic dye base on a salicylaldehyde derivative. The F₃ consists of diphenylacetylene as fluorogenic fragments and salicylaldehyde as a cyanide ion receptor resulting in the reduction of intramolecular charge transfer (ICT) process [80-82]. The F₃ can be used as cyanide fluorescent sensors using chromatographic-like technique [5]. It displays strong green emission at addition of cyanide ions and weak yellow fluorescence background at non-addition of cyanide ions. The structure and physical/chemical properties of 3,5-di(4-ethynyl-*N,N*-dimethylanily)-2-hydroxybenzaldehyde (F₃) are presented in Figure 2.6.



Appearance: Yellow solid

Molecular weight: 408.184

Water solubility: Insoluble

Absorption band: 335, 385 nm

Emission band: 444 nm

Figure 2.6 The structure and physical/chemical properties of 3,5-di(4-ethynyl-*N,N*-dimethylanily)-2-hydroxybenzaldehyde (F₃)

2.5 Literature Review

Many researches on electrospun fiber mats have been reported in colorimetric sensor applications.

- Sensing of chemical ions

Wang *et al.* (2002) fabricated an optical chemical sensor for metal ion (Fe^{3+} and Hg^{2+}) and 2,4-dinitrotoluene detection by electrospinning of poly(acrylic acid)-poly(pyrene methanol) as a fluorescent conjugated polymer. The fluorescence intensities decreased with increasing the concentration of analytes. These sensors showed high responsive fluorescence quenching due to the interactions of electron rich on poly(pyrene methanol) part and electron deficient quencher. In addition, this sensor exhibited high sensitivity due to high surface area-to-volume ratio of the fiber mat structure.

Li *et al.* (2010) [83] designed a colorimetric fiber mat based on 4-(2-pyridylazo)-1,3-benzenediol (PAR). The fiber mat responded with heavy metal ions, such as Hg^{2+} , Pb^{2+} , Cd^{2+} , Zn^{2+} , Ni^{2+} and Cu^{2+} with a color change from red-orange to dark-brown while light metals such as Ca^{2+} , Mg^{2+} and Al^{3+} did not create any color change. The color change of fiber mat was due to the coordinate of PAR with heavy metal ions. In addition, the colorimetric fiber showed good selectivity at different pH values.

Wang *et al.* (2011) [84] prepared the poly(methyl methacrylate-co-naphthalimide) fiber mat via electrospinning. The fluorescent fiber mat showed high sensitivity and selectivity toward Cu^{2+} over other metal ions in aqueous solution. The Cu^{2+} -naphthalimide complex exhibited a 48 nm blue-shift from 487 nm to 439 nm in fluorescence spectra.

Poltue *et al.* (2011) [10] demonstrated the electrospun dimethylglyoxime blended poly(caprolactone) fiber mat for nickel(II) ions sensing. The fiber mat turned from white to red in nickel solutions. Dimethylglyoxime (DMG) reacted with nickel(II) ions and formed a red complex of $\text{Ni}(\text{DMG})_2$.

Adeyemi *et al.* (2012) [85] developed a fluorescent nanofiber probe for the determination of Ni^{2+} via electrospinning of a covalently functionalized pyridylazo-2-naphthol-poly(acrylic acid) polymer. The Ni^{2+} quenched the fluorophore in a solid receptor-fluorophore. The fluorescent fiber mat switched off in the presence of Ni^{2+} .

Li *et al.* (2013) [86] designed a colorimetric sensor using nanogold probes immobilized on polyamide-6 membrane. Upon addition of lead(II) ions, the sensor was induced a pink to white color change. The ligand on nanogold was leached resulting in color change. The complexation between ligand and lead(II) ions occurred.

Ondigo *et al.* (2013) [87] reported the development of a colorimetric sensor for iron(II) ions sensing using 2-(2'-pyridyl) imidazole (PIMH) as a coloring agent. The poly(vinylbenzyl chloride) was spun and then the electrospun fiber mat was treated with the 2-(2'-pyridyl) imidazole (PIMH) for functionalization. When the fiber mat was used in the detection of iron(II) ions, the red-orange color appeared. PIMH-Fe^{2+} complexes were generated.

- **Sensing of gas**

Lv *et al.* (2010) [88] described a colorimetric and fluorescent nanofiber sensor which comprised of the synthesis between porphyrin moieties as fluorescence coloring agent and polyimide as polymer backbone. The electrospun porphyrinated polyimide nanofiber mat could rapidly detect hydrogen chloride gas via protonation process. The structure of porphyrin changed from planar to saddle. It showed the color change from red to fluorescent green after exposing to hydrogen chloride gas.

Wang *et al.* (2012) [11] developed a simple and highly sensitive colorimetric nanofiber mat for real-time formaldehyde gas sensing based on methyl yellow-impregnated nylon 6 membrane. The sensor altered color from yellow to red when it was exposed to formaldehyde. Methyl yellow as coloring agent was reacted with formaldehyde using sulfuric acid as catalyst.

- *Sensing of pH and others*

Schueren *et al.* (2010) [89] developed a nanofibrous pH-sensor by electrospinning with incorporated pH-indicator dyes. The pH-indicator addition had no influence on the average fiber diameter. Moreover, the fiber mat showed a clear color change with a change in pH.

In summary, the electrospinning can produce a colorimetric sensor using various coloring agents. This work aimed to prepare a simple zein blending with coloring agents fiber mat by the electrospinning and followed by crosslinking reaction using citric acid as a non-toxic crosslinker for ions sensing. Zein as a supporting natural polymer was used. Curcumin, difluoroboron curcumin ($\text{BF}_2\text{-CurOH}$) and 3,5-di(4-ethynyl-*N,N*-dimethylanily)-2-hydroxybenzaldehyde (F_3) as the coloring agents were selected as coloring agents. Nowadays, there is no report on the fabrication of zein blending with coloring agents for ions sensing.

CHAPTER III

EXPERIMENTAL SECTIONS

3.1 Apparatus

The used apparatus were listed in Table 3.1.

Table 3.1 Apparatus list

Apparatus	Model (company)
Analytical balance	SI-234 (Mettler-Toledo Ltd.)
Attenuated total reflection fourier transform infrared spectrometer (ATR-FT-IR)	Nicolet 6700 (Thermo Scientific)
Camera	DSC-WX100 (SONY)
Cover glasses	22x22 mm (Menzel-Glaser)
Diffuse reflectance ultraviolet – visible spectrophotometer (DR-UV-Vis)	UV-2500PC (Shimadzu)
High voltage power supply	EQ-30P1-L (230V) (Matsusada Precision Inc.)
Inductively coupled plasma-optical emission spectrometer (ICP-OES)	iCAP 6000 series (Thermo Scientific)
Nuclear magnetic resonance spectrometer (NMR)	Mercury Plus 400 (Varian)
Oven	UM500 (Mettmert)
pH meter	Seven Compact (Mettler Toledo)
Scanning electron microscope (SEM)	JSM-5410 LV (JEOL)
Syringe pump	NE-1000 (Prosense B.V.)

3.2 Chemicals

All chemicals were analytical reagent grade. The used chemicals were listed in Table 3.2.

Table 3.2 Chemical list

Chemical	Suppliers
Ammonium iron(II) sulfate hexahydrate	Merck
Ammonia solution (25%)	Merck
Ammonium iron(III) sulfate dodecahydrate	J.T. baker
Citric acid	Sigma-Aldrich
Curcumin	Thai-China Flavors & Fragrances Industry Co., Ltd.
Ethanol (absolute)	Merck
Metal standard solutions (1000 mg/L) of Ag, As, Cr, Cu, Fe, Hg, Ni and Pb	Merck
Metal standard solutions (1000 mg/L) of Co	BDH
Metal standard solutions (1000 mg/L) of Mn	Fisher scientific
Nitric acid (65%)	Merck
Sodium hydroxide (pellets)	Merck
Sodium tetraborate decahydrate	Merck
Zein (Z3625)	Sigma-Aldrich

3.2.1 Preparation of solution

All chemicals were used without purification. Deionized (DI) water was selected as the solvent.

Fe^{2+} stock solution

Fe^{2+} solution (1 M, 10 mL) was prepared by dissolving 3.9214 g of ammonium iron(II) sulfate hexahydrate ($(\text{NH}_4)_2\text{Fe}(\text{SO}_4)_2 \cdot 6\text{H}_2\text{O}$, MW = 392.14, Merck) in DI water.

Fe^{3+} stock solution

Fe^{3+} solution (10,000 mg/L, 10 mL) was prepared by dissolving 0.8635 g of ammonium iron(III) sulfate dodecahydrate ($(\text{NH}_4)_2\text{Fe}(\text{SO}_4)_2 \cdot 12\text{H}_2\text{O}$, MW = 482.20, J.T. Baker) in DI water.

Na^+ stock solution

Na^+ solution (1 M, 10 mL) was prepared by dissolving 0.8500 g of sodium nitrate (NaNO_3 , MW = 85.00, Fluka) in DI water.

K^+ stock solution

K^+ solution (1 M, 10 mL) was prepared by dissolving 1.011 g of potassium nitrate (KNO_3 , MW = 101.10, BDH) in DI water.

Ca^{2+} stock solution

Ca^{2+} solution (1 M, 10 mL) was prepared by dissolving 1.1098 g of calcium chloride (CaCl_2 , MW = 111.00, Merck) in DI water.

Ba²⁺ stock solution

Ba²⁺ solution (1 M, 10 mL) was prepared by dissolving 2.4428 g of barium chloride dihydrate (BaCl₂·2H₂O, MW = 244.28, Merck) in DI water.

Mg²⁺ stock solution

Mg²⁺ solution (1 M, 10 mL) was prepared by dissolving 1.3121 g of magnesium chloride dihydrate (MgCl₂·2H₂O, MW = 131.21, Merck) in DI water

B₄O₇²⁻ stock solution

B₄O₇²⁻ solution (1,000 mg/L, 25 mL) was prepared by dissolving 61.36 mg of sodium tetraborate decahydrate (Na₂B₄O₇·10H₂O, MW = 381.37, Merck) in DI water.

Sodium hydroxide solution

Sodium hydroxide solution (1 M, 50 mL) was prepared by dissolving 2.0000 g of sodium hydroxide (NaOH, MW = 40.00, Merck) in DI water.

All the required concentrations of solution were prepared by dilution of its stock solution.

3.3 Synthesis of Coloring Agents

3.3.1 Synthesis of Difluoroboron Curcumin (BF₂-CurOH)

Difluoroboron curcumin (BF₂-CurOH) was synthesized in methanol. The method was applied from Chaicharm *et al* [4, 90].

Curcumin (2.947 g) and borontrifluoride diethyl etherate (1.02 mL) were added to a two-necked round bottom flask containing and refluxed at 60 °C for 2 hours under nitrogen atmosphere. The reaction was stopped by cooling down at room temperature. The solvent was removed using a rotary evaporator. The red powder was purified via recrystallization using methanol/ethyl acetate (1:3) as solvent. The desired product was dried at room temperature and stored in a desiccator.

3.3.2 Synthesis of 3,5-di(4-ethynyl-*N,N*-dimethylanily)-2-hydroxybenzaldehyde (F₃)

3,5-di(4-ethynyl-*N,N*-dimethylanily)-2-hydroxybenzaldehyde (F₃) was provided by Organic Synthesis Research Unit (OSRU), Department of Chemistry, Faculty of Science, Chulalongkorn University. The method was described from Khumsri *et al* [91] and Niamnont *et al* [5].

Briefly, Iodine (24.90 g) and pyridine (20 mL) were added to a two-necked round bottom flask containing 20 mL of dioxane and stirred at 0 °C for 15 min. Then, 2-hydroxybenzaldehyde (3.00 g) was added in the solution. The reaction was reacted at reflux for 4 hours. The solvent was removed by a rotary evaporator. Sodium thiosulfate (20%wt/v) was added drop-wise on residual oil until it was turned light yellow. The mixture was purified by extraction with dichlorometane and washed with water. The water was removed using anhydrous magnesium sulfate. 2-Hydroxy-3,5-diiodobenzaldehyde was obtained via evaporation. Next, 2-hydroxy-3,5-diiodobenzaldehyde (0.93 g), bis(triphenylphosphine) palladium(II) dichloride (PdCl₂(PPh₃)₂) (132 mg), copper(I) iodide (36 mg) and triphenylphosphine (51 mg) were dissolved and mixed in the two-necked round bottom flask containing 10 mL

tetrahydrofuran. Then, triethylamine (10 mL) was added and followed by 4-ethynyl-*N,N*-dimethylaniline (0.49 g). The mixture solution was stirred at room temperature for 4 hours. The solid precipitate in the mixture solution was separated by filtration and then washed with dichloromethane. The desired product was conducted through a silica gel column using gradient solvents (pure hexane to dichloromethane/hexane (3:1)). The dried product was stored in a desiccator.

3.4 Characterization of Coloring Agents

Curcumin, difluoroboron curcumin (BF₂-CurOH) and 3,5-di(4-ethynyl-*N,N*-dimethylanily)-2-hydroxybenzaldehyde (F₃) as coloring agents were characterized by Fourier transform infrared spectrometer (FT-IR) and nuclear magnetic resonance spectrometer (NMR).

3.4.1 Fourier Transform Infrared Spectrometer (FT-IR)

FT-IR was used to identify the functional groups of the coloring agents. The FT-IR spectra were recorded in a wavenumber range of 400-4,000 cm⁻¹ with 32 scans at wavenumber resolution of ±4 cm⁻¹ using the attenuated total reflectance (ATR) mode.

3.4.2 Nuclear Magnetic Resonance Spectrometer (NMR)

NMR was used to confirm the structure of coloring agents. ¹H-NMR spectra were recorded in the chemical shift of 0-14 ppm with repetitions of 8 using deuterated solvents. DMSO-d₆ was used as the solvent for curcumin and difluoroboron curcumin (BF₂-CurOH). CDCl₃ was used as the solvent for 3,5-di(4-ethynyl-*N,N*-dimethylanily)-2-hydroxybenzaldehyde (F₃).

3.5 Preliminary Study of the Amount Coloring Agent on Zein Fiber Mats for Analysis of Ions

Firstly, the zein containing curcumin fiber mats were prepared by electrospinning and heat-induced amide crosslinking reaction using citric acid as crosslinker. The preparation method was adapted from Jiang *et al* [9]. and Reddy *et al* [92]. The weight ratios of curcumin/zein were varied from 0-15%wt/wt (curcumin/zein). Then, the fiber mats were examined in different concentrations (0-10 mg/L) of Fe^{3+} solution. The suitable curcumin-loaded zein fiber mat was investigated by eyes. It could be obviously distinguished from the intensity of color change in different concentrations of Fe^{3+} solution.

Exhaustively, the mixture solution was prepared by adding zein (1.0400 g) and citric acid (0.0936 g) in a tube containing 70% aqueous ethanol (2 mL). The pH of solution was adjusted to 4.9 by sodium hydroxide (0.125 g/mL in 70% aqueous ethanol). Next, the tube was sealed using parafilm and stored at room temperature for 48 hours. Then, curcumin (0, 7.28, 10.4, 31.2, 52.0, 72.8, 104.0, and 156.0 mg) was added into the solution. The total volume of solution was adjusted at 4 mL with 70% aqueous ethanol and shaken using an ultrasonic bath for 15 min. After that, the homogeneous solution was loaded in a 3 mL syringe. The syringe was put onto a syringe pump. The condition for fabrication of fiber mat was the applied voltage at 19.5 kV and the distance between the needle and the collector at 20 cm using the flow rate of 2 mL/hr. The fiber mat was collected on an aluminum foil covered collector. Next, the fiber mat was put in an oven at 150°C for 2.5 hours to allow the crosslinking reaction. After that, the fiber mat was cut into circle with diameter of 0.8 cm and weight in the range of 1.5-2.5 mg and used for sensing. After that, the sensing characteristics of the fiber mats were investigated by immersing the obtained fiber mats into the different concentrations (0, 1, 2, 3, 4, 5, 6, 7, 8, 9 and 10 mg/L) of Fe^{3+} solution in the pH of 2 at room temperature for 3 hours. The color changes of fiber mats were observed by naked-eye.

The amounts of difluoroboron curcumin (BF₂-CurOH) and 3,5-di(4-ethynyl-*N,N*-dimethylanily)-2-hydroxybenzaldehyde (F₃) loaded in zein fiber mat were firstly selected similarly with the amount of curcumin loaded in zein fiber mat.

3.6 Preparation of Zein Blending with Coloring Agents Fiber Mats

The preparation of suitable coloring agent loaded zein fiber mats were similar to the methodology described in section 3.5. Zein blending with curcumin fiber mat, zein blending with difluoroboron curcumin (BF₂-CurOH) fiber mat and zein blending with 3,5-di(4-ethynyl-*N,N*-dimethylanily)-2-hydroxybenzaldehyde (F₃) fiber mat were prepared by electrospinning and crosslinking reaction at 150 °C adapted the method described by Jiang *et al* [9] and Reddy *et al* [92].

3.6.1 Preparation of Zein Blending with Curcumin Fiber Mat

Briefly, zein (1.0400 g) and citric acid (0.0936 g) were added in a tube containing 70% aqueous ethanol (2 mL). The pH of solution was adjusted to 4.9 by sodium hydroxide (0.125 g/mL in 70% aqueous ethanol). Then, the tube was sealed using parafilm and stored at room temperature for 48 hours. Next, the curcumin (52.0 mg, 5%wt/wt (curcumin/zein)) was loaded into the solution. The total volume of solution was adjusted at 4 mL with 70% aqueous ethanol and shake using an ultrasonic bath for 15 min. Then, the homogeneous solution was loaded in a 3 mL syringe. The syringe was put onto a syringe pump. The condition for fabrication of fiber mat was the applied voltage at 19.5 kV and the distance between the needle and the collector at 20 cm using the flow rate 2 mL/hr. The fiber mat was collected on an aluminum foil covered collector. The fiber mat was put in an oven at 150 °C for 2.5 hours. After that, the fiber mat was cut into circle with diameter of 0.8 cm and weight in the range of 1.5-2.5 mg and used for all experiments.

3.6.2 Preparation of Zein Blending with Difluoroboron Curcumin (BF₂-CurOH) Fiber Mat

Concisely, the mixture was prepared by adding zein (1.0400 g) and citric acid (0.0936 g) in a tube containing 70% aqueous ethanol (2 mL). Next, the pH of solution was adjusted to 4.9 by sodium hydroxide (0.125 g/mL in 70% aqueous ethanol). The tube was sealed using parafilm and stored at room temperature for 48 hours. Then, difluoroboron curcumin (BF₂-CurOH) (2.60 mg, 0.25%wt/wt (curcumin/zein)) was loaded into the solution. The total volume of solution was adjusted at 4 mL with 70% aqueous ethanol and shake using an ultrasonic bath for 15 min. After that, the homogeneous solution was loaded in a 3 mL syringe. The syringe was put onto a syringe pump. The condition for fabrication of fiber mat was the applied voltage at 19.5 kV and the distance between the needle and the collector at 20 cm using the flow rate 2 mL/hr. The fiber mat was collected on an aluminum foil covered collector. The fiber mat was put in an oven at 150 °C for 2.5. After that, the fiber mat was cut into circle with diameter of 0.8 cm and weight in the range of 1.5-2.5 mg and used for all experiments.

3.6.3 Preparation of Zein Blending with 3,5-di(4-ethynyl-*N,N*-dimethylanily)-2-hydroxybenzaldehyde (F₃) Fiber Mat

Shortly, zein (1.0400 g) and citric acid (0.0936 g) were added in a tube containing 70% aqueous ethanol (2 mL). The pH of solution was adjusted to 4.9 by sodium hydroxide (0.125 g/mL in 70% aqueous ethanol). The tube was sealed using parafilm and stored at room temperature for 48 hours. After that, 3,5-di(4-ethynyl-*N,N*-dimethylanily)-2-hydroxybenzaldehyde (F₃) (1.04 mg, 0.1%wt/wt (curcumin/zein)) was added into the solution. The total volume of solution was adjusted at 4 mL with 70% aqueous ethanol and shake using an ultrasonic bath for 15 min. The homogeneous solution was loaded in a 3 mL syringe. The syringe was put onto a syringe pump. The condition for fabrication of fiber mat was the applied voltage at 19.5 kV and the distance between the needle and the collector at 20 cm using the

flow rate 2 mL/hr. The fiber mat was collected on an aluminum foil covered collector. Next, the fiber mat was put in an oven at 150 °C for 2.5 hours. After that, the fiber mat was cut into circle with diameter of 0.8 cm and weight in the range of 1.5-2.5 mg and used for all experiments.

3.7 Fiber Mats Characterization

The electrospun fiber mats were characterized by Fourier transform infrared spectrometry (FT-IR), diffuse reflectance ultraviolet-visible spectrophotometry (DRUV-Vis) and scanning electron microscopy (SEM).

3.7.1 Fourier Transform Infrared Spectrometer (FT-IR)

FT-IR was used to identify the functional groups of the electrospun fiber mats. ATIR-FT-IR spectra were recorded by using the procedure previously in the section 3.4.1.

3.7.2 Diffuse Reflectance Ultraviolet-visible Spectrophotometer (DR-UV-Vis)

DR-UV-Vis was used to investigate the diffuse reflectance of the electrospun fiber mats. The diffuse reflectance ultraviolet visible spectra were recorded in a wavenumber range of 200 – 800 cm⁻¹ by using barium sulfate as background substrate. The spectra were plotted between F(R) (Kubelka-Munk function) and wavelength (nm). The F(R) was calculated from the following equation [93].

$$F(R) = \frac{(1-R)^2}{2R}$$

When F(R) = Kubelka-Munk function

R = Reflectance of sample

3.7.3 Scanning Electron Microscope (SEM)

SEM was used to determine the morphology and the fiber diameter of the electrospun fiber mat. The sample was coated with gold. The SEM image was recorded with the accelerated voltage of 15 kV. The magnification at 5,000 was used for the measurement of a diameter of fiber. The average diameter and its standard deviation (n=30) of fibers were evaluated by Sem Afore program.

3.8 Fiber Mat Sensing Ability

The electrospun coloring agents-loaded zein fiber mats were tested for sensing of selected analytes by naked eye in triplicate. The fiber mat was immersed in 1 mL of sample solution for 3 hours. Then, the fiber mat was taken out. The free water at the surface of fiber mat was removed by filter paper and the fiber mat was photographed. For the difluoroboron curcumin (BF₂-CurOH) fiber mat, the photograph was taken under 20W black light lamp. Then, the picture at a test zone was analyzed using image J software in gray mode. The mean gray value and its standard deviation (n=3) was evaluated.

3.8.1 Influence of pH

For the curcumin-loaded zein fiber mat, 1 and 10 mg/L Fe³⁺ solutions in the pH range of 1-5 were examined. DI water in the pH range of 1-5 as the control solution were evaluated.

For the difluoroboron curcumin (BF₂-CurOH)-loaded zein fiber mat, 100 mg/L B₄O₇²⁻ solutions in the pH range of 7-10 were tested. DI water in the pH range of 7-10 as the control solution were investigated.

For the 3,5-di(4-ethynyl-*N,N*-dimethylanily)-2-hydroxybenzaldehyde (F₃)-loaded zein fiber mat, 10 and 100 mg/L Fe³⁺ solutions in the pH range of 1-5 were investigated. DI water in the pH range of 1-5 as the control solution were examined.

3.8.2 Effect of Interferences

The interferences of 17 metal ions (Ag^+ , As^{5+} , Ba^{2+} , Ca^{2+} , Cd^{2+} , Co^{2+} , Cr^{3+} , Cu^{2+} , Fe^{2+} , Hg^{2+} , K^+ , Mn^{2+} , Na^+ , Ni^{2+} , Pb^{2+} , Zn^{2+} and Mg^{2+} (200 μM)) were examined under the optimal pH from the experiment described in section 3.8.1.

3.8.3 Limit of Detection (LOD) and Method Validation

LOD is defined as the lowest concentration of analyte which produces the minimum intensity of color change of fiber mat. It can be visually differentiated by the naked eye.

For the curcumin-loaded zein fiber mat, the different concentrations (0.1, 0.2, 0.3, 0.4, 0.5, 1.0 and 5.0 mg/L) of Fe^{3+} solutions were investigated. In addition, curcumin-loaded zein fiber mat was examined for qualitative (yes/no response) and quantitative testing [94]. The series concentrations (0.1, 0.2, 0.3, 0.4, 0.5, 1.0 and 5.0 mg/L) of Fe^{3+} solutions were investigated as assay of 1 and 2. The DI water as assay of 1-14 was used for acting as iron-free solution.

For the 3,5-di(4-ethynyl-*N,N*-dimethylanily)-2-hydroxybenzaldehyde (F_3)-loaded zein fiber mat, the different concentrations (0.3, 0.6, 0.9, 1, 3, 8, 10, 20, 30, 40, 50, 60, 70, 80, 90, 100, 200, 300, 400 and 500 mg/L) of Fe^{3+} solutions were tested.

3.9 Applications

For the assessment of the developed fiber mats sensing, the real samples were applied. All real samples were filtrated by 0.45 μm cellulose membrane and preserved with nitric acid at pH 2 and kept in polypropylene bottles.

3.9.1 Curcumin Fiber Mat for the Determination of Iron(III) Ions

Bottled drinking waters (I, II and mineral), tap water and Chulalongkorn University pond water as real samples were used. 100 μL of 50, 100 and 500 mg/L Fe^{3+} solution were spiked in real water samples in a 10 mL volumetric flask. All of the real samples were tested using curcumin-loaded zein fiber mat. The concentration of Fe^{3+} solutions in real samples were evaluated using the inductively coupled plasma-optical emission spectrometer (ICP-OES). The ICP-OES operating conditions for Fe evaluation are shown in Table 3.3

Table 3.3 The ICP-OES operating conditions for Fe evaluation

Operating conditions	
Fe emission wavelength	259.9 nm
RF power	1150 W
Analysis pump rate	50 rpm
Auxiliary gas flow	0.5 L/min
Nebulizer gas flow	0.6 L/min
Coolant gas flow	12 L/min

The Fe^{3+} standard solution in the concentration 0, 2, 4, 6, 8 and 10 mg/L were used as a calibration standard for ICP-OES.

3.9.2 Difluoroboron Curcumin (BF₂-CurOH) Fiber Mat for Ammonia

Sensing

The concentrated ammonia solution (13.4 mol/L) was dropped with the volume of 20, 50 and 100 μL using a micropipette in a closed bottle (volume size = $7.96 \times 10^{-6} \text{ m}^3$; diameter = 1.5 cm, height = 4.5 cm). The BF₂-CurOH-loaded zein fiber mat was hung above ammonia solution. After that, the bottle was put in boiling water bath for 30 min. The ammonia solution was completely evaporated. The fiber mat was taken out and photographed immediately. 20 μL of DI water was also used as a control for sensing application.

3.9.3 3,5-di(4-ethynyl-*N,N*-dimethylanily)-2-hydroxybenzaldehyde (F₃)

Fiber Mat for the Determination of Iron (III) Ions

Tap water, Chulalongkorn University pond water and ground water as real samples were used. 100 μL of 3,000 and 7,000 mg/L Fe³⁺ solutions were spiked in real water samples in a 10 mL volumetric flask. All of the real samples were tested using F₃-loaded zein fiber mat. The concentrations of Fe³⁺ in real samples were examined using inductively coupled plasma-optical emission spectrometry (ICP-OES). The ICP-OES operating conditions for Fe measurement are described in section 3.9.1. The Fe³⁺ standard solution in the concentration 0, 2, 4, 6, 8, 10, 20, 30, 40, 50, 60, 70, 80, 90 and 100 mg/L were used for a calibration of ICP-OES.

3.10 Preparation of Film Sensing for Comparison with Fiber Mat

For a comparison of fiber mat and film sensing efficiency, the zein blending with curcumin film was prepared by hand casting and heat-induced amide crosslinking reaction using citric acid as crosslinker. The method was adapted from Bualom *et al* [95], Jiang *et al* [9] and Reddy *et al* [92].

Briefly, the mixture solution was prepared by adding zein (1.0400 g) and citric acid (0.0936 g) in a tube containing 70% aqueous ethanol (2 mL). The pH of solution was adjusted to 4.9 by sodium hydroxide (0.125 g/mL in 70% aqueous ethanol). The tube was sealed using parafilm and stored at room temperature for 48 hours. After that, the curcumin (52.0 mg, 5%wt/wt (curcumin/zein)) was added into the solution. The total volume of solution was adjusted at 4 mL with 70% aqueous ethanol and shake using ultrasonic bath for 15 min. Next, the cover glass was cleaned using ethanol and acetone. Then, 30 μ L of the homogeneous solution was pipetted onto clean cover glass and casted by hand. Finally, the cast film was put in an oven at 150 °C for 2.5 hours to allow the crosslinking reaction. Curcumin-loaded zein film containing 5%wt/wt (curcumin/zein) was obtained and used for Fe³⁺ sensing. In addition, the morphology of film was investigated by scanning electron microscope (SEM). The SEM image was recorded using the same procedure described in section 3.7.3.

For fiber mat, the curcumin-loaded zein fiber mat containing 5%wt/wt (curcumin/zein) was prepared by electrospinning followed the method described in section 3.6.1.

For the assessment of the efficiency sensing, fiber mat and film were immersed in 3 mL 10 mg/L of Fe³⁺ solution at pH 2 for 3 hours. After that, the fiber mat and film were taken out. The free water at the surface was removed by a filter paper and the sensors were photographed.

CHAPTER IV

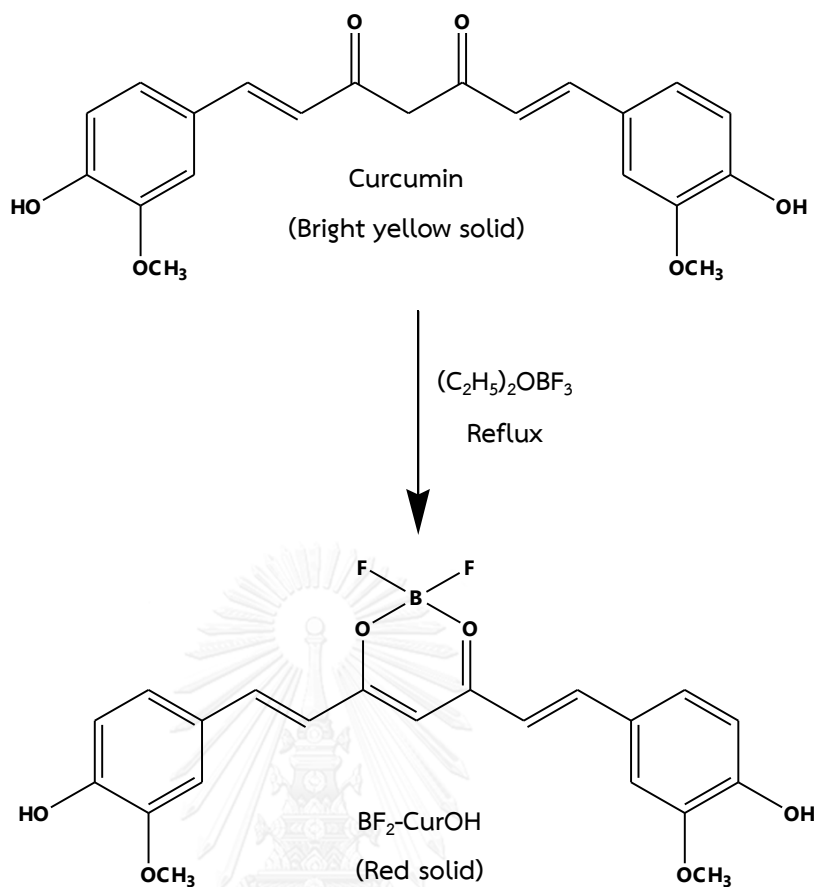
RESULTS AND DISCUSSION

Zein blended with coloring agents (curcumin, difluoroboron curcumin ($\text{BF}_2\text{-CurOH}$) and 3,5-di(4-ethynyl-*N,N*-dimethylanily)-2-hydroxybenzaldehyde (F_3)) fiber mats were prepared by electrospinning. The curcumin-loaded zein fiber mat for iron(III) ions sensing, the $\text{BF}_2\text{-CurOH}$ -loaded zein fiber mat for ammonia sensing and the F_3 -loaded zein fiber mat for iron(III) ions sensing were examined using the naked-eye. This work consists of seven parts including (1) synthesis of coloring agents, (2) characterization of coloring agents, (3) preliminary study of the amount of coloring agent on zein fiber mats for analysis of ions, (4) electrospun zein blending with curcumin fiber mats, (5) electrospun zein blending with difluoroboron curcumin ($\text{BF}_2\text{-CurOH}$), (6) electrospun zein blending with 3,5-di(4-ethynyl-*N,N*-dimethylanily)-2-hydroxybenzaldehyde (F_3) and (7) comparison of fiber mat and film sensing efficiency.

4.1 Synthesis of Coloring Agents

4.1.1 Synthesis of Difluoroboron Curcumin ($\text{BF}_2\text{-CurOH}$)

Difluoroboron curcumin ($\text{BF}_2\text{-CurOH}$) was synthesized from yellow powder of curcumin. Curcumin was modified with borontrifluoride diethyl etherate ($(\text{C}_2\text{H}_5)_2\text{OBF}_3$). The red powder of $\text{BF}_2\text{-CurOH}$ was obtained in 61% yield. The synthesis of difluoroboron curcumin ($\text{BF}_2\text{-CurOH}$) was illustrated in Scheme 4.1.

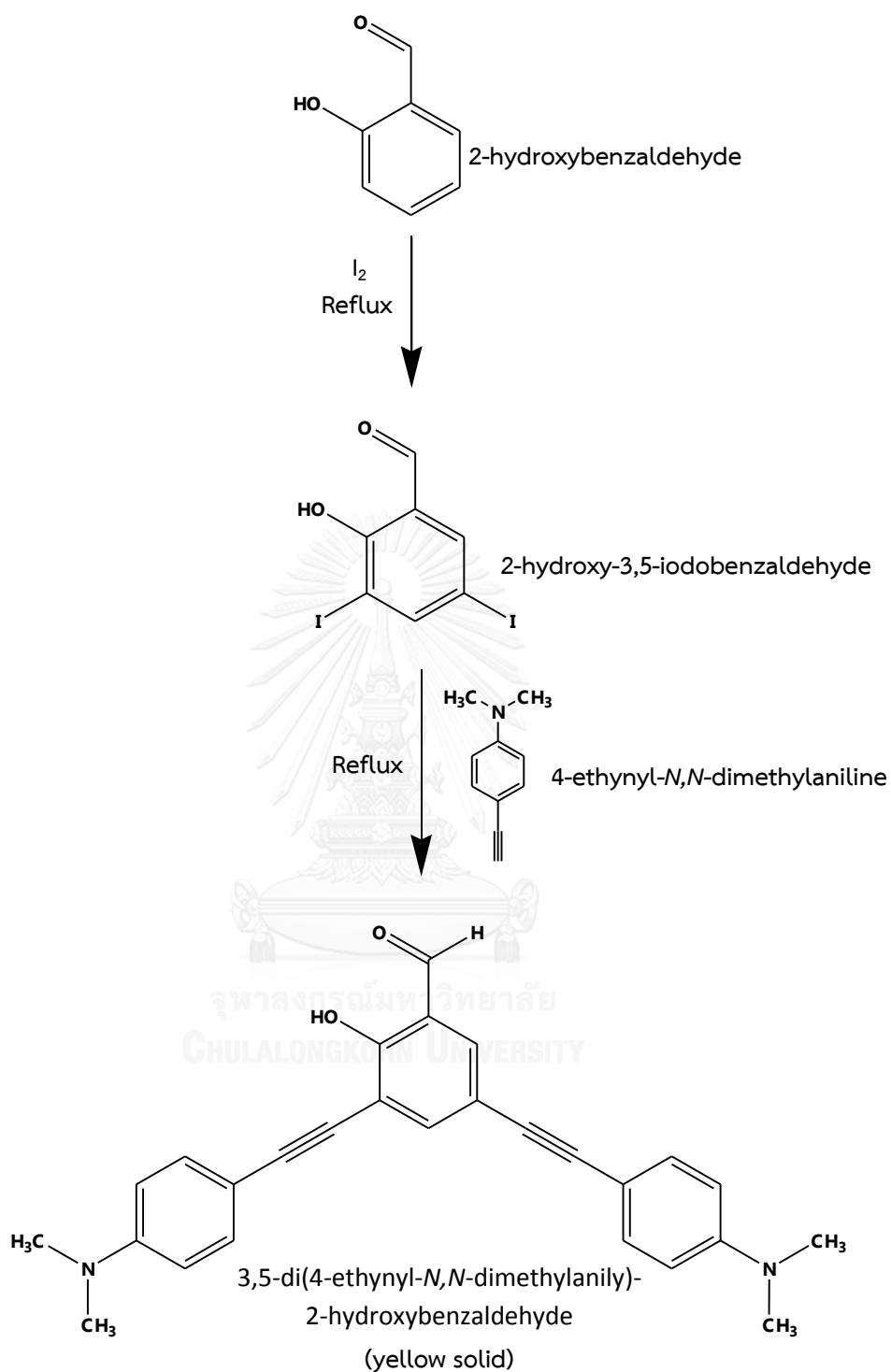


Scheme 4.1 Synthesis of difluoroboron curcumin ($\text{BF}_2\text{-CurOH}$) [4, 90]

4.1.2 Synthesis of 3,5-di(4-ethynyl-*N,N*-dimethylanily)-2-hydroxybenzaldehyde (F_3)

The green powder of 3,5-di(4-ethynyl-*N,N*-dimethylanily)-2-hydroxybenzaldehyde (F_3) was provided by Organic Synthesis Research Unit (OSRU), Chulalongkorn University. The result was described from Khumsri *et al* [91] and Niamnont *et al* [5].

Briefly, 3,5-di(4-ethynyl-*N,N*-dimethylanily)-2-hydroxybenzaldehyde (F_3) was synthesized from 2-hydroxybenzaldehyde. 2-Hydroxybenzaldehyde was doubly iodinated and doubly coupled with 4-ethynyl-*N,N*-dimethylaniline. The yellow powder of F_3 was obtained in 41% yield. The synthesis of 3,5-di(4-ethynyl-*N,N*-dimethylanily)-2-hydroxybenzaldehyde (F_3) was illustrated in Scheme 4.2.



Scheme 4.2 The synthesis of 3,5-di(4-ethynyl-*N,N*-dimethylanily)-2-hydroxybenzaldehyde (F_3) [5, 91]

4.2 Characterization of Coloring Agents

All coloring agents (curcumin, difluoroboron curcumin ($\text{BF}_2\text{-CurOH}$) and 3,5-di(4-ethynyl-*N,N*-dimethylanily)-2-hydroxylbenzaldehyde (F_3)) were characterized by Fourier transform infrared spectroscopy (FT-IR) and nuclear magnetic resonance spectroscopy (NMR).

4.2.1 Curcumin

4.2.1.1 Fourier Transform Infrared Spectroscopy (FT-IR)

The curcumin was characterized by FT-IR. The IR spectrum of curcumin was shown in Figure 4.1. The characteristic bands of curcumin were observed at $1022 \text{ (s)} \text{ cm}^{-1}$ assigned to C-O stretching band of ether, $1503 \text{ (s)} \text{ cm}^{-1}$ assigned to C-H stretching band of alkane, $1600 \text{ (m)} \text{ cm}^{-1}$ assigned to C=C stretching band of alkene, $1623 \text{ (m)} \text{ cm}^{-1}$ assigned to C=O stretching band of carbonyl group and $3304 \text{ (m, broad)} \text{ cm}^{-1}$ assigned to O-H stretching band of hydroxyl group. This accorded with the results described by Zebib *et al* [96] and Kim *et al* [97].



Figure 4.1 FT-IR spectrum of curcumin

4.2.1.2 Nuclear Magnetic Resonance Spectroscopy (NMR)

Curcumin was characterized by $^1\text{H-NMR}$. The NMR spectrum of curcumin in $\text{DMSO-}d_6$ was shown in Figure 4.2. $^1\text{H-NMR}$ signals (400 MHz, $\text{DMSO-}d_6$) of curcumin were observed at 9.71 ppm (s, 2H) of hydroxyl group, 7.54 ppm ($J = 16.0$ Hz, d, 2H) of aromatic group, 7.32 ppm (s, 2H) of aromatic group, 7.16 ppm ($J = 12.0$ Hz, d, 2H) of aromatic group, 6.82 ppm ($J = 8.0$ Hz, d, 2H) of alkene group, 6.75 ppm ($J = 16.0$ Hz, d, 2H) of alkene group, 6.07 ppm (s, 2H) of alkane group and 3.84 ppm (s, 6H) of methoxy group. This matched with the results described by Suwantong *et al* [98].

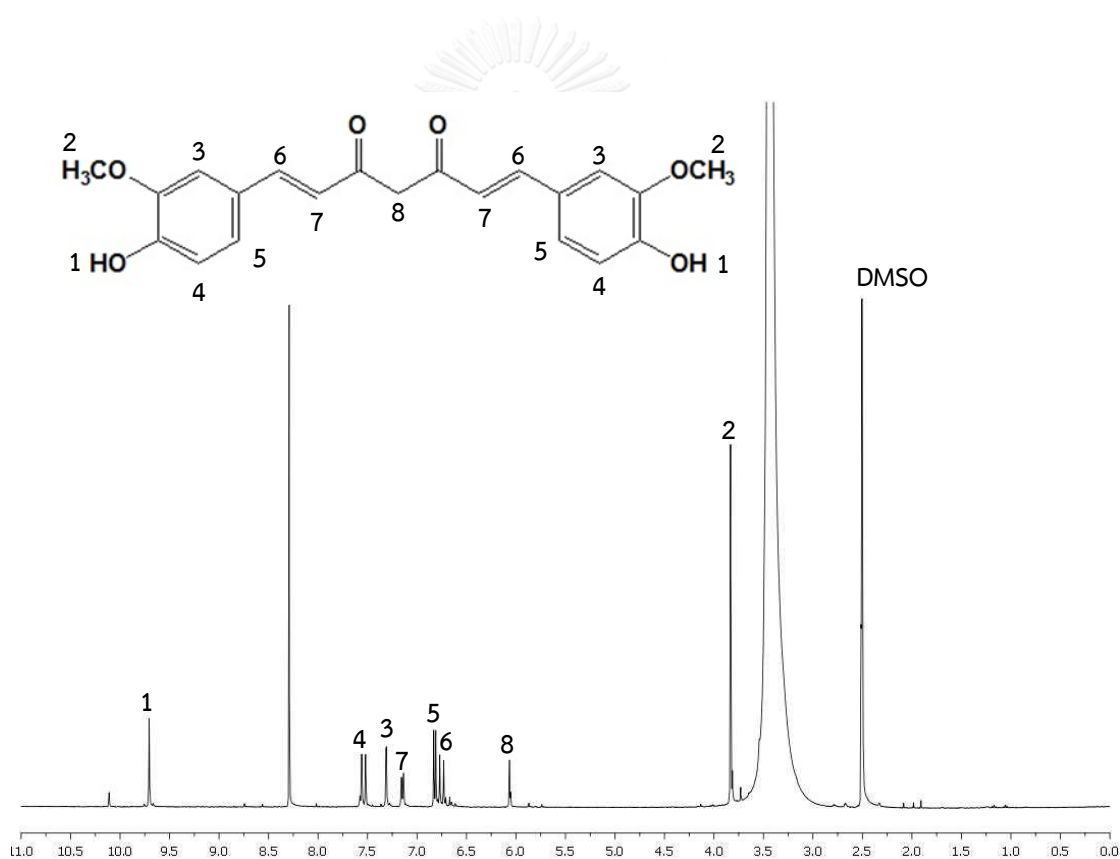


Figure 4.2 $^1\text{H-NMR}$ spectrum of curcumin in $\text{DMSO-}d_6$

4.2.2 Difluoroboron Curcumin (BF₂-CurOH)

4.2.2.1 Fourier Transform Infrared Spectroscopy (FT-IR)

The difluoroboron curcumin (BF₂-CurOH) was characterized by FT-IR. The IR spectrum of BF₂-CurOH was shown in Figure 4.3. The absorption bands of curcumin and borondifluoride units were found. For the curcumin unit, the characteristic bands of BF₂-CurOH were observed at 1062 (s) cm⁻¹ for C-O stretching of ether, 1496 (s) cm⁻¹ for C-H stretching of alkane, 1584 (m) cm⁻¹ for C=C stretching band of alkene, 1609 (m) cm⁻¹ for C=O stretching of carbonyl group and 3483 (m, broad) cm⁻¹ for O-H stretching of hydroxyl group. For borondifluoride unit, the characteristic bands of BF₂-CurOH were observed at 1386 (m) cm⁻¹ for B-O stretching of borate group. Gao *et al* [99] reported that the IR absorption band of borate linkage (B-O) appeared at 1350 cm⁻¹. Moreover, FT-IR spectrum of BF₂-CurOH presented a new peak of borate group at 1386 cm⁻¹ when comparison with IR spectrum of curcumin (Figure 4.1).

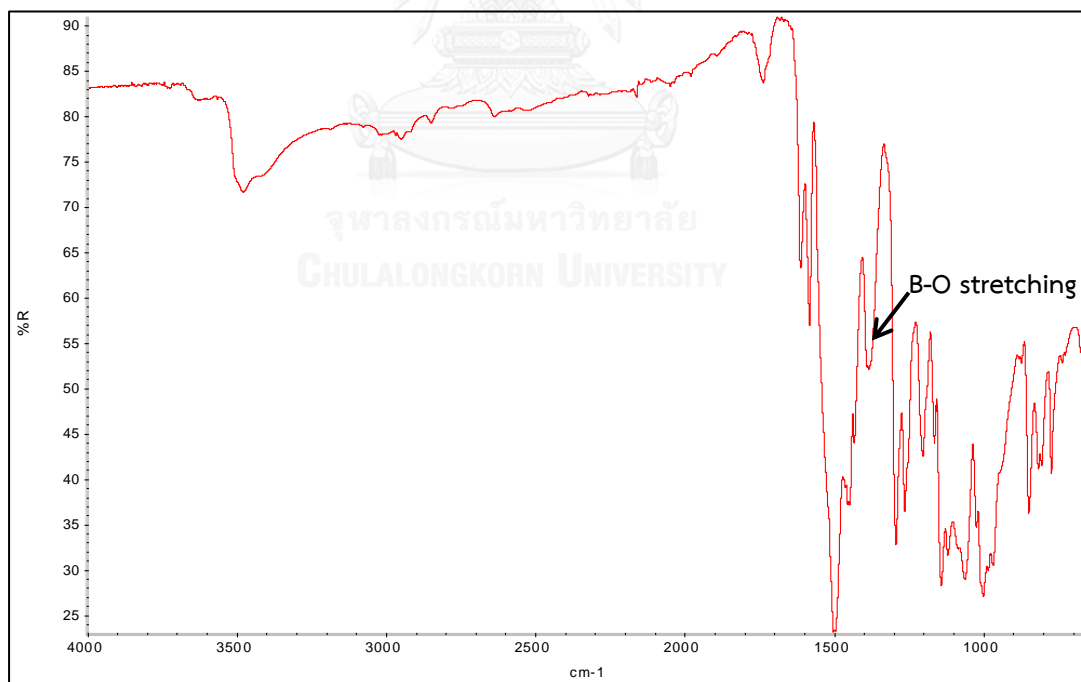


Figure 4.3 FT-IR spectrum of difluoroboron curcumin (BF₂-CurOH)

4.2.2.2 Nuclear Magnetic Resonance Spectroscopy (NMR)

The difluoroboron curcumin ($\text{BF}_2\text{-CurOH}$) was characterized by $^1\text{H-NMR}$. The NMR spectrum of $\text{BF}_2\text{-CurOH}$ in $\text{DMSO-}d_6$ was shown in Figure 4.4. $^1\text{H-NMR}$ signals (400 MHz, $\text{DMSO-}d_6$) of $\text{BF}_2\text{-CurOH}$ were observed at 10.15 ppm (s, 2H) of hydroxyl group, 7.91 ppm ($J = 16.0$ Hz, d, 2H) of aromatic group, 7.46 ppm (s, 2H) of aromatic group, 7.34 ppm ($J = 8.0$ Hz, d, 2H) of aromatic group, 7.01 ppm ($J = 16.0$ Hz, d, 2H) of alkene group, 6.88 ppm ($J = 8.0$ Hz, d, 2H) of alkene group, 6.46 ppm (s, 2H) of alkane group and 3.85 ppm (s, 6H) of methoxy group. When compared $^1\text{H-NMR}$ spectrum of $\text{BF}_2\text{-CurOH}$ and curcumin, $^1\text{H-NMR}$ signals of $\text{BF}_2\text{-CurOH}$ showed the downfield shift because borondifluoride unit was an electron withdrawing group [4, 90].

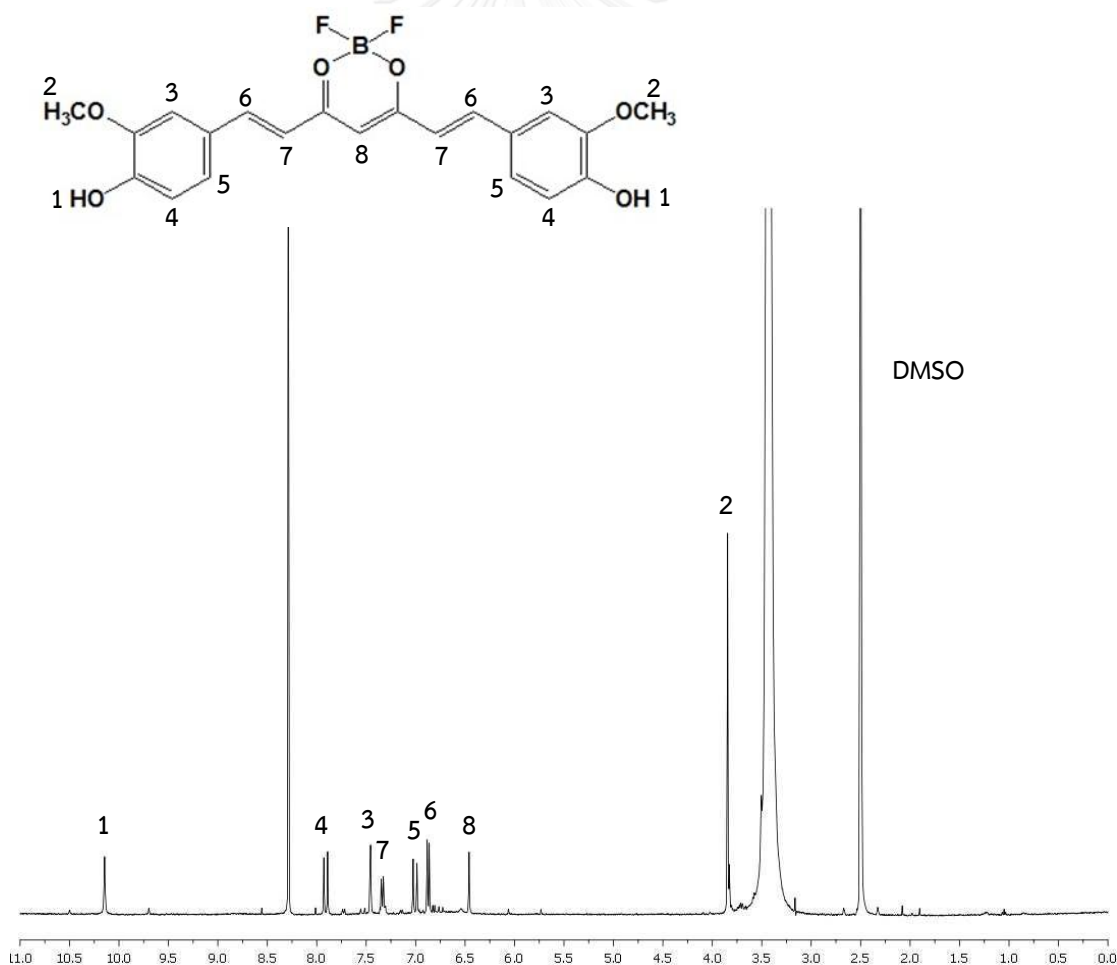


Figure 4.4 $^1\text{H-NMR}$ spectrum of difluoroboron curcumin ($\text{BF}_2\text{-CurOH}$) in $\text{DMSO-}d_6$

4.2.3 3,5-di(4-ethynyl-*N,N*-dimethylanily)-2-hydroxybenzaldehyde (F₃)

4.2.3.1 Fourier Transform Infrared Spectroscopy (FT-IR)

3,5-Di(4-ethynyl-*N,N*-dimethylanily)-2-hydroxybenzaldehyde (F₃) was characterized by FT-IR. The IR spectrum of F₃ was shown in Figure 4.5. The absorption bands of salicylaldehyde and diphenylacetylene units were found. For the salicylaldehyde unit, the characteristic bands of F₃ were observed at 1608 (s) cm⁻¹ for C=O stretching of aldehyde, 2798 (s) and 2851 (s) cm⁻¹ for C-H stretching of aldehyde and 3433 (broad) cm⁻¹ for O-H stretching band of hydroxyl group. For diphenylacetylene unit, the characteristic bands of F₃ were observed at 1189 (m) cm⁻¹ for C-N stretching of tertiary amine group, 2204 (m) cm⁻¹ for C=C stretching of alkyne group and 2919 (m) cm⁻¹ for C-H stretching of aromatic.

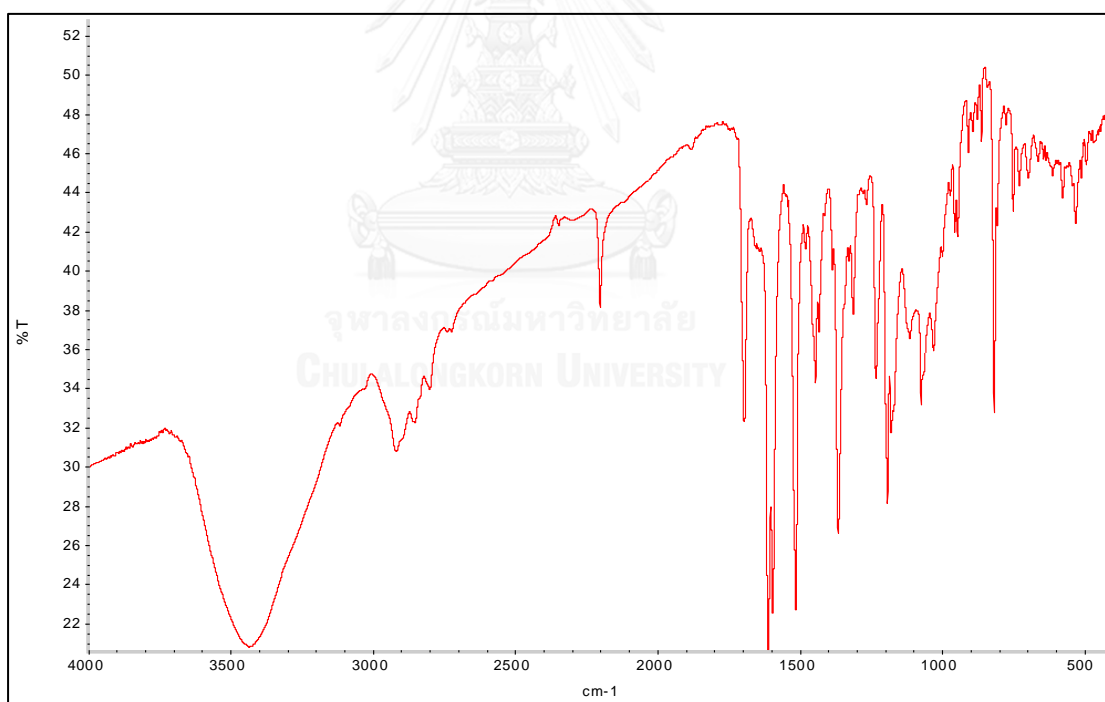


Figure 4.5 FT-IR spectrum of 3,5-di(4-ethynyl-*N,N*-dimethylanily)-2-hydroxybenzaldehyde (F₃)

4.2.3.2 Nuclear Magnetic Resonance Spectroscopy (NMR)

3,5-Di(4-ethynyl-*N,N*-dimethylanily)-2-hydroxybenzaldehyde (F_3) was characterized by $^1\text{H-NMR}$. The NMR spectrum of F_3 in CDCl_3 was shown in Figure 4.6. $^1\text{H-NMR}$ signals (400 MHz, CDCl_3) of F_3 were observed at 10.55 ppm (s, 1H) of aldehyde group, 7.68 ppm (s, 1H) of aromatic group, 7.78 ppm ($J = 8.0$ Hz, d, 2H) aromatic group, 7.43 ppm ($J = 8.0$ Hz, d, 2H) of aromatic group, 6.82 ppm (s, 1H) of aromatic group, 6.78 ppm ($J = 8.0$ Hz, d, 2H) of aromatic group, 6.68 ppm ($J = 8.0$ Hz, d, 2H) of aromatic group, 3.05 ppm (s, 6H) of methyl group, 3.00 ppm (s, 6H) of methyl group and 2.61 ppm (s, 6H) of hydroxyl group. This corresponded with the results described by Khumsri *et al* [91] and Niamnont *et al* [5].

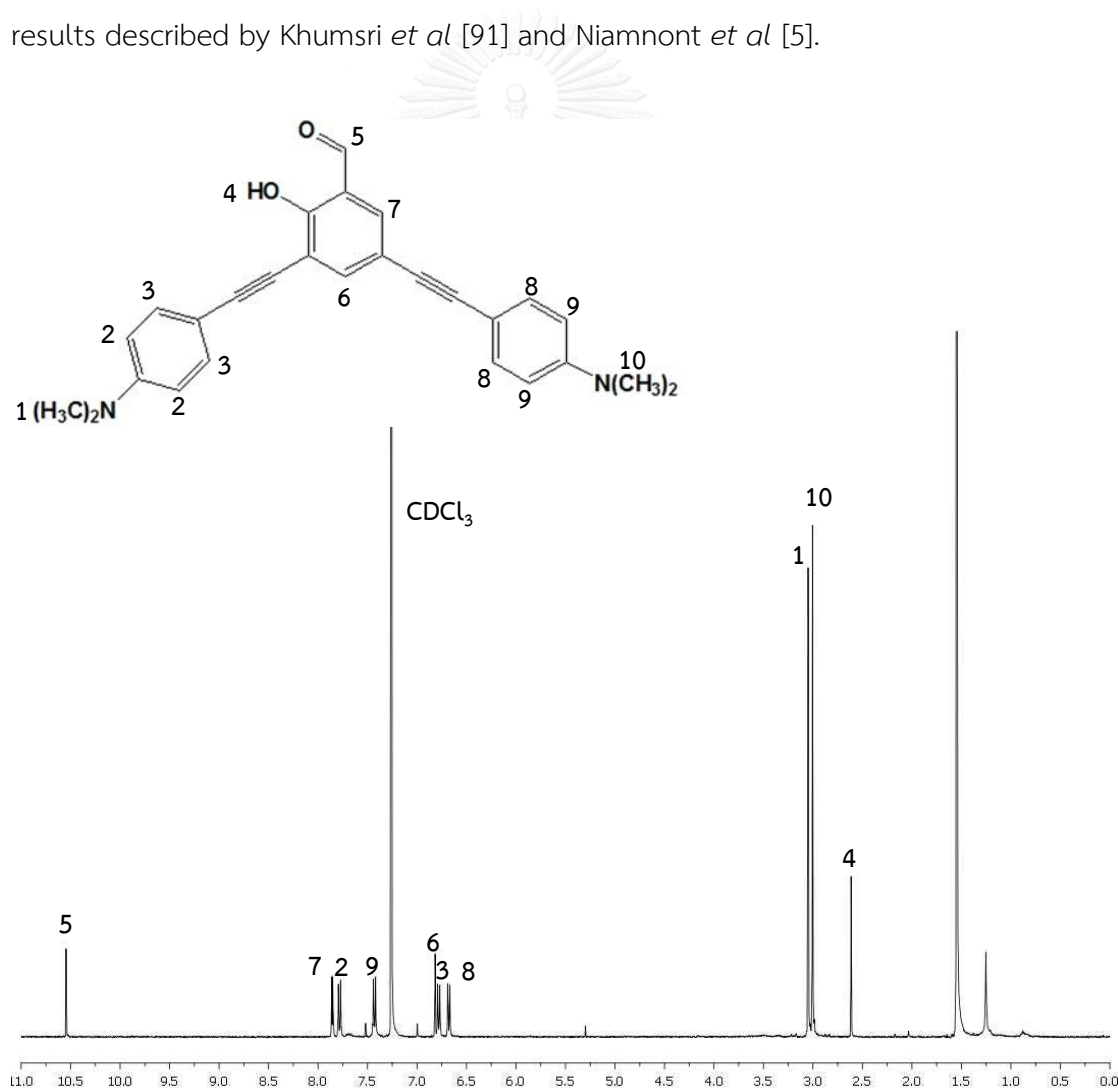


Figure 4.6 $^1\text{H-NMR}$ spectrum of 3,5-di(4-ethynyl-*N,N*-dimethylanily)-2-hydroxybenzaldehyde (F_3) in CDCl_3




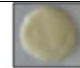



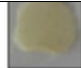


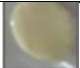



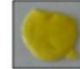

















































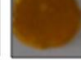























4.3 Preliminary Study of the Amount of Coloring Agent on Zein Fiber Mats for Analysis of Ions

Amounts coloring agents were studied to find the suitable fiber mats for sensing objective. The color change of suitable fiber mats should be highly and obviously distinguished from their original color at different concentrations of specific ions solution.

Firstly, curcumin-loaded zein fiber mats with 0-15%wt/wt (curcumin/zein) were prepared for iron(III) ions sensing by the naked-eye. Curcumin-loaded zein fiber mats were immersed into DI water and 1-10 mg/L of Fe^{3+} solutions at pH 2. Figure 4.7 displays the photographs of curcumin fiber mats with varying amount of curcumin immersed in DI water and solutions of different concentrations of Fe^{3+} . At equal to or above 3%wt/wt (curcumin/zein) of curcumin-loaded zein fiber mat, the color of fiber mats in 1-10 mg/L of Fe^{3+} solution were differently changed from DI water as blank solution while below 3%wt/wt (curcumin/zein) of curcumin-loaded zein fiber mat, no color change was observed. The amount of coloring agent at below 3%wt/wt (curcumin/zein) of curcumin-loaded zein fiber mat was not suitable in sensing while the fiber mats having equal to or above 7%wt/wt (curcumin/zein) did not exhibit color change comparing to the control mats (immersing in DI water) caused by a background effect [10]. The change in color intensity of fiber mats in solutions of different concentrations of Fe^{3+} was not obviously observed. Therefore, 5%wt/wt (curcumin/zein) curcumin-loaded zein fiber mat was selected for Fe^{3+} sensing. The change in color intensity was easily and obviously distinguished when employed in different concentrations of Fe^{3+} solution.

Next, 5%wt/wt (BF_2 -CurOH/zein) fiber mat and 5%wt/wt (F_3 /zein) fiber mat were prepared. It was found that the blending failed. These coloring agents were not completely dissolved in zein solution. Thus, the maximum amount of BF_2 -CurOH and F_3 that was capable to completely and homogeneously dissolve in zein solution were investigated. It was found that 0.25%wt/wt of BF_2 -CurOH-loaded zein fiber mat and 0.1%wt/wt of F_3 -loaded zein fiber mat could be obtained. The mats with smoothly spread color were observed.

In conclusion, 5%wt/wt (curcumin/zein) fiber mat, 0.25%wt/wt (BF₂⁻CurOH/zein) fiber mat and 0.1%wt/wt (F₃/zein) fiber mat were selected for further experiments.

Curcumin (%wt/wt)	Concentration of Fe (III) ions (ppm)										
	DI	1	2	3	4	5	6	7	8	9	10
0											
0.7											
1											
3											
5											
7											
10											
15											

Conditions: Sample volume = 1 mL, time = 3 h, room temperature, pH=2

Figure 4.7 Photographs of curcumin-loaded zein fiber mats with varying amount of curcumin immersed in DI water and different concentrations of Fe³⁺

4.4 Electrospun Zein Blending with Curcumin Fiber Mats

In this section, 5%wt/wt (curcumin/zein) fiber mat was fabricated by electrospinning, followed by the crosslinking reaction. The morphology of curcumin-loaded zein fiber mat was investigated by scanning electron microscopy (SEM). The functional groups of curcumin-loaded zein fiber mat were characterized by Fourier transform infrared spectroscopy (FT-IR). The color characteristic of curcumin-loaded zein fiber mat was investigated by diffuse reflectance ultraviolet-visible spectroscopy (DR-UV-Vis). The naked-eye sensing for iron(III) ions was examined and applied in real water samples.

4.4.1 Morphology of Curcumin-loaded Zein Fiber Mat

The morphology of curcumin-loaded zein fiber mat was investigated by scanning electron microscopy (SEM). The SEM images of curcumin fiber mat before and after immersing in DI water were presented in Figure 4.8. Before immersing in DI water, the morphology of dry curcumin fiber mat exhibited satisfactory fiber mats observed by straight and smooth fibers. The average diameter of dry curcumin fiber mat was 586 ± 131 nm (mean \pm S.D., n=30). After immersing in DI water, the morphology of wet curcumin fiber mat showed considerable swelling yet maintaining their fibrous networks. It indicated that the fiber mat was completely crosslinked by heat-induced amide crosslinking. In actuality, an uncrosslinked zein fiber mat is water soluble. It becomes water insoluble when there is a crosslinking [9, 67]. The average diameter of wet curcumin-loaded zein fiber mat increased to 1381 ± 384 nm (mean \pm S.D., n=30). Moreover, the curcumin-loaded zein fiber mat preserved yellow color mat after immersing in DI water. The curcumin could be efficiently retained in the zein fiber mat. This retaining action can be ascribed to the H-bonding intermolecular force between the polypeptide chains of zein and the hydroxyl groups of curcumin.

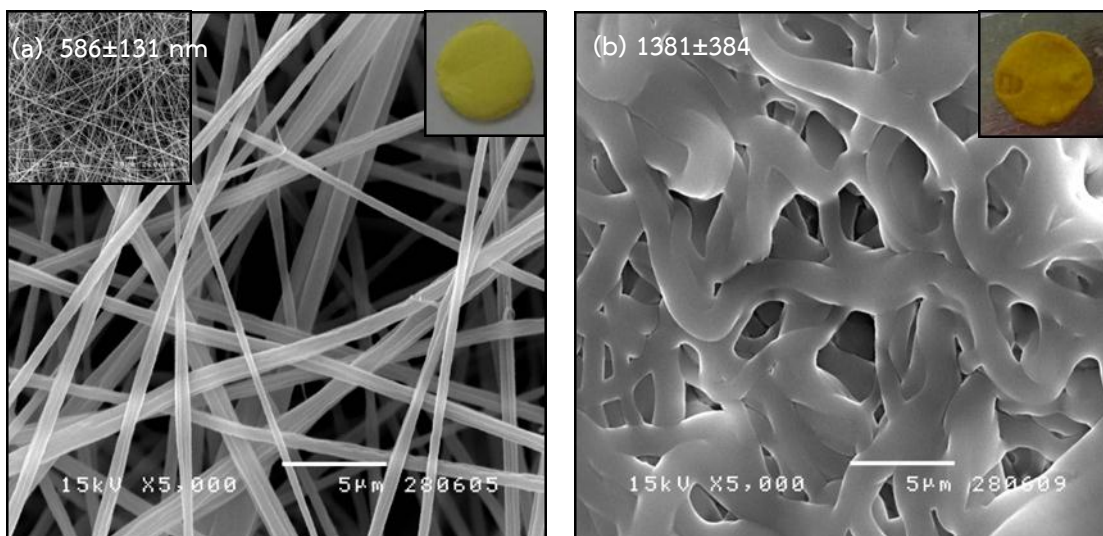


Figure 4.8 SEM images (5,000x magnification) of (a) dry and (b) wet curcumin-loaded zein fiber mats before and after immersing in DI water at room temperature for 3 hours. Inset: SEM image (750x magnification) and the photographs of curcumin-loaded zein fiber mats (upper right corner).

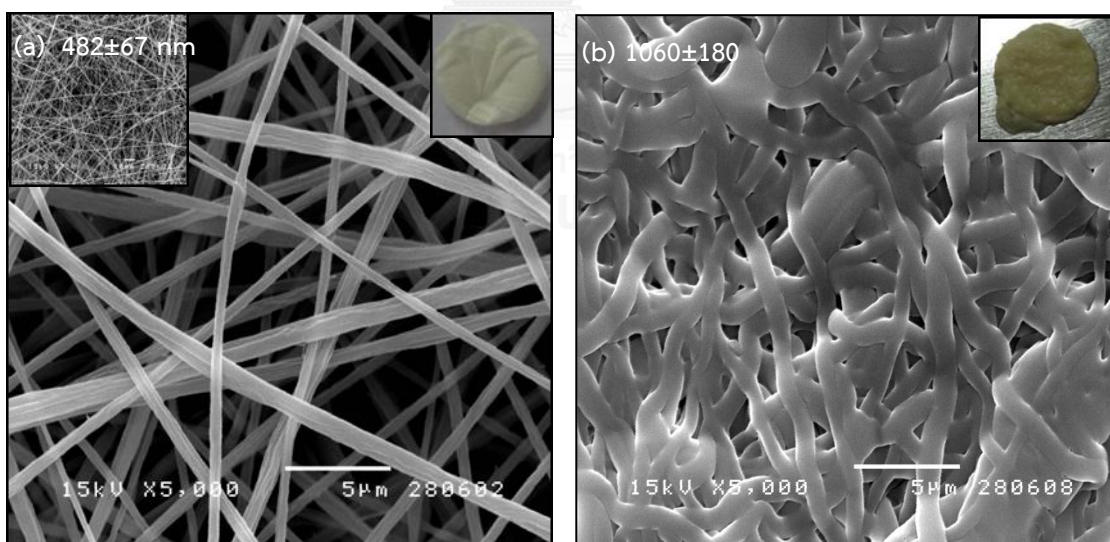


Figure 4.9 SEM images (5,000x magnification) of (a) dry and (b) wet zein fiber mats before and after immersing in DI water at room temperature for 3 hours. Inset: SEM image (750x magnification) and the photographs of zein fiber mats (upper right corner).

In addition, the morphology of zein fiber mat was investigated by scanning electron microscopy (SEM). The SEM images of zein fiber mat before and after immersing in DI water were showed in Figure 4.9. The zein fiber mat has white color. The average diameter of dry and wet zein fiber mats were 482 ± 67 nm and 1060 ± 180 nm (mean \pm S.D., n=30), respectively. The morphology of zein fiber mat and curcumin fiber mat were compared. From Figures 4.8 and 4.9, the morphology of both fiber mats was similarly found. The small amount curcumin blending with zein did not affected the morphology and diameter of fiber mats. When a small amount of curcumin was added into zein solution, the average diameter of curcumin fiber mat was insignificantly increased due to the fact that the viscosity of mixture solution slightly increased and affecting the electrospinning [25, 100].

4.4.2 FT-IR Characterization of Curcumin-loaded Zein Fiber Mat

The curcumin-loaded zein fiber mat was characterized by FT-IR. The IR spectrum of curcumin-loaded zein fiber mat was shown in Figure 4.10. The absorption bands of zein unit and curcumin were investigated. For the zein unit, the characteristic bands of curcumin-loaded zein fiber mat were observed at 1515 (m-s) cm^{-1} for N-H bending of amide II group, 1645 (s) cm^{-1} for C=O stretching of amide I group and 3286 (m, broad) and 3057 (w) cm^{-1} for N-H stretching of secondary amide group. For the curcumin unit, the characteristic bands of curcumin-loaded zein fiber mat were not appeared probably because of low amount of curcumin blending with zein at 5%w/w (curcumin/zein) fiber mat. However, the curcumin-loaded zein fiber mat presented yellow color of curcumin. These showed significantly different color intensities on mat from the white zein fiber mat (Figures 4.8 and 4.9).

In addition, the zein fiber mat was characterized by FT-IR. The IR spectrum of zein fiber mat was shown in Figure 4.11. The characteristic bands of zein fiber mat were observed at 1515 (m-s) cm^{-1} assigned to N-H bending band of amide II group, 1645 (s) cm^{-1} assigned to C=O stretching band of amide I group and 3286 (m, broad) and 3057 (w) cm^{-1} assigned to N-H stretching band of secondary amide group.

Moreover, the IR spectrum of zein fiber mat and zein powder was compared. The IR spectrum of zein powder was shown in Figure 4.12. Both spectra exhibited a very similar characteristic absorption bands. This implied that the electrospinning did not change functional groups of materials.

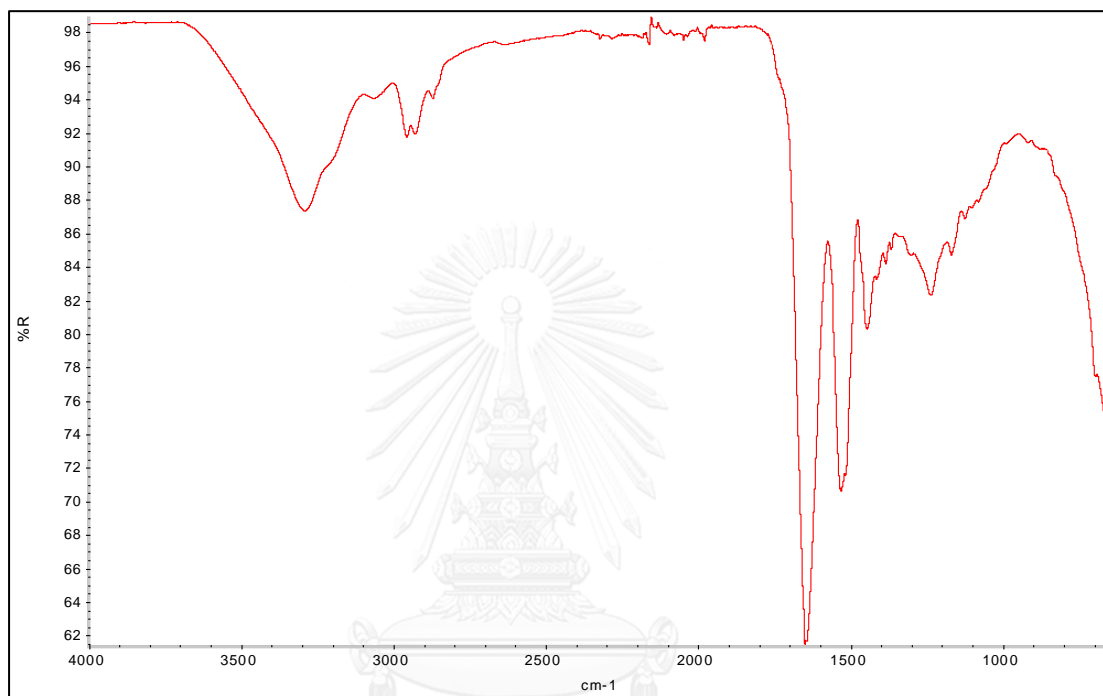


Figure 4.10 FT-IR spectrum of curcumin-loaded zein fiber mat

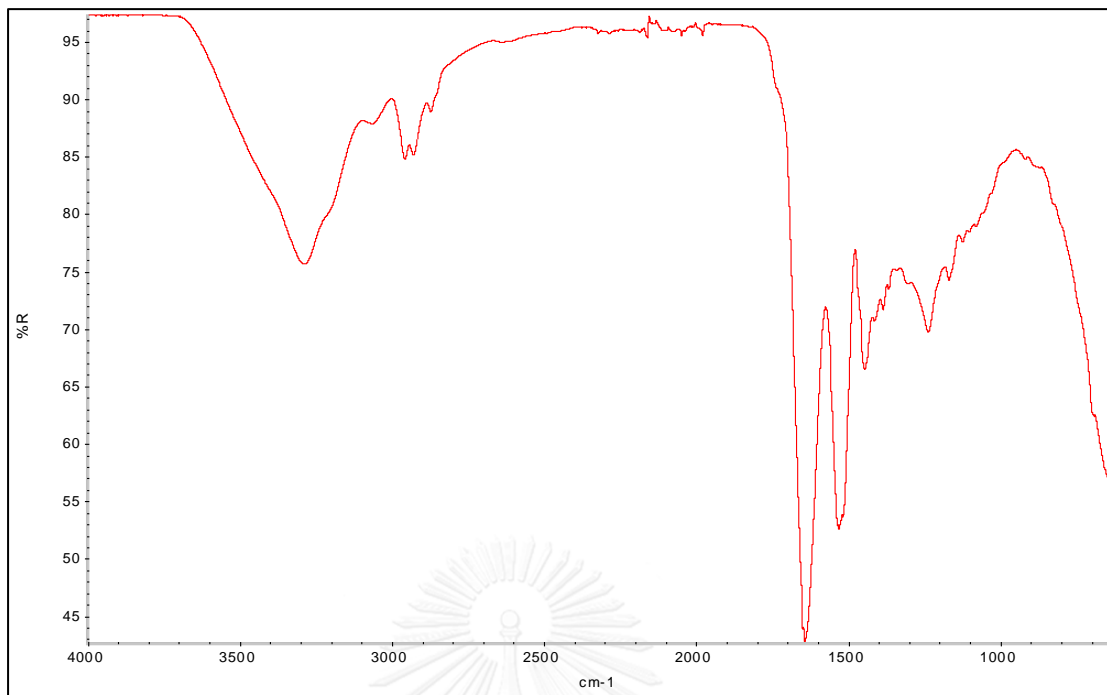


Figure 4.11 FT-IR spectrum of zein fiber mat

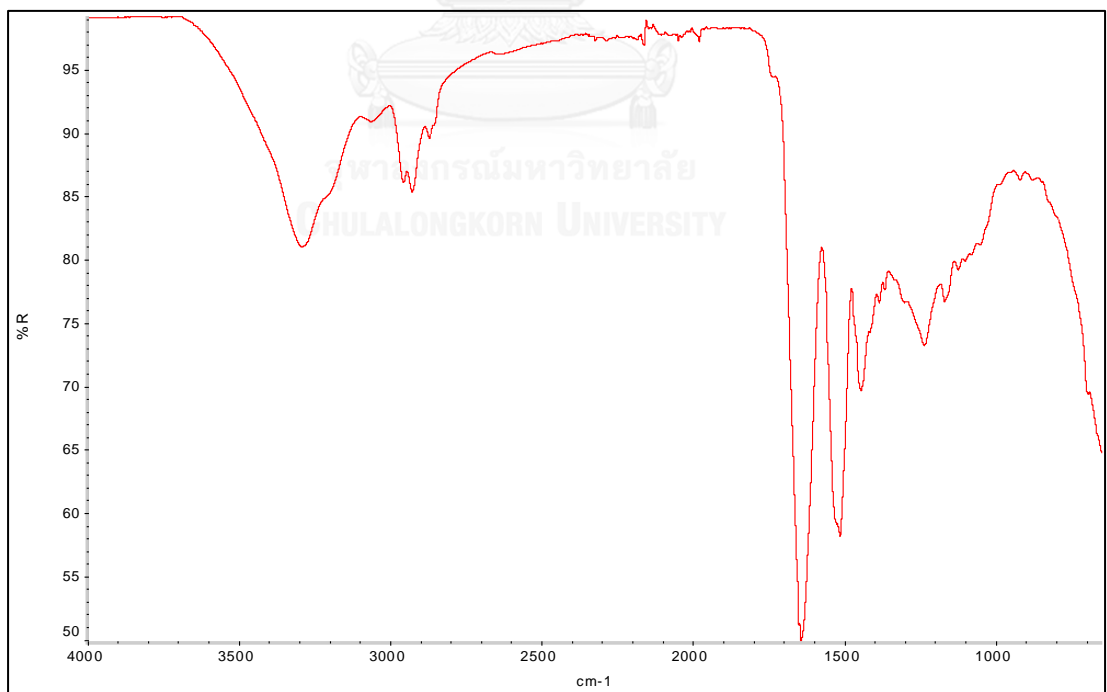


Figure 4.12 FT-IR spectrum of zein powder

4.4.3 DR-UV-Vis Characterization of Curcumin-loaded Zein Fiber Mat

The curcumin-loaded zein fiber mat was characterized by DR-UV-Vis. The DR-UV-Vis spectrum of curcumin-loaded zein fiber mat was shown in Figure 4.13. The maximum absorption of curcumin-loaded zein fiber mat was found at 424 nm. This agreed with the absorption band of an enol form of curcumin [101]. In addition, the zein fiber mat was also characterized by DR-UV-Vis. In Figure 4.14, the absorption band of zein fiber mats had the maximum at 424 nm (λ_{\max}). The DR-UV-Vis spectrum of curcumin-loaded zein fiber mat was significantly different from the DR-UV-Vis spectra of zein fiber mat. This can be supported that the incorporating of curcumin into the zein fiber mat was obtained.

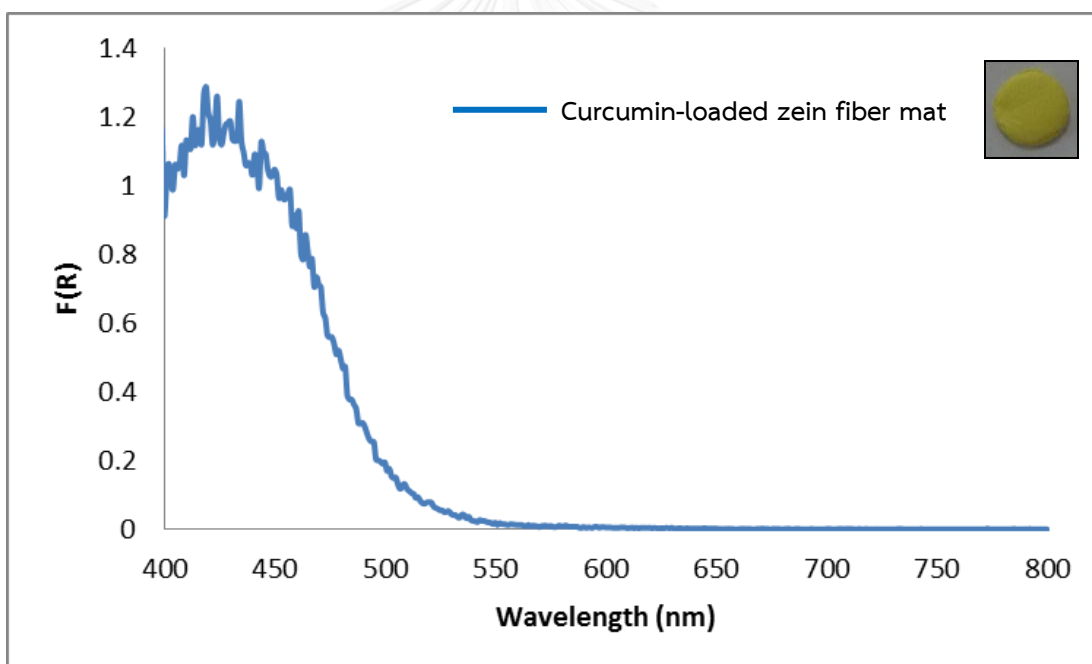


Figure 4.13 DRUV-Vis spectrum of curcumin-loaded zein fiber mat (Inset shows the photograph of curcumin-loaded zein fiber mat.)

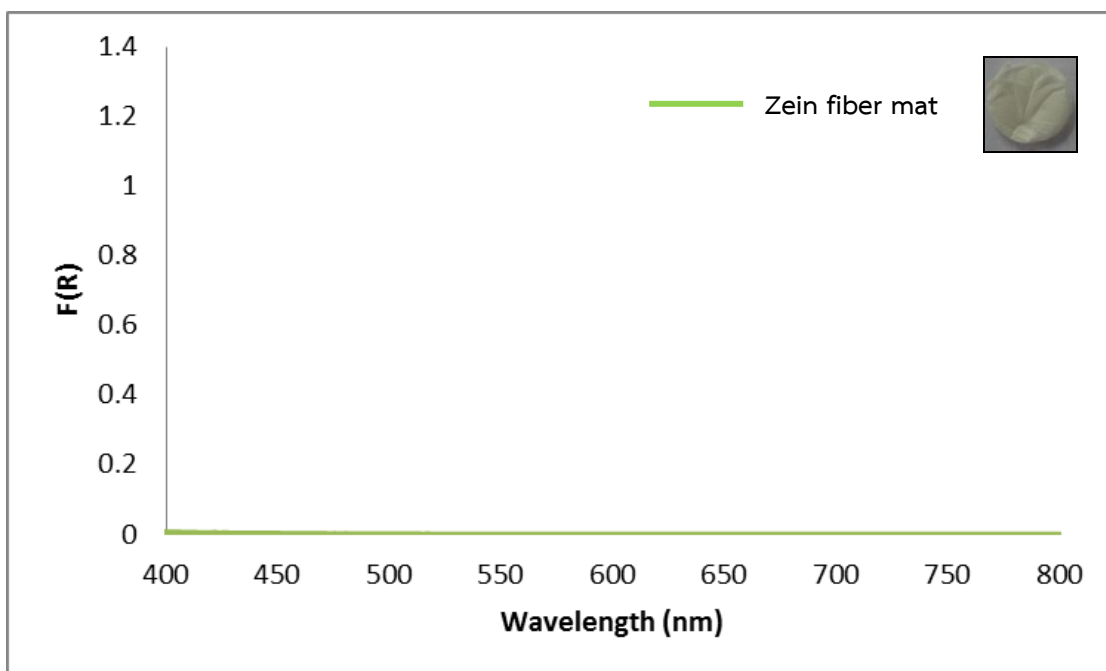


Figure 4.14 DRUV-Vis spectrum of zein fiber mat (Inset shows the photograph of zein fiber mat.)

4.4.4 Naked-eye Sensing for Iron(III) Ions

Concerning the study of influence of pH, 1 and 10 mg/L Fe^{3+} solution were prepared in the pH range of 1 to 5 to avoid the formation of insoluble metal hydroxides. Moreover, the color of curcumin can self-shift at the pH above 7.4 acting as a pH indicator [102]. The photographs of curcumin-loaded zein fiber mats after immersed into DI water and Fe^{3+} solution at different pHs were displayed in Figure 4.15. At pH 1-3, the color of curcumin-loaded zein fiber mats changed from yellow to brown in the presence of Fe^{3+} while the in DI water, a blank solution, did not change. The most sensitive color change was observed at pH 2. The reason for this phenomenon is explained by the stability of an enol form that is generally present in acidic solution. This enol form of curcumin can serve as a ligand in curcumin-metal complex [75, 103]. The conjugated system is disturbed causing a color change. The complex formation of curcumin and iron(III) ion was shown in Scheme 4.3.

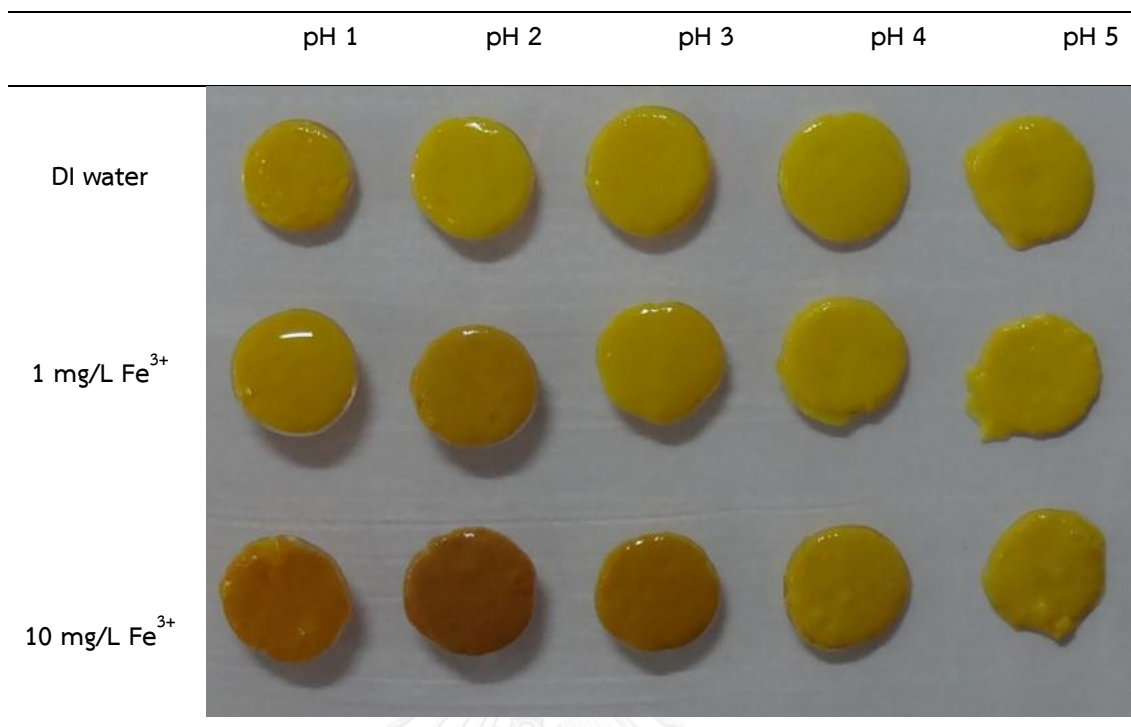
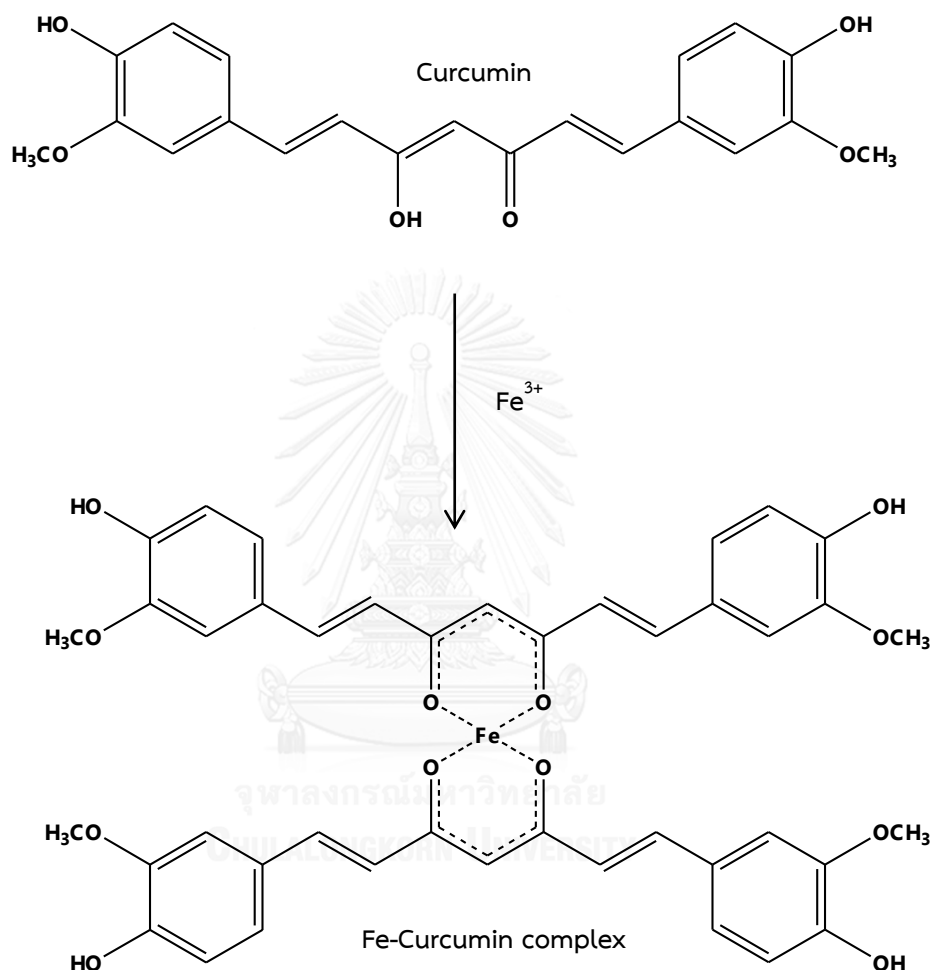


Figure 4.15 Photographs of curcumin-loaded zein fiber mats immersed in DI water and Fe³⁺ solution at different pHs (sample volume = 1 mL, time = 3 hours, room temperature).

Regarding the study of effect of interferences, 17 metal ions (Ag⁺, As⁵⁺, Ba²⁺, Ca²⁺, Cd²⁺, Co²⁺, Cr³⁺, Cu²⁺, Fe²⁺, Hg²⁺, K⁺, Mn²⁺, Na⁺, Ni²⁺, Pb²⁺, Zn²⁺ and Mg²⁺) of 200 μM was prepared at pH 2. In Figure 4.16, the photographs of the curcumin-loaded zein fiber mats after immersing into various metal ion solutions were presented. After dipping into the presence of Fe³⁺, the color of the curcumin-loaded zein fiber mat was changed only. For the presence of other metal solutions, the color of the curcumin-loaded zein fiber mat was remained similarly to nonexistence of Fe³⁺ in DI water. The selectivity of curcumin-loaded zein fiber mat to Fe³⁺ can be described to the Hard Soft Acid Base (HSAB) theory. Fe³⁺ is classified as hard Lewis acid. The enol functionality of curcumin is classified as hard Lewis base. Meanwhile other metal ions are classified as soft and borderline acids. The hard Lewis acid prefers to bind to hard Lewis base while soft and borderline acids do not prefer to bind to hard Lewis base

from HSAB theory. Therefore, Fe^{3+} sensing with curcumin fiber mat was free from interferences by other metal ions.



Scheme 4.3 The complex formation of curcumin and iron(III) ion

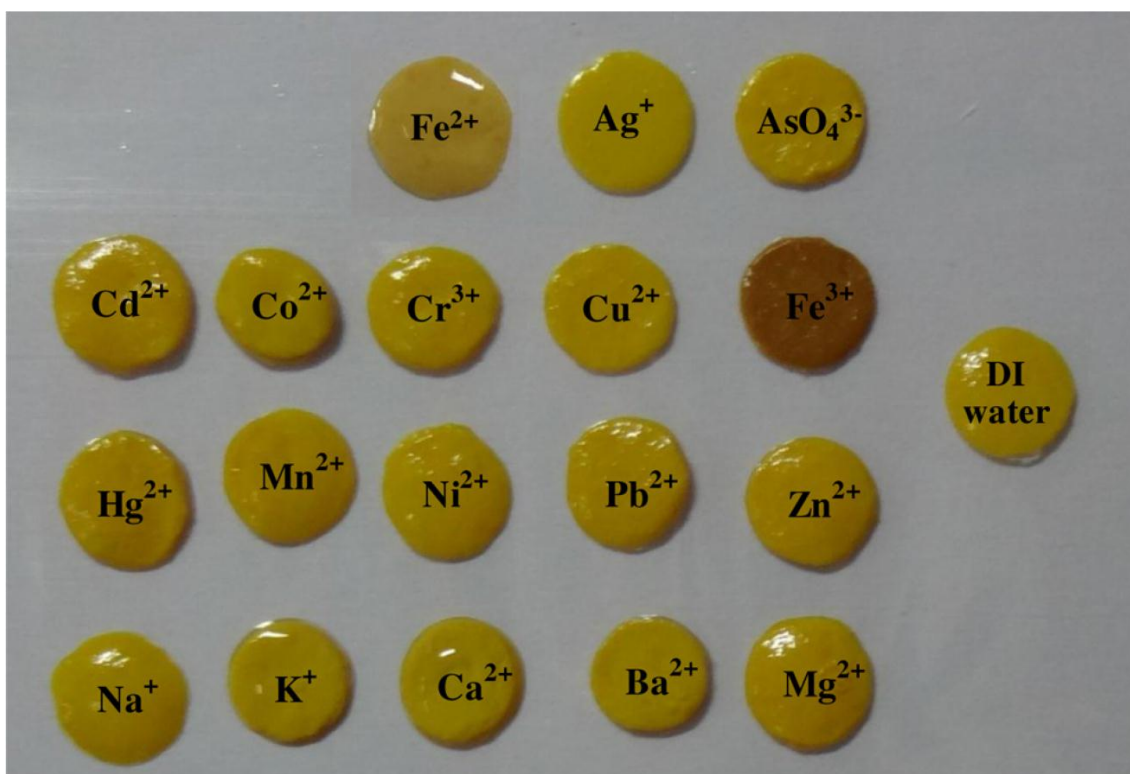


Figure 4.16 Photographs of the curcumin-loaded zein fiber mats after immersing into various metal ion solutions (concentrations= 200 μ M, pH = 2, sample volume= 1 mL, time= 3 hours)

For qualitative and quantitative testing, the color change of curcumin-loaded zein fiber mats were investigated by varying the concentration (0.1, 0.2, 0.3, 0.4, 0.5, 1.0 and 5.0 mg/L) of Fe^{3+} solution at pH 2. DI water at pH 2 was applied as Fe free solution. The photographs of the curcumin fiber mats after immersing into solutions at different concentrations of Fe^{3+} for qualitative (yes/no response) and quantitative testing (1: positive response, 0: null response) were shown in Figure 4.17. A positive response (1) signifies “with color change” while a null response (0) signifies “no color change”. At the concentration of Fe^{3+} equal to or greater than 0.4 mg/L, the color change of curcumin-loaded zein fiber mats were observed. Moreover, the color of curcumin-loaded zein fiber mats was not changed at below 0.4 mg/L Fe^{3+} solution. Therefore, the visual detection limit was found at 0.4 mg/L. Furthermore, the intensity of color change of the curcumin-loaded zein fiber mat increased

proportionally with increasing concentration of Fe^{3+} . These changed from yellow to dark-brown. Moreover, the response time of the curcumin-loaded zein fiber mat depended on the concentration of Fe^{3+} . For the solutions containing 5.0 mg/L, 1.0 mg/L and lower than 1 mg/L of Fe^{3+} solution, the color change of curcumin-loaded zein fiber mat were initially observed at 5 min, 60 min and 90 min, respectively.

		[Fe^{3+}], mg/L						
		0.1	0.2	0.3	0.4	0.5	1.0	5.0
Assay 1		0	0	0	1	1	1	1
		0	0	0	1	1	1	1
		Control (Fe free solution)						
Assay 1-14		0	0	0	0	0	0	0
		0	0	0	0	0	0	0
		Conditions: Sample volume = 1 mL, Time = 3 hours, pH = 2, Room temperature						

Figure 4.17 The photographs of the curcumin-loaded zein fiber mats after immersing into solutions at different concentration of Fe^{3+} for qualitative. (yes/no response) and quantitative testing (1: positive response, 0: null response)

In addition, the curcumin-loaded zein fiber mats after immersing in different concentrations of Fe^{3+} solutions at pH 2 were characterized by DR-UV-Vis. Figure 4.18 shows the DR-UV-Vis spectra of curcumin-loaded zein fiber mats after immersing for 3 hours in different concentrations of Fe^{3+} at pH 2. The new absorption band of curcumin- Fe^{3+} complex at the region of 620-660 nm was found. This was significantly different from the absorption band of curcumin fiber mat in DI water. The result agreed with the report of Tcnnesen *et al* [104].

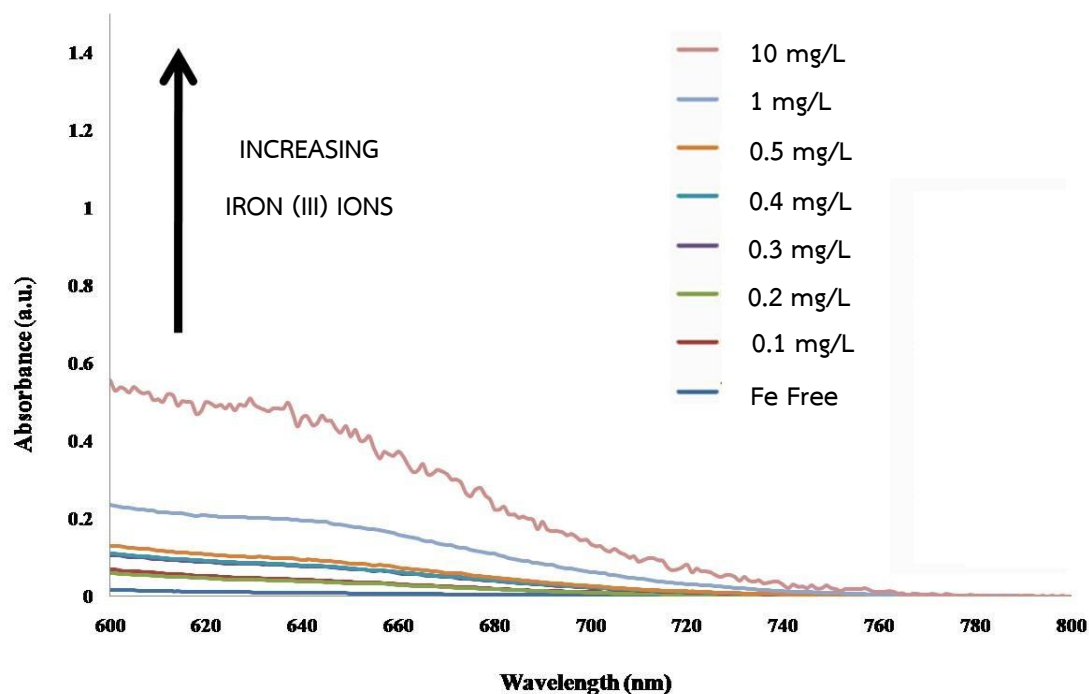



Figure 4.18 DR-UV-Vis spectra of curcumin-loaded zein fiber mats after immersing for 3 hours in different concentrations of Fe^{3+} at pH 2

4.4.5 Analysis of Real Water Samples

In Thailand, the amount of iron in water is prescribed by the Pollution Control Department. The maximum acceptable concentration and maximum allowable concentration of iron for potable water are 0.5 and 1.0 mg/L, respectively [105].

In term of colorimetric detection, the curcumin-loaded zein fiber mat can be easily used to analyze qualitatively and quantitatively by comparing with a calibration color chart. The photographs of the curcumin-loaded zein fiber mat after immersing in real water samples and the color calibration chart were shown in Figure 4.19. For comparative purpose, all concentrations of Fe^{3+} in solutions were determined using the inductively coupled plasma-optical emission spectrometer (ICP-OES). For five different real water samples, the curcumin-loaded zein fiber mat was tested. When dipping into all non-spiked real samples, the color of the curcumin-loaded zein fiber mats did not change. This implies that the concentration of Fe^{3+} in all non-spiked real sample was below 0.4 mg/L as the LOD of the proposed naked eye method. From the results determined by ICP-OES, the Fe concentrations of all non-spiked real samples are in the range of 0.07-0.09 mg/L. For spiked real samples at 0.5, 1.0 and 5.0 mg/L, the degree of brown color of the curcumin-loaded zein fiber mat increased in accordance with the color calibration chart. The present naked-eye detection on curcumin-loaded zein fiber mat produced a satisfied accuracy comparing with ICP-OES result as the reference method [106].

In conclusion, the proposed procedure can be used for iron(III) ions sensing in potable water and surface water samples.

Samples	Non-spiked	Spiked level (mg/L)			Color calibration chart
		0.5	1.0	5.0	
Drinking water I	0.07	0.58	1.06	4.81	
Drinking water II	0.07	0.59	1.08	5.38	
Mineral water	0.07	0.57	1.06	4.84	
Tap water	0.09	0.60	1.08	5.08	
Pond water	0.08	0.58	1.09	5.16	

Condition: Sample volume = 1 mL, Time = 3 hours, pH = 2, Room temperature.

The values indicated on the concentration of Fe determined by ICP-OES.

Figure 4.19 Photographs of the curcumin fiber mat after immersing in real water samples (left) and the color calibration chart (right)

4.5 Electrospun Zein Blending with Difluoroboron Curcumin

In this section, 0.25%wt/wt (difluoroboron curcumin (BF₂-CurOH)/zein) fiber mat was established by electrospinning and amide crosslinking reaction. The morphology of BF₂-CurOH-loaded zein fiber mat was investigated by scanning electron microscopy (SEM). The functional groups of BF₂-CurOH-loaded zein fiber mat were characterized by Fourier transform infrared spectroscopy (FT-IR). The diffuse reflectance of BF₂-CurOH-loaded zein fiber mat was characterized by diffuse reflectance ultraviolet-visible spectroscopy (DR-UV-Vis). Finally, the applicability of ammonia sensing was investigated.

4.5.1 Morphology of BF₂-CurOH-loaded Zein Fiber Mat

The morphology of difluoroboron curcumin (BF₂-CurOH)-loaded zein fiber mat was investigated by scanning electron microscopy (SEM). The SEM images of BF₂-CurOH-loaded zein fiber mat before and after immersing in DI water were presented in Figure 4.20. Before immersing in DI water, the morphology of dry BF₂-CurOH-loaded zein fiber mat presented smooth and straight fibers. The average diameter of dry BF₂-CurOH-loaded zein fiber mat was 429±89 nm (mean±S.D., n=30). After immersing in DI water, the morphology of wet BF₂-CurOH fiber mat exhibited swelling with maintaining their fibrous networks. The average diameter of wet BF₂-CurOH-loaded zein fiber mat increased to 840±174 nm (mean±S.D., n=30). This result indicated that the fiber mat was fully crosslinked [9, 67]. Moreover, the BF₂-CurOH-loaded curcumin fiber mat preserved orange color on zein mat after immersing in DI water. It indicated that BF₂-CurOH could be efficiently retained in the zein fiber mat. This retaining action can be attributed to the H-bonding intermolecular force between the polypeptide chains of zein and the hydroxyl groups of BF₂-CurOH.

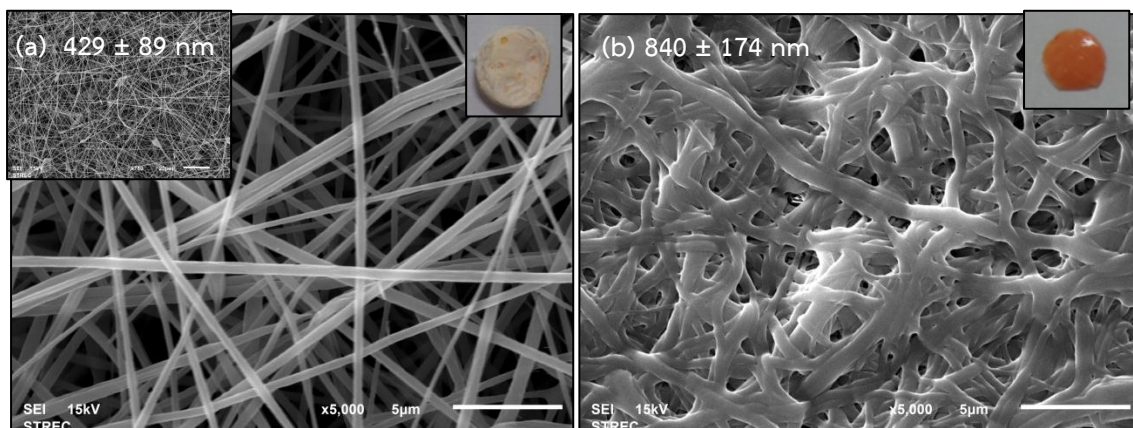


Figure 4.20 SEM images (5,000x magnification) of (a) dry and (b) wet difluoroboron curcumin ($\text{BF}_2\text{-CurOH}$)-loaded zein fiber mats before and after immersing in DI water at room temperature for 3 hours. Inset: SEM image (750x magnification) and the photograph of $\text{BF}_2\text{-CurOH}$ -loaded zein fiber mats (upper right corner)

4.5.2 FT-IR Characterization of $\text{BF}_2\text{-CurOH}$ -loaded Zein Fiber Mat

The difluoroboron curcumin ($\text{BF}_2\text{-CurOH}$)-loaded zein fiber mat was characterized by FT-IR. The IR spectrum of $\text{BF}_2\text{-CurOH}$ -loaded zein fiber mat was shown in Figure 4.21. The absorption bands of zein unit and difluoroboron curcumin were investigated. For the zein unit, the characteristic bands of $\text{BF}_2\text{-CurOH}$ -loaded zein fiber mat were observed at $1515 \text{ (m-s) cm}^{-1}$ assigned to N-H bending band of amide II group, 1645 (s) cm^{-1} assigned to C=O stretching band of amide I group and $3286 \text{ (m, broad) and } 3057 \text{ (w) cm}^{-1}$ assigned to N-H stretching band of secondary amide group. For the difluoroboron curcumin unit, the characteristic bands of $\text{BF}_2\text{-CurOH}$ -loaded zein fiber mat were not observed. This supposed reason is due to a low amount of $\text{BF}_2\text{-CurOH}$ blending with zein solution at 0.25%wt/wt ($\text{BF}_2\text{-CurOH/zein}$). Nevertheless, the $\text{BF}_2\text{-CurOH}$ -loaded zein fiber mat has orange color of $\text{BF}_2\text{-CurOH}$.

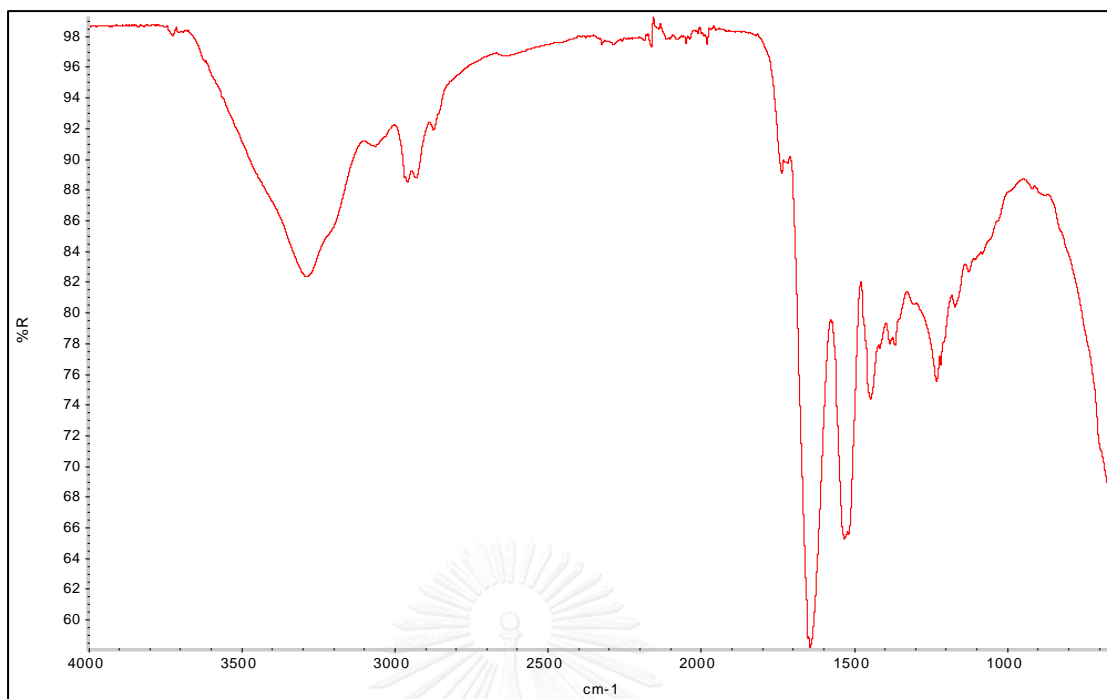


Figure 4.21 FT-IR spectrum of difluoroboron curcumin ($\text{BF}_2\text{-CurOH}$)-loaded zein fiber mat

4.5.3 DR-UV-Vis Characterization of $\text{BF}_2\text{-CurOH}$ -loaded Zein Fiber Mat

The difluoroboron curcumin ($\text{BF}_2\text{-CurOH}$)-loaded zein fiber mat was characterized by DR-UV-Vis. The DR-UV-Vis spectrum of $\text{BF}_2\text{-CurOH}$ -loaded zein fiber mat was shown in Figure 4.22. The absorption band of $\text{BF}_2\text{-CurOH}$ -loaded zein fiber mat was found at the region of 425 to 600 nm. This agreed with the absorption bands of difluoroboron curcumin powder (red powder) [4, 90]. In Figure 4.23, the absorption band of $\text{BF}_2\text{-CurOH}$ powder was found at the region of 525 to 600 nm. In addition, the absorption band of zein fiber mat was not found as shown in Figure 4.24. This result implied that the blending of $\text{BF}_2\text{-CurOH}$ with zein fiber mat was achieved.

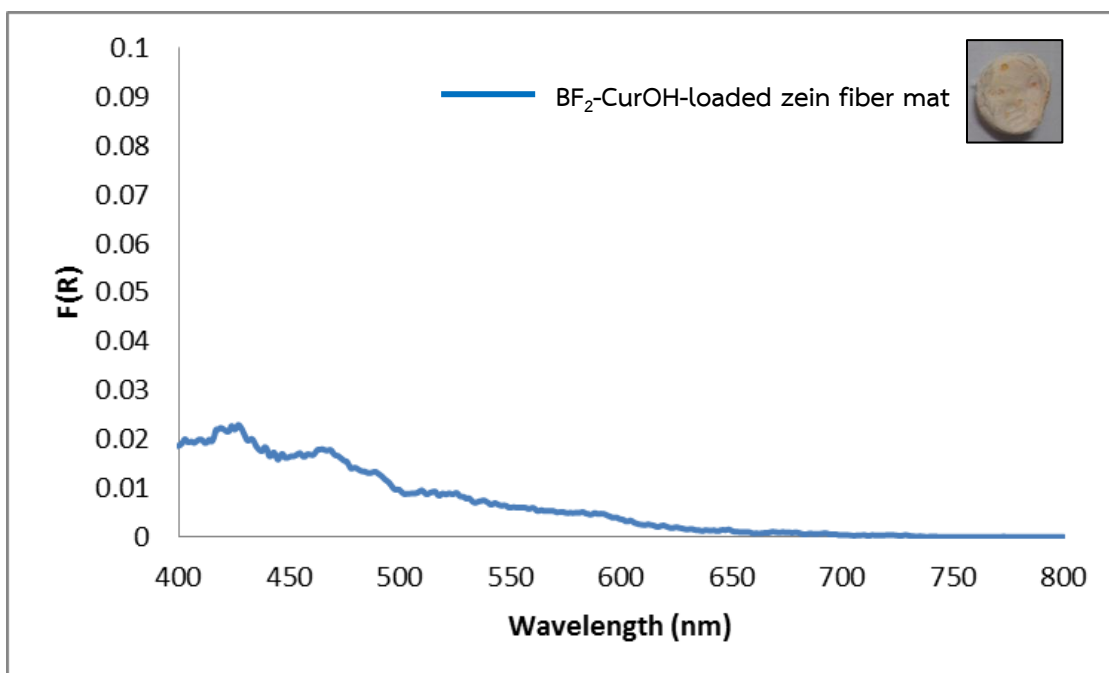


Figure 4.22 DR-UV-Vis spectrum of difluoroboron curcumin ($\text{BF}_2\text{-CurOH}$)-loaded zein fiber mat (Inset shows the photograph of $\text{BF}_2\text{-CurOH}$ -loaded zein fiber mat.)

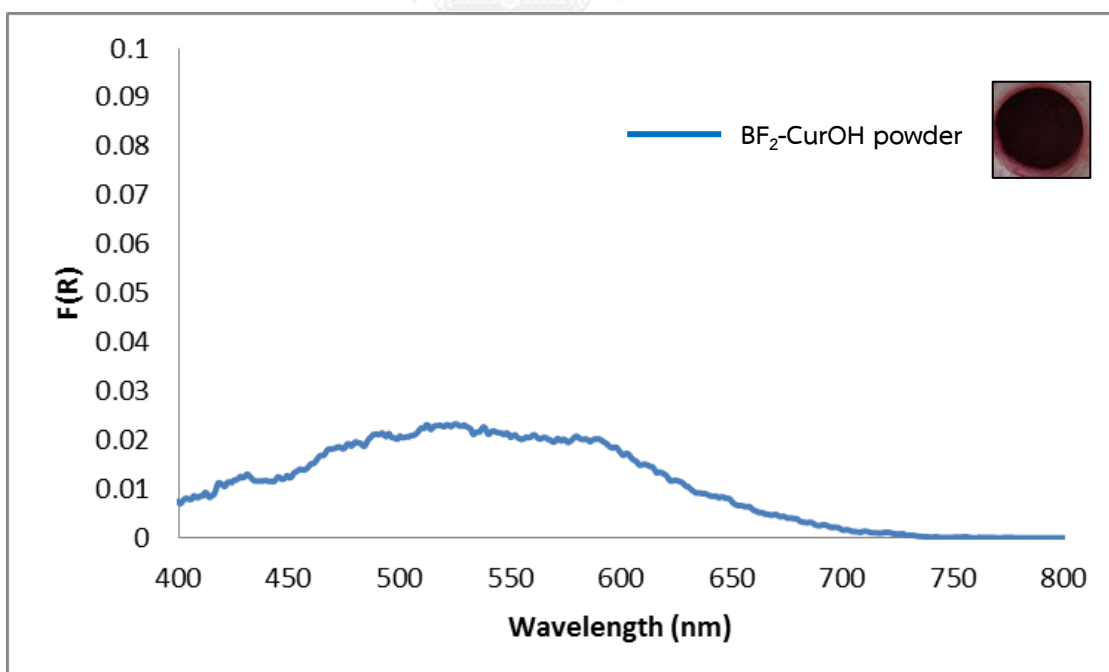


Figure 4.23 DR-UV-Vis spectrum of difluoroboron curcumin ($\text{BF}_2\text{-CurOH}$) powder (Inset shows the photograph of $\text{BF}_2\text{-CurOH}$ powder.)

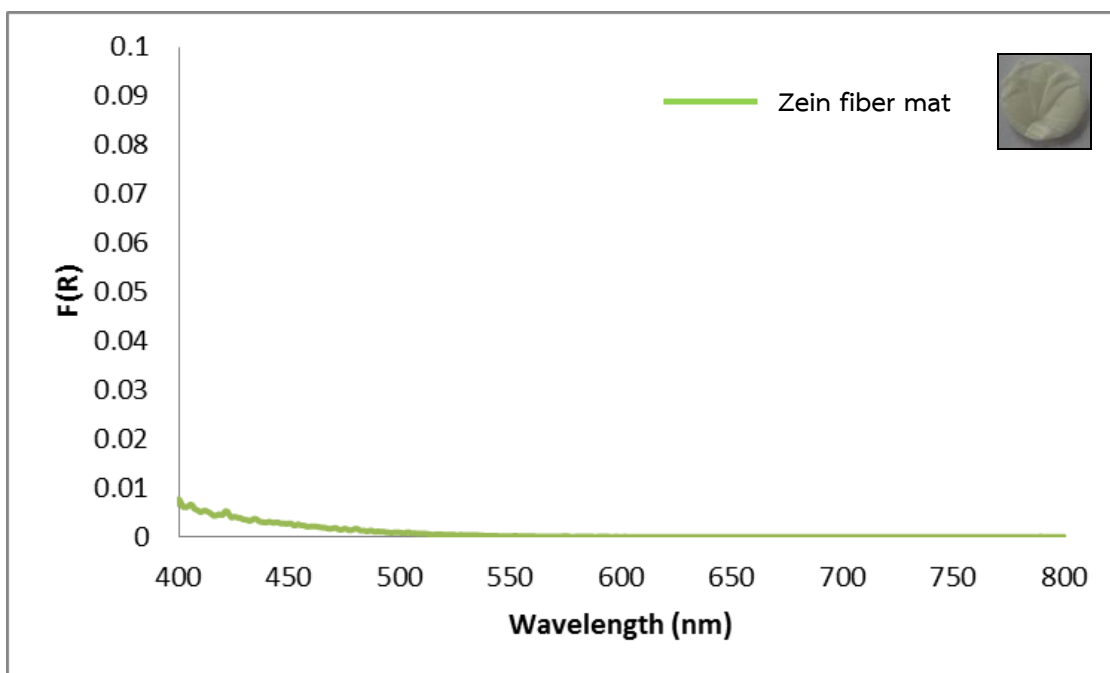


Figure 4.24 DR-UV-Vis spectrum of zein fiber mat (Inset shows the photograph of zein fiber mat.)

4.5.4 Applicability of Borax Sensing

$\text{BF}_2\text{-CurOH}$ could be changed its molecular structure by strongly basic anions since the deprotonation occurred at its hydroxyl groups [4, 90]. $\text{B}_4\text{O}_7^{2-}$ solution was a basic anion with a low acid dissociation constant ($\text{pK}_a = 9.23$) that may be abstract protons from the hydroxyl groups in $\text{BF}_2\text{-CurOH}$ resulting in the change of $\text{BF}_2\text{-CurOH}$ color by disturbance of the π -conjugate system.

Regarding the study of influence of pH, 100 mg/L of $\text{B}_4\text{O}_7^{2-}$ solution and DI water as free $\text{B}_4\text{O}_7^{2-}$ sample were prepared in the pH range of 7 to 10. The photographs of difluoroboron curcumin ($\text{BF}_2\text{-CurOH}$)-loaded zein fiber mat after immersing into DI water and $\text{B}_4\text{O}_7^{2-}$ solution at different pHs were shown in Figure 4.25. At pH 10, the color of $\text{BF}_2\text{-CurOH}$ -loaded zein fiber mat changed upon the presence of $\text{B}_4\text{O}_7^{2-}$ while absented of $\text{B}_4\text{O}_7^{2-}$ the color did not change. However, it was unfortunate that the $\text{BF}_2\text{-CurOH}$ -loaded zein fiber mat could not maintain its fiber morphology at pH 9-10. It became distorted and exploded on fiber morphology,

probably due to zein protein denaturation under high basic conditions. However, these phenomena might be useful to apply in basic gas sensing.

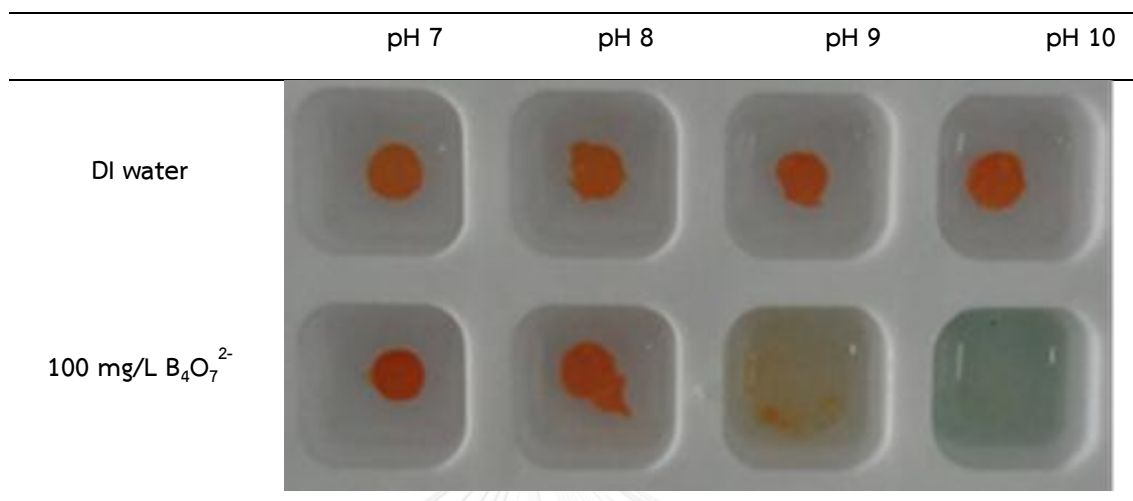


Figure 4.25 Photographs of difluoroboron curcumin (BF_2 -CurOH)-loaded zein fiber mat immersed in DI water and $B_4O_7^{2-}$ solution at different pHs (sample volume = 1 mL, time = 3 hours)

4.5.5 Applicability of Ammonia Sensing

Ammonia is the most attractive of basic gas sensing. It is colorless toxic gas that causes damage to health and environment. Ammonia was enormously produced in many applications such as fertilizers, refrigerant chemical and urine from humans and animals [107, 108]. The maximum allowable concentration of ammonia at the working place for 8 hours is 25 ppm (18 mg/m^3 of air). This is regulated by the National Institute for Occupational Safety and Health in U.S. Department of Health and Human Services.

In term of applicability of ammonia gas sensing, the color changing of BF_2 -CurOH-loaded zein fiber mat was investigated by varying the concentration of NH_3 at 572.4, 1,431 and 2,862 mg/L. The photographs of BF_2 -CurOH-loaded zein fiber mat

after being exposed to ammonia gas at different concentrations were shown in Figure 4.26. The color of BF₂-CurOH-loaded zein fiber mats changed under presence of ammonia gas while the one in the air without ammonia gas did not change. One possible reason for this phenomenon is described by the strong intermolecular charge transfer (ICT) process [4, 90, 109]. BF₂-CurOH contains methoxy phenol as electron donor parts at both conjugated *pi*-system and difluoroboron enolate as electron acceptor. In the presence of NH₃, BF₂-CurOH was assumed to undergo the deprotonation of hydroxyl groups by NH₃. The negative charges could delocalize through *pi*-conjugated bond to acceptor unit resulting in a strong *pi*-delocalization. The color change of BF₂-CurOH was occurred. The intermolecular charge transfer (ICT) process of BF₂-CurOH + NH₃ was shown in Scheme 4.4. Moreover, the degree of color change of the BF₂-CurOH-loaded zein fiber mat increased proportionally with the increasing concentration of ammonia gas, from orange to dark-green.

In conclusion, the result demonstrated that this method can be applied for ammonia gas sensing by the naked-eye.

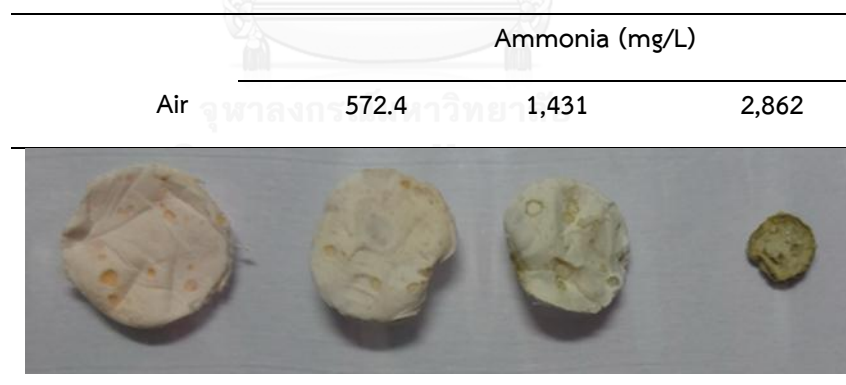
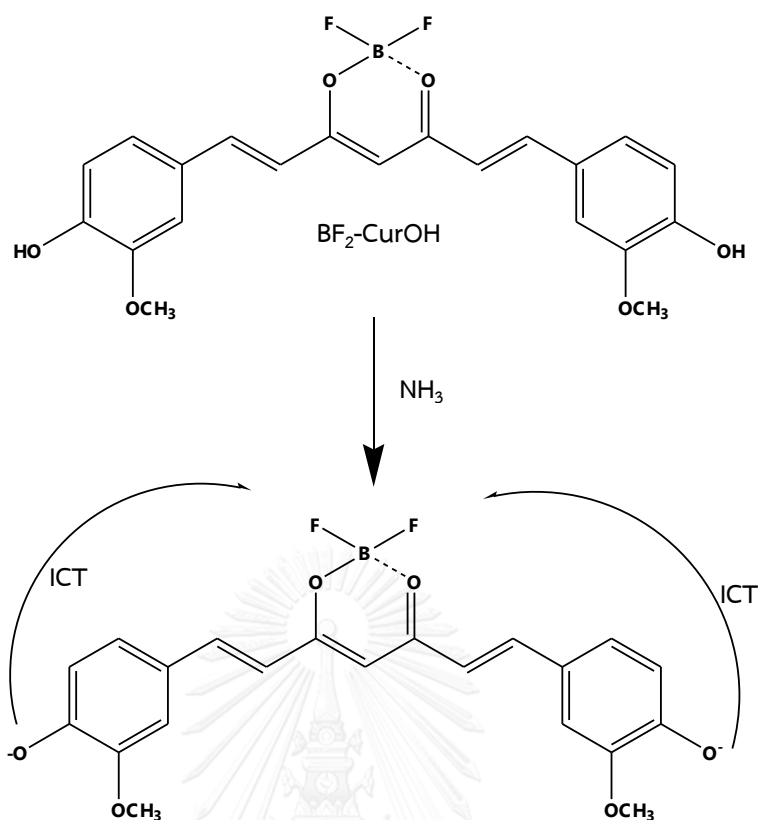


Figure 4.26 The photographs of BF₂-CurOH fiber mat after exposing to ammonia gas at different concentrations (time = 30 min, in a boiling water bath)



Scheme 4.4 The ICT process of $\text{BF}_2\text{-CurOH} + \text{NH}_3$

4.6 Electrospun Zein Blending with 3,5-di(4-ethynyl-*N,N*-dimethylanily)-2-hydroxybenzaldehyde (F₃)

In this section, 0.1%wt/wt (3,5-di(4-ethynyl-*N,N*-dimethylanily)-2-hydroxybenzaldehyde (F₃)/zein) fiber mat was fabricated by electrospinning and then crosslinking reaction. The morphology of F₃-loaded zein fiber mat was investigated by scanning electron microscopy (SEM). The functional groups of F₃-loaded zein fiber mat were characterized by Fourier transform infrared spectroscopy (FT-IR). The diffuse reflectance of F₃-loaded zein fiber mat was recorded by diffuse reflectance ultraviolet-visible spectroscopy (DR-UV-Vis). In addition, the naked-eye sensing for iron(III) ions were examined and real water samples were tested.

4.6.1 Morphology of F₃-loaded Zein Fiber Mat

The morphology of F₃-loaded zein fiber mat was investigated by scanning electron microscopy (SEM). The SEM images of F₃-loaded zein fiber mat before and after immersing in DI water were shown in Figure 4.27. The morphology of dry F₃-loaded zein fiber mat show fine fibers without node. It exhibited swelling and maintaining their fibrous networks after immersing in DI water. The average diameter of dry and wet F₃-loaded zein fiber mat were 394±65 nm and 559±197 nm (mean±S.D., n=30), respectively.

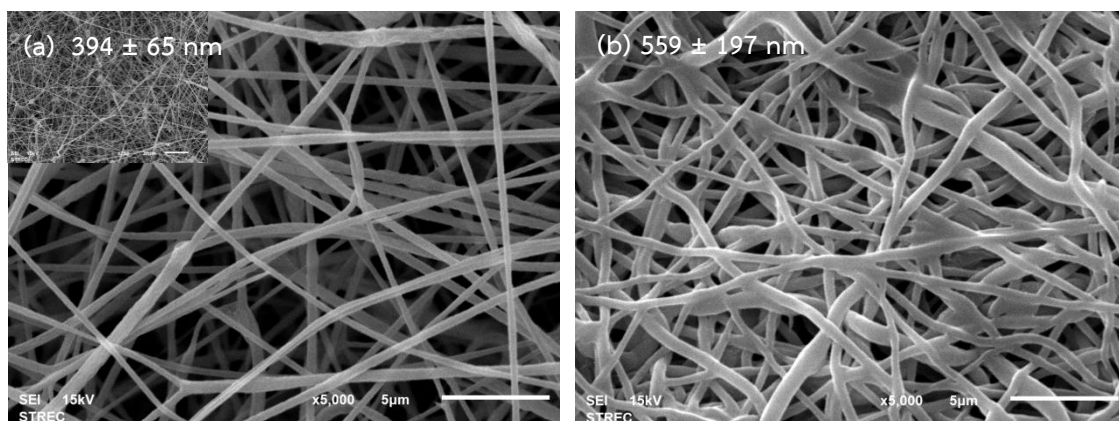


Figure 4.27 SEM images (5,000x magnification) of (a) dry and (b) wet 3,5-di(4-ethynyl-*N,N*-dimethylanily)-2-hydroxybenzaldehyde (F_3)-loaded zein fiber mats before and after immersing in DI water at room temperature for 3 hours (Inset: SEM image (750x magnification))

4.6.2 FT-IR Characterization of F_3 -loaded Zein Fiber Mat

The F_3 -loaded zein fiber mat was characterized by FT-IR. The IR spectrum of F_3 -loaded zein fiber mat was shown in Figure 4.28. The absorption bands of zein and F_3 unit were investigated. For the zein unit, the characteristic bands of curcumin-loaded zein fiber mat were observed at $1515 \text{ (m-s)} \text{ cm}^{-1}$ for N-H bending of amide II group, $1645 \text{ (s)} \text{ cm}^{-1}$ for C=O stretching of amide I group and 3286 (m, broad) and $3057 \text{ (w)} \text{ cm}^{-1}$ for N-H stretching of secondary amide group. For the F_3 unit, the characteristic bands of F_3 -loaded zein fiber mat were not found because of low amount of F_3 loaded in zein fiber mat, 0.1%wt/wt (F_3 /zein).

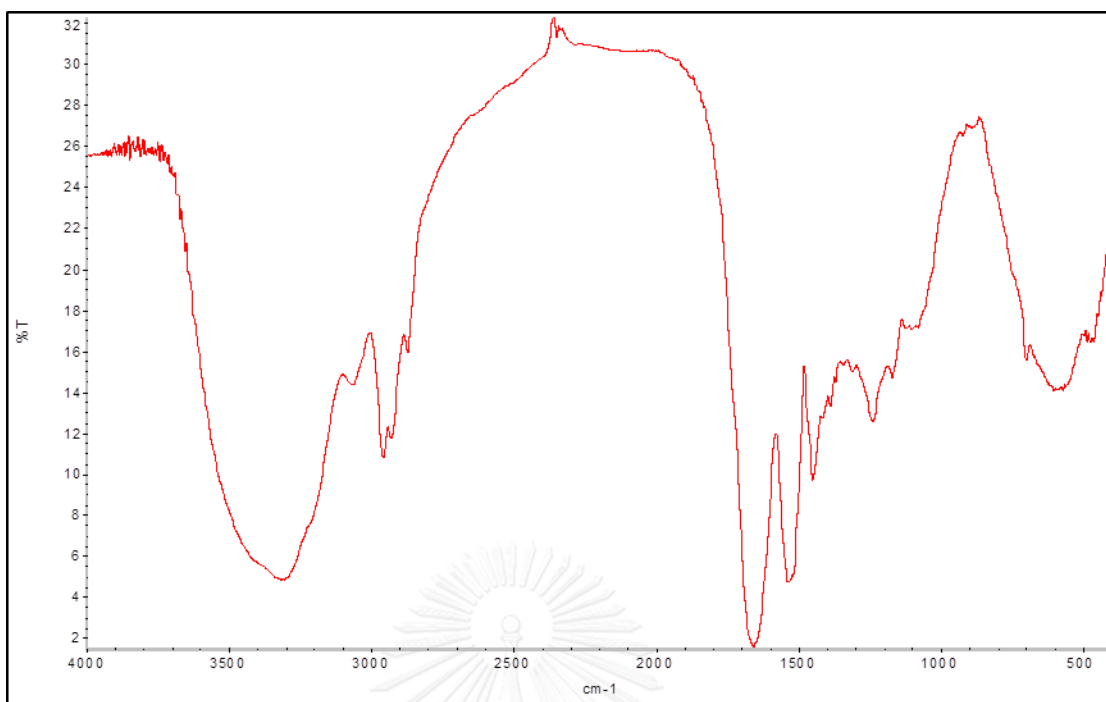


Figure 4.28 FT-IR spectrum of 3,5-di(4-ethynyl-*N,N*-dimethylanily)-2-hydroxybenzaldehyde (F_3)-loaded zein fiber mat

4.6.3 DR-UV-Vis Characterization of F_3 -loaded Zein Fiber Mat

The F_3 -loaded zein fiber mat was characterized by DR-UV-Vis. The DR-UV-Vis spectrum of F_3 -loaded zein fiber mat was shown in Figure 4.29. The absorption bands of F_3 -loaded zein fiber mat were found at 279 and 326 nm. Khumsri *et al* [91] and Niamnont *et al* [5] were reported that F_3 in 90% DMSO/10 mM HEPES buffer pH 7.4 showed two absorption bands at 335 and 385 nm.

Normally, F_3 is a weak fluorescence synthetic dye. F_3 -loaded zein fiber mat was observed by eyes under 20W black light lamp and comparison with zein fiber mat. The photographs of zein fiber mats and F_3 -loaded zein fiber mat were shown in Figure 4.30. The F_3 -loaded zein fiber mat presented as weak green fluorescence while zein fiber mat showed as non-fluorescence.

In conclusion, this result can be indicated that the incorporating of F_3 into the zein fiber mat was created.

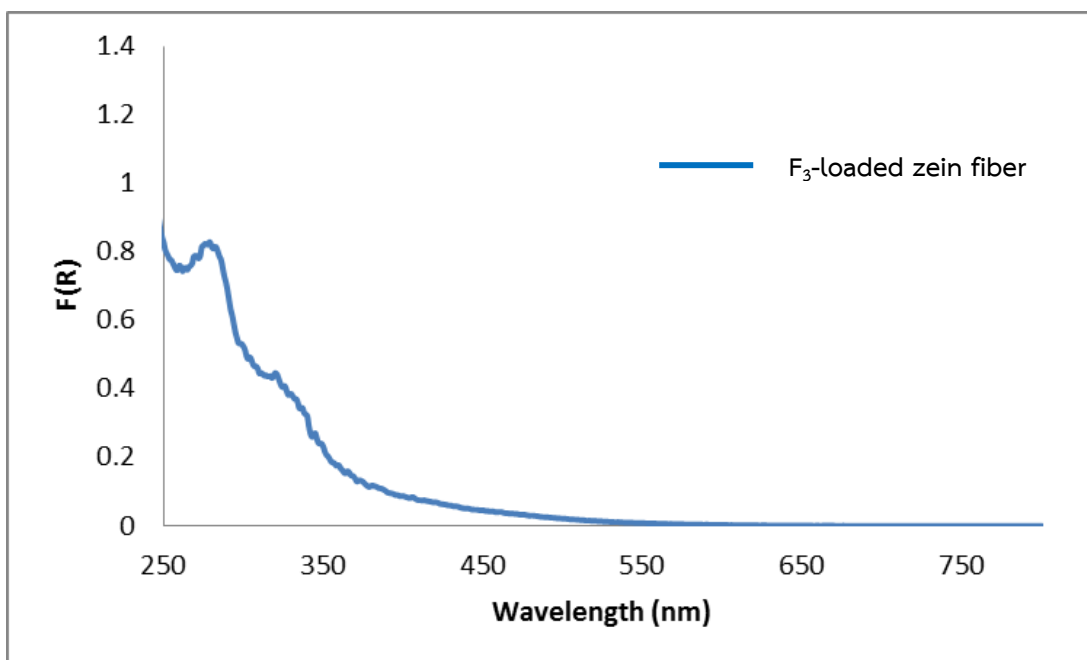


Figure 4.29 DR-UV-Vis spectrum of 3,5-di(4-ethynyl-*N,N*-dimethylanily)-2-hydroxybenzaldehyde (F_3)-loaded zein fiber mat

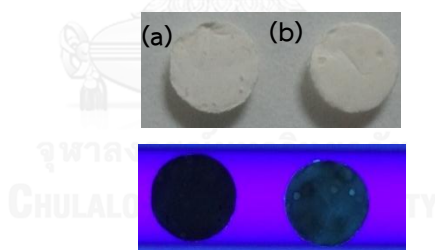


Figure 4.30 The photographs of (a) zein fiber mat and (b) 3,5-di(4-ethynyl-*N,N*-dimethylanily)-2-hydroxybenzaldehyde (F_3)-loaded zein fiber mat under fluorescent lamp (Top) and 20W black light lamp (bottom)

4.6.4 Naked-eye Sensing for Iron(III) Ions

The F₃-loaded zein fiber mat was examined as fluorescent sensor for iron(III) ions sensing. It was observed under 20W black light lamp. For obtaining quantitative data, the mean gray value and its standard deviation (n=3) was evaluated from the photograph of F₃-loaded zein fiber mat using image J software. The mean gray value decreased inversely proportionally with the increasing shade color to dark [20].

Regarding the study of influence of pH, 10 and 100 mg/L of Fe³⁺ solution were prepared at pH 1, 2, 3, 4 and 5. The mean color intensity at various pH values was presented in Figure 4.31. It was found that the most sensitive color change was observed at pH 2. The shade colors of F₃-loaded zein fiber mat was changed from weak green fluorescence to dark in the presence of Fe³⁺ as shown in Figure 4.32. The reason for this phenomenon is explained by occurred quenching with Fe³⁺. This agreed with the results published by Ye *et al* [110]. In the absence of Fe³⁺, F₃ displays weak fluorescence. It contains diphenylacetylene as fluorogenic units which have many conjugated systems. Upon excitation with light, the emission of radiation occurs. On the other hand, the fluorescence intensity of F₃ was reduced into dark upon increasing the concentration of Fe³⁺. This quenching may be due to the formation of coordination complexes between Fe³⁺ ions and oxygen atom on salicylaldehyde groups. It inhibited the emission properties. The proposed quenching mechanism of F₃ + Fe³⁺ was shown in Scheme 4.5. For 100 mg/L of Fe³⁺ solution at the pH range of 3 to 5, the mean color intensity of F₃-loaded zein fiber mat did not decrease because Fe³⁺ was precipitated. Therefore, pH 2 was chosen in this experiment.

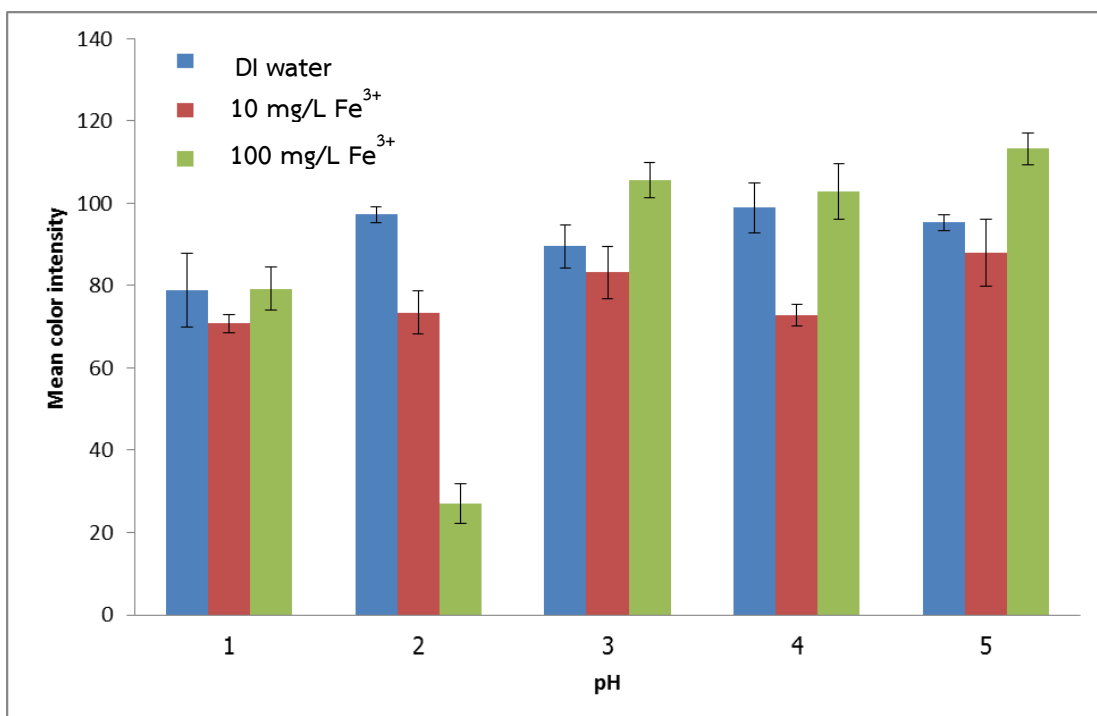


Figure 4.31 The mean color intensity at various pH values (sample volume = 1 mL, 3 hours, under 20 W black light)


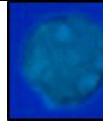
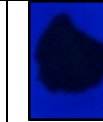
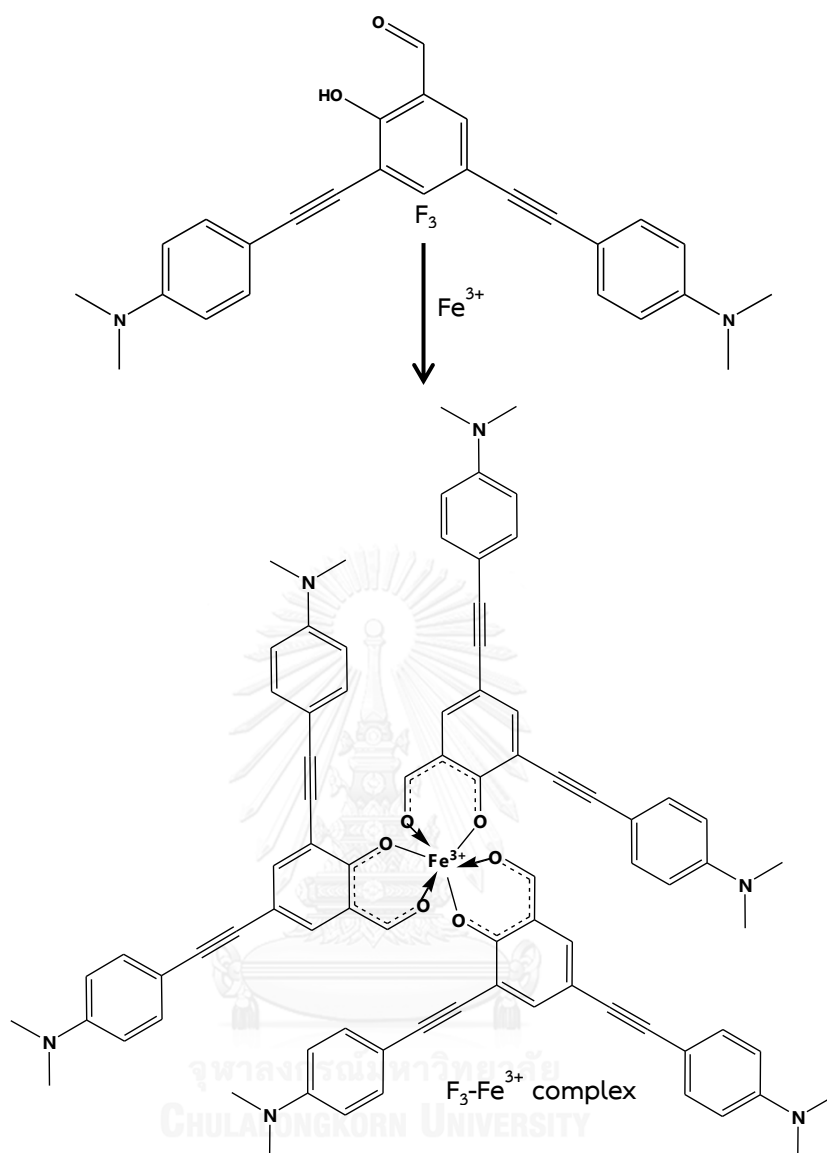
DI water	Fe ³⁺ (mg/L)	
	10	100
		

Figure 4.32 Photographs of 3,5-di(4-ethynyl-*N,N*-dimethylanily)-2-hydroxybenzaldehyde (F₃)-loaded zein fiber mats immersed in DI water and Fe³⁺ solution at pH 2 (sample volume = 1 mL, 3 hours, under 20 W black light)



Scheme 4.5 The proposed quenching mechanism of $F_3 + Fe^{3+}$

Concerning the study of effect of interferences, 17 metal ions (Ag^+ , As^{5+} , Ba^{2+} , Ca^{2+} , Cd^{2+} , Co^{2+} , Cr^{3+} , Cu^{2+} , Fe^{2+} , Hg^{2+} , K^+ , Mn^{2+} , Na^+ , Ni^{2+} , Pb^{2+} , Zn^{2+} and Mg^{2+}) of 200 μM were prepared at pH 2. The photographs of F_3 -loaded zein fiber mats after immersing into various metal ion solutions were shown in Figure 4.33. It was found that the color of the F_3 -loaded zein fiber mat was significantly changed to dark only after dipping into the solution of Fe^{3+} . For the solution of other metal ions, the color of the F_3 -loaded zein fiber mat remained the same as the blank test using only DI water, the fiber mat exhibited weak green fluorescence. It implied that the

fluorescence was quenched by Fe^{3+} . Aydin *et al.* and Buss *et al.* reported that salicylaldehyde group showed strong affinity to Fe^{3+} [111, 112]. In addition, the mean color intensity with various metal ion solutions was evaluated by image J software as shown in Figure 4.34. The mean gray value significantly dropped only in the presence of Fe^{3+} . Therefore, F_3 -loaded zein fiber mats colorimetrically responded selectively to Fe^{3+} .

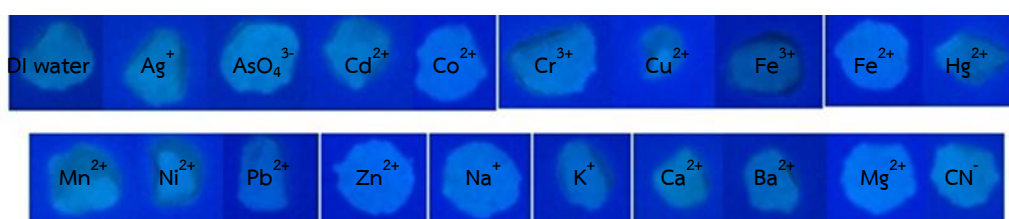


Figure 4.33 Photographs of F_3 fiber mats after immersing into various solutions (concentration = 200 μM , pH = 2, sample volume = 1 mL, 3 hours, under 20 W black light)

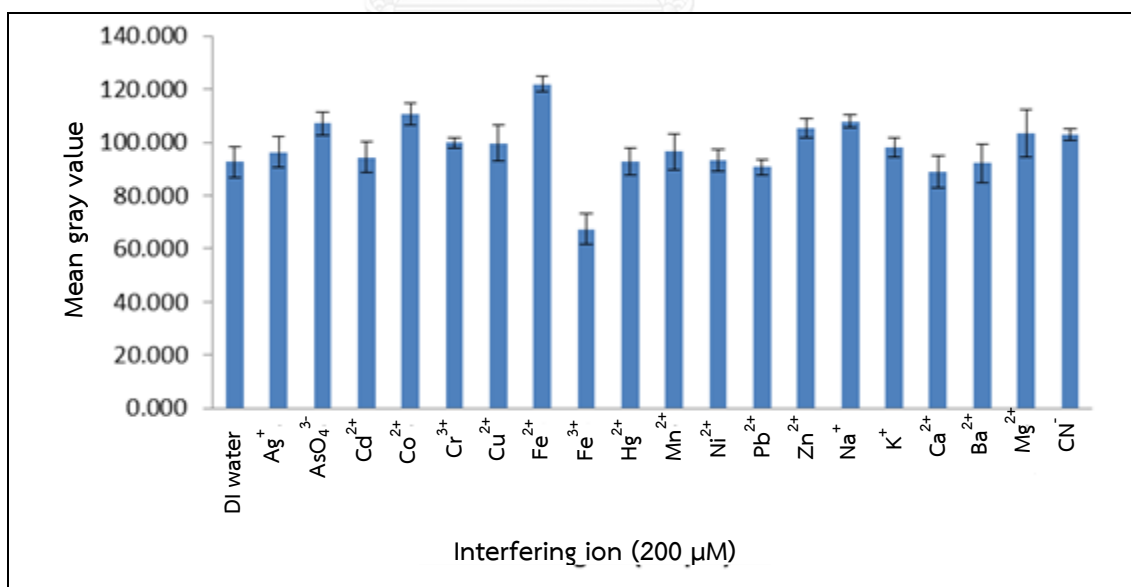


Figure 4.34 The mean color intensity with various metal ion solutions (concentration = 200 μM , pH = 2, sample volume = 1 mL, 3 hours, under 20 W black light)

For the qualitative analysis, the color change of F₃-loaded zein fiber mat was investigated by varying the concentration of Fe³⁺ from 0-500 mg/L. The photographs of the F₃-loaded zein fiber mats after immersing into solutions at different concentrations were shown in Figure 4.35. It was found that the color change of the F₃ fiber mat was observed at the concentration of Fe³⁺ equal to or greater than 10 mg/L. For the concentration Fe³⁺ below 10 mg/L, the color of F₃-loaded zein fiber mats was not significantly changed. The stable color change of F₃-loaded zein fiber mats was observed at 3 hours.

For the quantitative analysis, the mean color intensity with various concentration of Fe³⁺ was shown in Figure 4.36. The result showed that the mean color intensity decreased with increasing concentration of Fe³⁺. In addition, the mean color intensity and concentrations of Fe³⁺ in the range of 20-50 mg/L was plotted in Figure 4.37. This graph acting as the calibration graph for Fe³⁺ sensing was linear with a coefficient of determination (R²) of 0.989 and the linear equation of $y = -1.69x + 113.84$.

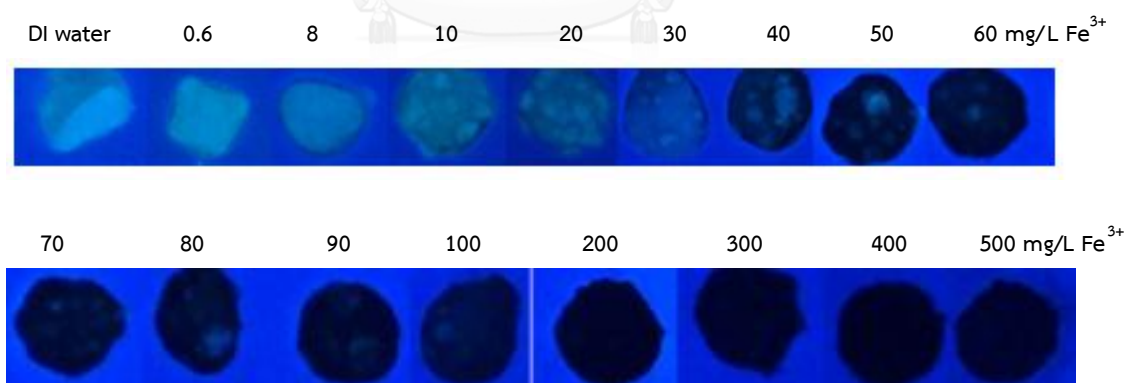


Figure 4.35 The photographs of the F₃-loaded zein fiber mats after immersing into solutions at different concentration (pH = 2, sample volume = 1 mL, 3 hours, under 20 W black light)

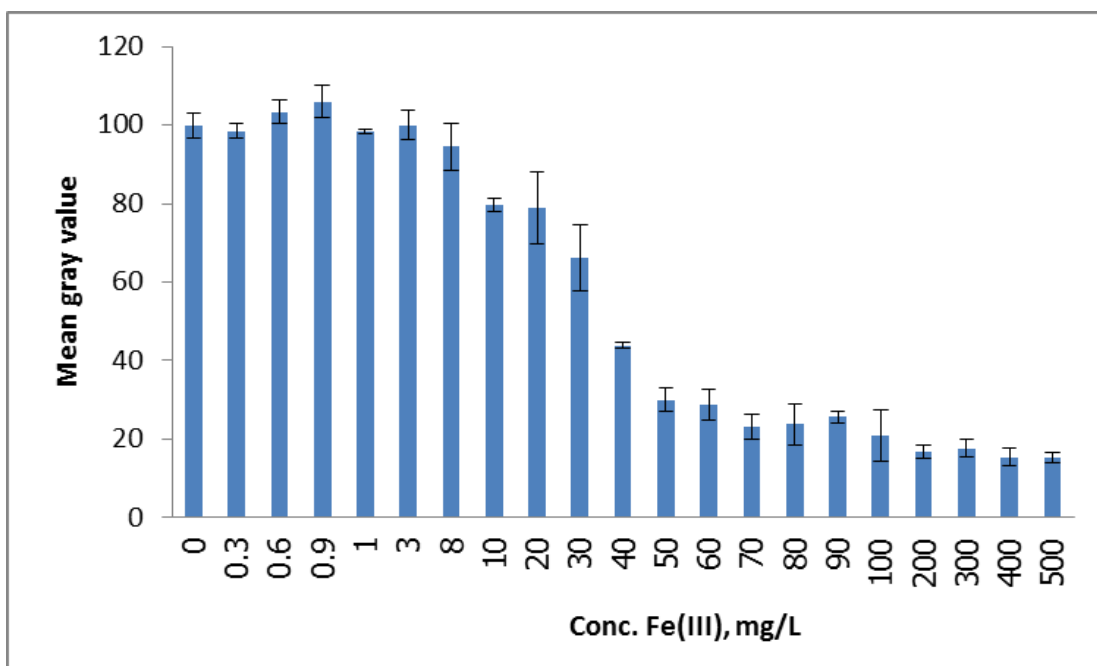


Figure 4.36 The mean color intensity and concentration of Fe^{3+} in various concentrations (pH = 2, sample volume = 1 mL, 3 hours, under 20 W black light)

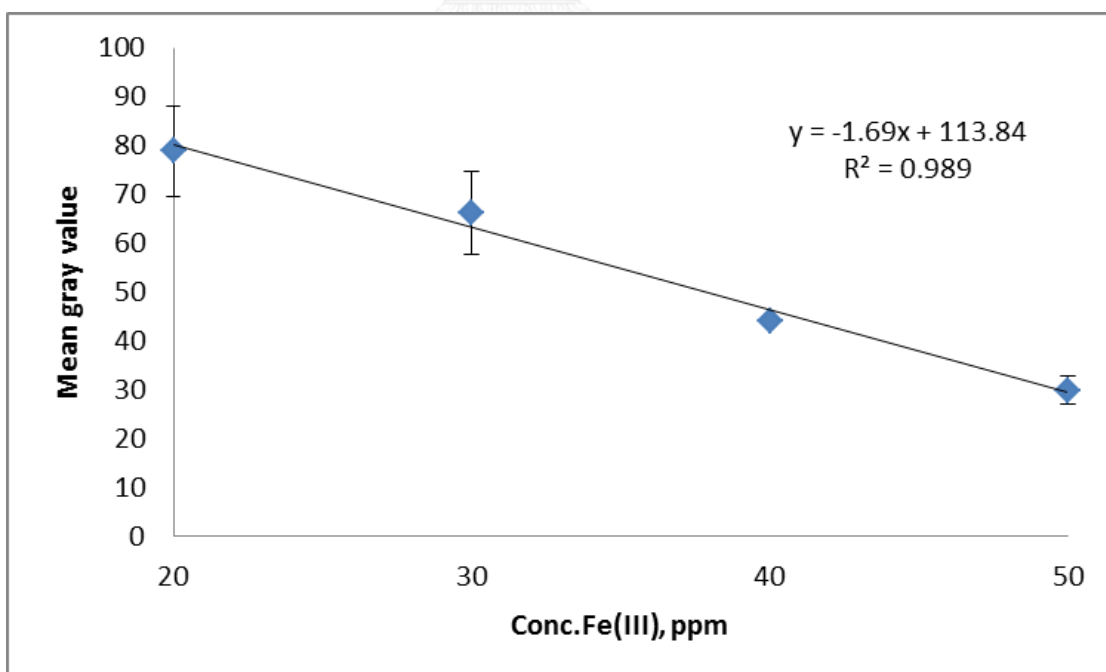


Figure 4.37 The calibration graph for Fe^{3+} sensing (pH = 2, sample volume = 1 mL, 3 hours, under 20 W black light)

4.6.5 Analysis of Real Water Samples

The high concentration of iron was focused to analyze for some application such as ground water, mine wastewater and industrial wastewater. The applicability of the proposed method was evaluated by determination of Fe^{3+} in three real water samples including ground water, pond water and tap water. The comparative results of Fe(III) ion concentration determined by the naked-eye, Image J software and inductively coupled plasma-optical emission spectrometer (ICP-OES) as shown in Figure 4.38. The concentration of Fe^{3+} was verified by ICP-OES [106].

For qualitative test, the color change of F_3 -loaded zein fiber mat can be easily used to analyze qualitatively by comparing with a calibration color chart. The calibration color chart was shown in Figure 4.35. It was found that the color of F_3 -loaded zein fiber mat did not change when dipping into all non-spiked real samples. It indicates that the concentration of Fe^{3+} in all non-spiked real water samples was below 10 mg/L as the LOD of the proposed naked eye method. From the results determined by ICP-OES, the Fe concentrations of all non-spiked real water samples are in the range of 0.12-0.31 mg/L. In addition, the shade color of the F_3 -loaded zein fiber mat increased to dark for spiked real samples. These imply that the concentration of Fe^{3+} in all spiked real water sample was equal or upper 10 mg/L.

For quantitative test, the mean color intensity of F_3 fiber mat can be used to analyze quantitatively using the calibration graph for Fe^{3+} sensing. The calibration graph for Fe^{3+} sensing was shown in Figure 4.37. The linear equation is $y = -1.69x + 113.84$ in the range of 20-50 mg/L Fe^{3+} solution. The fiber mats of spiked real water samples were determined by image J software. It was found that the result from image J software detection produced moderately accuracy comparing with the result from ICP-OES. The reason may be suggested that some species in real sample waters could have reaction with F_3 -loaded zein fiber. The mean color intensity was decreased.



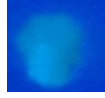

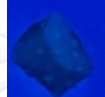

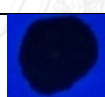


Real samples	[Fe ³⁺], ppm			
	Naked-eye	Image J	ICP-OES	
Ground water	<10		n.d.	0.31 ± 0.02
Pond water	<10		n.d.	0.13 ± 0.03
Tap water	<10		n.d.	0.12 ± 0.00
Ground water	>10		39.8 ± 7.0	28.9 ± 0.3
Pond water	>10		32.3 ± 4.9	28.8 ± 0.5
Tap water	>10		37.8 ± 3.7	28.8 ± 0.5
Ground water	>10		n.d.	64.0 ± 0.04
Pond water	>10		n.d.	61.66 ± 1.8
Tap water	>10		n.d.	60.0 ± 2.3
Condition: pH = 2, sample volume = 1 mL, 3 hours, under 20 W black light				
The values indicated on the concentration of Fe determined by ICP-OES.				

Figure 4.38 The comparative results of Fe(III) ion concentration determined by naked-eye, Image J software and ICP-OES

4.7 Comparison of Fiber Mat and Film Sensing Efficiency

5%wt/wt (curcumin/zein) of curcumin-loaded zein film was prepared by hand casting. The morphology of curcumin-loaded zein film and zein film were investigated by scanning electron microscopy (SEM). The SEM images of curcumin film and zein film before and after immersing in DI water were shown in Figure 4.39. The morphology of dry film exhibits flat form. After immersing in DI water, the morphology of wet film showed rough form with low porosity.

For comparison of fiber mat and film sensing efficiency, 5%wt/wt (curcumin/zein) of curcumin-loaded zein film and 5%wt/wt (curcumin/zein) of curcumin-loaded zein fiber mat were tested into 10 mg/L of Fe^{3+} solution at pH 2 for 3 hours. The photographs of curcumin-loaded zein film and curcumin-loaded zein fiber mat after immersing into 10 mg/L of Fe^{3+} solution were shown in Figure 4.40. It was found that the color of curcumin-loaded zein fiber mat was significantly changed from yellow to dark brown while the color of curcumin-loaded zein film was slightly change from yellow to light brown after immersing into 10 mg/L of Fe^{3+} solution for 3 hours. In addition, the degree of color change of curcumin-loaded zein film increased from yellow to dark brown after immersing in 10 mg/L of Fe^{3+} in solution for 24 hours. The photographs of curcumin film after immersing in 10 mg/L of Fe^{3+} solution for 24 hours was shown in Figure 4.41. The result indicates that the film takes time longer than fiber mat for sensing. The reason for this phenomenon is explained by the surface area of material that is generally a factor on reaction rate. The rate of reaction increases with increasing the surface area.

In conclusion, the fiber mat sensing efficiency was higher than the cast film.

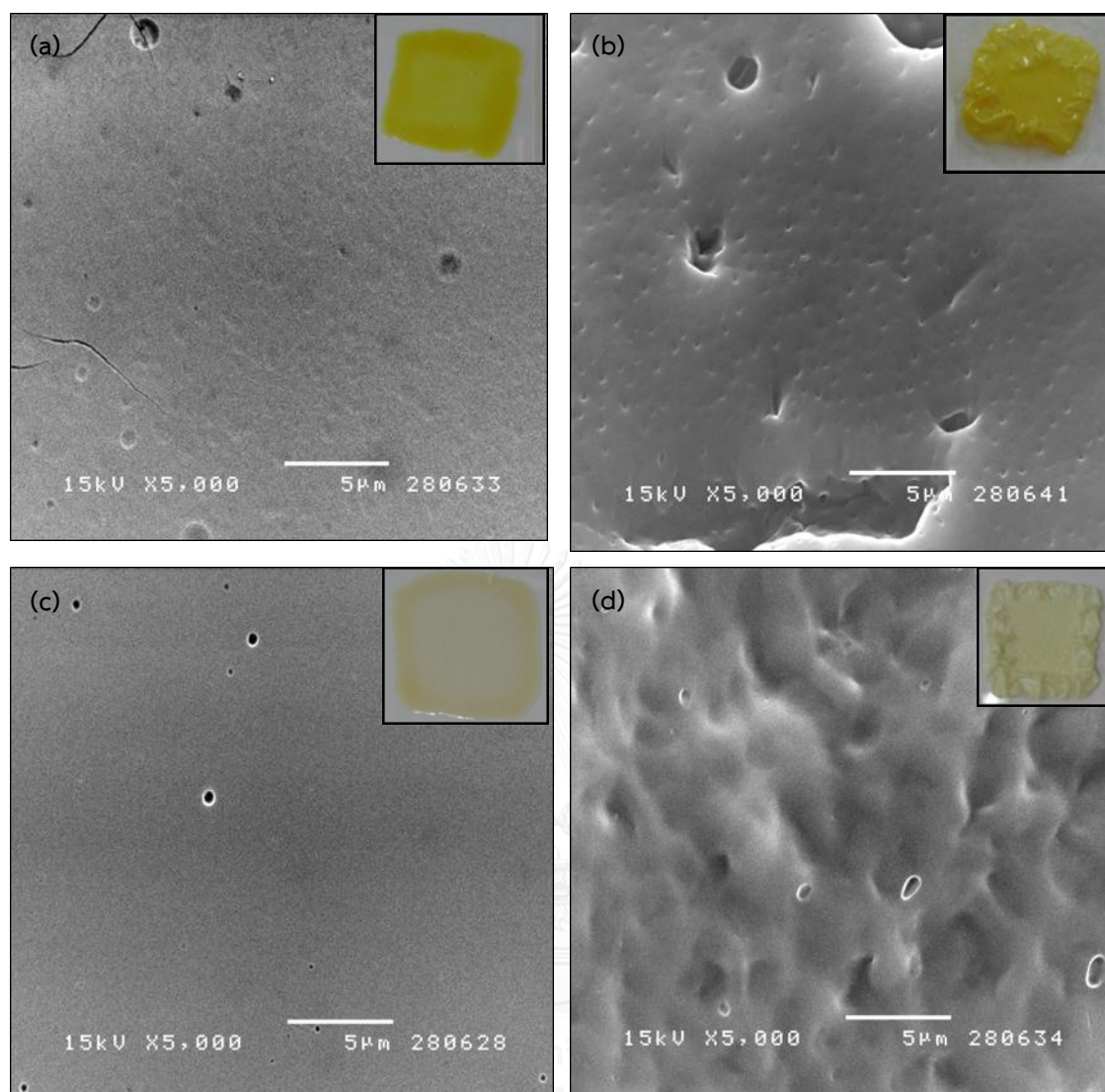


Figure 4.39 SEM images (5,000x magnification) of (a) dry and (b) wet curcumin-loaded zein film (c) dry and (d) wet zein film before and after immersing in DI water at room temperature for 3 hours (Inset: the photographs of films (upper right corner))

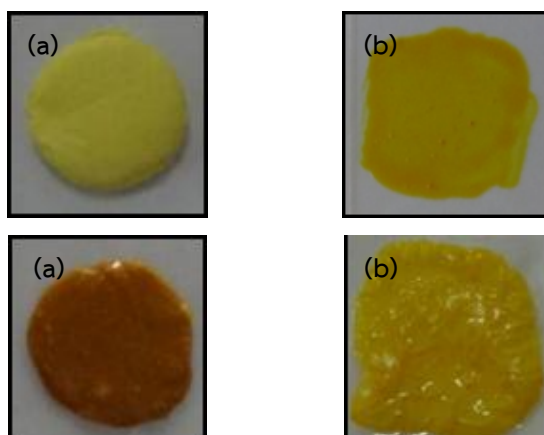


Figure 4.40 The photographs of curcumin-loaded zein (a) fiber mat and (b) film before (top) and after (bottom) immersed into 10 mg/L of Fe^{3+} solution (sample volume = 3 mL, time = 3 hours, room temperature)

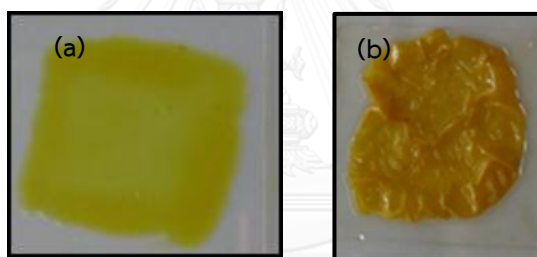


Figure 4.41 The photographs of curcumin-loaded zein film before (a) and after (b) immersed in 10 mg/L of Fe^{3+} solution for 24 hours (sample volume = 3 mL, room temperature).

CHAPTER V

CONCLUSION AND SUGGESTIONS

5.1 Conclusion

Difluoroboron curcumin ($\text{BF}_2\text{-CurOH}$) was synthesized from curcumin and borontrifluoride diethyletherate. 3,5-Di(4-ethyl-*N,N*-dimethylanily)-2-hydroxybenzaldehyde (F_3) was synthesized from 2-hydroxybenzaldehyde and 4-ethynyl-*N,N*-dimethylaniline. Curcumin, $\text{BF}_2\text{-CurOH}$ and F_3 were applied as coloring agents. All coloring agents were characterized by Fourier transform infrared spectroscopy (FT-IR) and nuclear magnetic resonance spectroscopy (NMR). The results from all characterization techniques could evidently confirm the structures of the coloring agents.

The zein blending with coloring agents (curcumin, $\text{BF}_2\text{-CurOH}$ and F_3) fiber mats was fabricated by electrospinning and amide crosslinking. All fiber mats were characterized by scanning electron microscopy (SEM), Fourier transform infrared spectroscopy (FT-IR) and diffuse reflectance ultraviolet-visible spectroscopy (DRUV-Vis). After that, fiber mats sensing ability were investigated by naked-eye.

From preliminary study, the amount of coloring agent on zein fiber mats for analysis of ions was investigated. It was found that the optimum coloring agent loading for analysis of ions could be achieved at 5%wt/wt (curcumin/zein) of curcumin-loaded zein fiber mat, 0.25%wt/wt ($\text{BF}_2\text{-CurOH}$ /zein) of BF_2 -loaded zein fiber mat and 0.1%wt/wt (F_3 /zein) of F_3 -loaded zein fiber mat.

For an electrospun zein blending with curcumin fiber mat, the SEM image showed satisfactory non-woven fiber mat with an average diameter of 586 ± 131 nm. The DR-UV-Vis spectrum showed the maximum absorption band at 424 nm. The concentration of Fe^{3+} solution was determined by naked-eye detection after dipping fiber mat into the solution. The color of fiber mat changed from yellow to brown in the presence of Fe^{3+} . The effect of pH and interfering metal ions (Ag^+ , As^{5+} , Ba^{2+} , Ca^{2+} , Cd^{2+} , Co^{2+} , Cr^{3+} , Cu^{2+} , Fe^{2+} , Hg^{2+} , K^+ , Mn^{2+} , Na^+ , Ni^{2+} , Pb^{2+} , Zn^{2+} and Mg^{2+}) were

investigated. It was found that the optimal sensing condition was at pH 2 without any significant interfering ions. The intensity of color change increased in agreement with the increasing concentration of Fe^{3+} . Its optical detection limit was 0.4 mg/L. This method could be practically used for analysis of Fe^{3+} in potable water samples with a good accuracy comparing with the reference method by inductive coupled plasma optical emission spectrometry (ICP-OES).

For an electrospun zein blending with difluoroboron curcumin ($\text{BF}_2\text{-CurOH}$) fiber mat, the SEM image showed fiber network before and after immersing in DI water with an average diameter of 429 ± 89 nm and 840 ± 174 nm, respectively. The DR-UV-Vis spectrum showed the absorption band at the region of 425 to 600 nm. The $\text{B}_4\text{O}_7^{2-}$ solution in the pH range 7 to 10 was determined by naked-eye detection after dipping fiber mat into the solution. The color of fiber mat changed from orange to green in the presence of $\text{B}_4\text{O}_7^{2-}$. Unfortunately, the fiber mat could not maintain fiber morphology. It became distorted and exploded on fiber morphology. The applicability for ammonia gas sensing was examined. It was found that the color of fiber mat changed from orange to green as a result of intermolecular charge transfer (ICT) process. The intensity of changing color increased in accordance with the increasing concentration of NH_3 . The result implied that this method can be used for ammonia sensing by naked-eye.

For an electrospun zein blending with 3,5-di(4-ethyl-*N,N*-dimethylanily)-2-hydroxybenzaldehyde (F_3) fiber mat, the average diameter of fibers mat was 394 ± 65 nm. The DR-UV-Vis spectrum showed the absorption band at 279 and 326 nm. The shade colors of fiber mat changed from weak green fluorescence to dark in the presence of Fe^{3+} . The effect of solution pH and co-existing metal ions (Ag^+ , As^{5+} , Ba^{2+} , Ca^{2+} , Cd^{2+} , Co^{2+} , Cr^{3+} , Cu^{2+} , Fe^{2+} , Hg^{2+} , K^+ , Mn^{2+} , Na^+ , Ni^{2+} , Pb^{2+} , Zn^{2+} and Mg^{2+}) were examined. It was found that the optimal sensing condition was at pH 2 without significant effect of interfering ions. The visual detection limit was 10 mg/L. For quantitative detection, the mean gray value was evaluated from the photograph of fiber mat using image J software. It was found that the graph between the mean gray value and the concentration of Fe^{3+} in the range of 20-50 mg/L was linear with a

coefficient of determination (R^2) of 0.989. The fiber mat via image J software detection was applied to the determination of concentration Fe^{3+} in potable water, surface water and ground water samples with moderately accuracy comparing with the result from ICP-OES detection.

In addition, the fiber mat efficiency was compared with the cast film. 5%wt/wt (curcumin/zein) fiber mat and film were observed after immersing in 10 mg/L of Fe^{3+} solution at pH 2. It was found that the film took time longer than the fiber mat for Fe^{3+} sensing. Therefore, the fiber mat sensing efficiency was higher than the film.

In conclusion, the simple coloring agent-loaded zein fiber mats for analysis of ions as new optical sensors were successfully established by electrospinning and followed amide crosslinking using citric acid as a non-toxic crosslinker. This technique is easy to use, low cost and fall in environmental friendly technique.

5.2 Suggestions for Future Work

For an electrospun zein blending with difluoroboron curcumin ($\text{BF}_2\text{-CurOH}$), a suitable method for ammonia gas sensing should be further studied in a flow gas system. Moreover, it is well known that an electrospun coloring agent-loaded zein fiber mat as a colorimetric sensor is easily developed. The natural coloring agent can be applied for many external stimuli sensing such as chemicals, pH, temperature, humidity.

REFERENCES

- [1] Gomez-Estaca, J., Balaguer, M.P., Gavara, R., and Hernandez-Munoz, P. Formation of zein nanoparticles by electrohydrodynamic atomization: effect of the main processing variables and suitability for encapsulating the food coloring and active ingredient curcumin. Food Hydrocolloids 28 (2012): 82-91.
- [2] Borsari, M., Ferrari, E., Grandi, R., and Saladini, M. Curcuminoids as potential new iron-chelating agent: spectroscopic, polarographic and potentiometric study on their Fe(III) complexing ability. Inorganica Chimica Acta 328 (2002): 61-68.
- [3] Kuswandi, B., Jayus, Larasati, T.S., Abdullah, A., and Heng, L.Y. Real-time monitoring of shrimp spoilage using on-package sticker sensor based on natural dye of curcumin. Food Analytical Methods 5 (2011): 881-889.
- [4] Chaicham, A., Kulchat, S., Tumcharern, G., Tuntulani, T., and Tomapatanaget, B. Synthesis, photophysical properties, and cyanide detection in aqueous solution of BF₂-curcumin dyes. Tetrahedron 66 (2010): 6217-6223.
- [5] Niamnont, N., Khumsri, A., Promchat, A., Tumcharern, G., and Sukwattanasinitt, M. Novel salicylaldehyde derivatives as fluorescence turn-on sensors for cyanide ion. Journal of Hazardous Materials 280 (2014): 458-463.
- [6] Mecitoğlu, Ç., Yemenicioğlu, A., Arslanoğlu, A., Elmacı, Z.S., Korel, F., and Çetin, A.E. Incorporation of partially purified hen egg white lysozyme into zein films for antimicrobial food packaging. Food Research International 39 (2006): 12-21.
- [7] Dong, J., Sun, Q., and Wang, J.Y. Basic study of corn protein, zein, as a biomaterial in tissue engineering, surface morphology and biocompatibility. Biomaterials 25 (2004): 4691-4697.
- [8] Wang, H.J., Lin, Z.X., Liu, X.M., Sheng, S.Y., and Wang, J.Y. Heparin-loaded zein microsphere film and hemocompatibility. Journal of Controlled Release 105 (2005): 120-131.

- [9] Jiang, Q., Reddy, N., and Yang, Y. Cytocompatible cross-linking of electrospun zein fibers for the development of water-stable tissue engineering scaffolds. Acta Biomaterialia 6 (2010): 4042-4051.
- [10] Poltue, T., Rangkupan, R., Dubas, S.T., and Dubas, L. Nickel (II) ions sensing properties of dimethylglyoxime/poly(caprolactone) electrospun fibers. Materials Letters 65 (2011): 2231-2234.
- [11] Wang, X., Si, Y., Wang, J., Ding, B., Yu, J., and Al-Deyab, S.S. A facile and highly sensitive colorimetric sensor for the detection of formaldehyde based on electro-spinning/netting nano-fiber/nets. Sensors and Actuators B: Chemical 163 (2012): 186-193.
- [12] Kaur, N., and Kumar, S. Colorimetric metal ion sensors. Tetrahedron 67 (2011): 9233-9264.
- [13] Jia, M.-Y., and Feng, L. Recent progresses in optical colorimetric/fluorometric sensor array. Chinese Journal of Analytical Chemistry 41 (2013): 795-802.
- [14] Yang, Z., Zhang, K., Gong, F., Li, S., Chen, J., Ma, J.S., Sobenina, L.N., Mikhaleva, A.I., Trofimov, B.A., and Yang, G. A highly selective fluorescent sensor for fluoride anion based on pyrazole derivative: naked eye "no-yes" detection. Journal of Photochemistry and Photobiology A: Chemistry 217 (2011): 29-34.
- [15] Wanichacheva, N., Praikaew, P., Suwanich, T., and Sukrat, K. "Naked-eye" colorimetric and "turn-on" fluorometric chemosensors for reversible Hg²⁺ detection. Spectrochimica Acta Part A: Molecular Biomolecular Spectroscopy 118 (2014): 908-914.
- [16] Goswami, S., Manna, A., Paul, S., Aich, K., Das, A.K., and Chakraborty, S. Highly reactive (<1min) ratiometric probe for selective 'naked-eye' detection of cyanide in aqueous media. Tetrahedron Letters 54 (2013): 1785-1789.
- [17] Park, J.J., Kim, Y.-H., Kim, C., and Kang, J. Naked eye detection of fluoride and pyrophosphate with an anion receptor utilizing anthracene and nitrophenyl group as signaling group. Tetrahedron Letters 52 (2011): 2759-2763.
- [18] Dutta, D., Sarma, T.K., Chowdhury, D., and Chattopadhyay, A. A polyaniline-containing filter paper that acts as a sensor, acid, base, and endpoint indicator

- and also filters acids and bases. Journal of Colloid Interface Science 283 (2005): 153-159.
- [19] Puntang, S., Siripornnoppakhun, W., Sukwattanasinitt, M., and Ajavakom, A. Solvent colorimetric paper-based polydiacetylene sensors from diacetylene lipids. Journal of Colloid and Interface Science 364 (2011): 366-372.
- [20] Zhou, M., Yang, M., and Zhou, F. Paper based colorimetric biosensing platform utilizing cross-linked siloxane as probe. Biosensors and Bioelectronics 55 (2014): 39-43.
- [21] Ozay, H., and Ozay, O. Rhodamine based reusable and colorimetric naked-eye hydrogel sensors for Fe³⁺ ion. Chemical Engineering Journal 232 (2013): 364-371.
- [22] Isaad, J., El Achari, A., and Malek, F. Bio-polymer starch thin film sensors for low concentration detection of cyanide anions in water. Dyes and Pigments 97 (2013): 134-140.
- [23] Wang, W., Yang, Q., Sun, L., Wang, H., Zhang, C., Fei, X., Sun, m., and Li, Y. Preparation of fluorescent nanofibrous film as a sensing material and adsorbent for Cu²⁺ in aqueous solution via copolymerization and electrospinning. Journal of Hazardous Materials 194 (2011): 185-192.
- [24] Reneker, D.H., and Yarin, A.L. Electrospinning jets and polymer nanofibers. Polymer 49 (2008): 2387-2425.
- [25] Bhardwaj, N., and Kundu, S.C. Electrospinning: a fascinating fiber fabrication technique. Biotechnology Advances 28 (2010): 325-347.
- [26] Li, D., and Xia, Y. Electrospinning of nanofibers: reinventing the wheel? Advanced Materials 16 (2004): 1151-1170.
- [27] Reneker, D.H., and Fong, H. Polymeric nanofibers: introduction USA: Oxford University Press, 2006.
- [28] Taylor, G. Electrically driven jets. Mathematical and Physical Sciences 313 (1969): 453-475.

- [29] Shin, Y.M., Hohman, M.M., Brenner, M.P., and Rutledge, G.C. Experimental characterization of electrospinning: the electrically forced jet and instabilities. Polymer 42 (2001): 9955-9967.
- [30] Li, Dan., and Xia, Y. Electrospinning of nanofibers: reinventing the wheel? Advanced Materials 16 (2004): 1151-1170.
- [31] Huang, Z.-M., Zhang, Y.Z., Kotaki, M., and Ramakrishna, S. A review on polymer nanofibers by electrospinning and their applications in nanocomposites. Composites Science and Technology 63 (2003): 2223-2253.
- [32] Jiang, H., Fang, D., Hsiao, B.S., Chu, B., and Chen, W. Optimization and characterization of dextran membranes prepared by electrospinning. Biomacromolecules 5 (2004): 326-333.
- [33] Huang, L., Nagapudi, K., Apkarian, R.P., and Chaikof, E.L. Engineered collagen-PEO nanofibers and fabrics. Journal of Biomaterials Science, Polymer Edition 12 (2001): 979-993.
- [34] Zhao, Z., Li, J., Yuan, X., Li, X., Zhang, Y., and Sheng, J. Preparation and properties of electrospun poly(vinylidene fluoride) membranes. Journal of Applied Polymer Science 97 (2005): 466-474.
- [35] Zhang, C., Yuan, X., Wu, L., Han, Y., and Sheng, J. Study on morphology of electrospun poly(vinyl alcohol) mats. European Polymer Journal 41 (2005): 423-432.
- [36] Kim, B., Park, H., Lee, S.H., and Sigmund, W.M. Poly(acrylic acid) nanofibers by electrospinning. Materials Letters 59 (2005): 829-832.
- [37] Son, W.K., Youk, J.H., Lee, T.S., and Park, W.H. The effects of solution properties and polyelectrolyte on electrospinning of ultrafine poly(ethylene oxide) fibers. Polymer 45 (2004): 2959-2966.
- [38] Jun, Z., Youling, Y., Kehua, W., Jian, S., and Sicong, L. Surface modification of segmented poly(ether urethane) by grafting sulfo ammonium zwitterionic monomer to improve hemocompatibilities. Colloids and Surfaces B: Biointerfaces 28 (2003): 1-9.

- [39] Chen, V.J., and Ma, P.X. Nano-fibrous poly(L-lactic acid) scaffolds with interconnected spherical macropores. Biomaterials 25 (2004): 2065-2073.
- [40] Demir, M.M., Yilgor, I., Yilgor, E., and Erman, B. Electrospinning of polyurethane fibers. Polymer 43 (2002): 3303-3309.
- [41] Gupta, P., Elkins, C., Long, T.E., and Wilkes, G.L. Electrospinning of linear homopolymers of poly(methyl methacrylate): exploring relationships between fiber formation, viscosity, molecular weight and concentration in a good solvent. Polymer 46 (2005): 4799-4810.
- [42] Koski, A., Yim, K., and Shivkumar, S. Effect of molecular weight on fibrous PVA produced by electrospinning. Materials Letters 58 (2004): 493-497.
- [43] Ki, C.S., Baek, D.H., Ganga, K.D., Lee, K.H., Um, I.C., and Park, Y.H. Characterization of gelatin nanofiber prepared from gelatin-formic acid solution. Polymer 46 (2005): 5094-5102.
- [44] Geng, X., Kwon, O.H., and Jang, J. Electrospinning of chitosan dissolved in concentrated acetic acid solution. Biomaterials 26 (2005): 5427-5432.
- [45] Buchko, C.J., Chena, L.C., Shena, Y., and Martin, D.C. Processing and microstructural characterization of porous biocompatible protein polymer thin films. Polymer 40 (1999): 7397-7407.
- [46] Sill, T.J., and Recum, H.A. Electrospinning: applications in drug delivery and tissue engineering. Biomaterials 29 (2008): 1989-2006.
- [47] Zuo, W., Zhu, M., Yang, W., Yu, H., Chen, Y., and Zhang, Y. Experimental study on relationship between jet instability and formation of beaded fibers during electrospinning. Polymer Engineering and science (2005): 704-709.
- [48] Mit-uppatham, C., Nithitanakul, M., and Supaphol, P. Ultrafine electrospun polyamide-6 fibers: effect of solution conditions on morphology and average fiber diameter. Macromolecular Chemistry Physics 205 (2004): 2327-2338.

- [49] Desai, K., Kit, K., Li, J., Davidson, P.M., Zivanovic, S., and Meyer, H. Nanofibrous chitosan non-wovens for filtration applications. Polymer 50 (2009): 3661-3669.
- [50] Ignatova, M., Manolova, N., and Rashkov, I. Novel antibacterial fibers of quaternized chitosan and poly(vinyl pyrrolidone) prepared by electrospinning. European Polymer Journal 43 (2007): 1112-1122.
- [51] Khadka, D.B., and Haynie, D.T. Protein- and peptide-based electrospun nanofibers in medical biomaterials. Nanomedicine 8 (2012): 1242-1262.
- [52] Chigome, S., and Torto, N. A review of opportunities for electrospun nanofibers in analytical chemistry. Analytica Chimica Acta 706 (2011): 25-36.
- [53] Torres-Giner, S., Gimenez, E., and Lagaron, J.M. Characterization of the morphology and thermal properties of zein prolamine nanostructures obtained by electrospinning. Food Hydrocolloids 22 (2008): 601-614.
- [54] Argos, P., Pedersen, K., Marks, M.D., and Larkins, B.A. Structural model for maize zein proteins. The Journal of Biological Chemistry 257 (1982): 9984-9990.
- [55] Shukla, R., and Cheryan, M. Zein: the industrial protein from corn. Industrial Crops and Products 13 (2001): 171-192.
- [56] Wang, Q., Geil, P., and Padua, G. Role of hydrophilic and hydrophobic interactions in structure development of zein films. Journal of Polymers and the Environment 12 (2004): 197-202.
- [57] Miyoshi, T., Toyohara, K., and Minematsu, H. Preparation of ultrafine fibrous zein membranes via electrospinning. Polymer International 54 (2005): 1187-1190.
- [58] Selling, G.W., Biswas, A., Patel, P., Walls, D.J., Dunlap, C., and Wei, Y. Impact of solvent on electrospinning of zein and analysis of resulting fibers. Macromolecular Chemistry and Physics 208 (2007): 1002-1010.
- [59] Yao, C., Li, X., Song, T., Li, Y., and Pu, Y. Biodegradable nanofibrous membrane of zein/silk fibroin by electrospinning. Polymer International 58 (2009): 396-402.

- [60] Torres-Giner, S., Ocio, M.J., and Lagaron, J.M. Novel antimicrobial ultrathin structures of zein/chitosan blends obtained by electrospinning. Carbohydrate Polymers 77 (2009): 261-266.
- [61] Kayaci, F., and Uyar, T. Electrospun zein nanofibers incorporating cyclodextrins. Carbohydrate Polymers 90 (2012): 558- 568.
- [62] Yang, J.M., Zha, L.S., Yu, D.G., and Liu, J. Coaxial electrospinning with acetic acid for preparing ferulic acid/zein composite fibers with improved drug release profiles. Colloids Surf B Biointerfaces 102 (2013): 737-743.
- [63] Neo, Y.P., Ray, S., Jin, j., Gizdavic-Nikolaidis, M., Nieuwoudt, M.K., Liu, D., and Quek S.Y. Encapsulation of food grade antioxidant in natural biopolymer by electrospinning technique: a physicochemical study based on zein-gallic acid system. Food Chemistry 136 (2013): 1013-1021.
- [64] Gong, S., Wang, H., Sun, Q., Xue, S.T., and Wang, J.Y. Mechanical properties and in vitro biocompatibility of porous zein scaffolds. Biomaterials 27 (2006): 3793-3799.
- [65] Yao, C., Li, X., and Song, T. Electrospinning and crosslinking of zein nanofiber mats. Journal of Applied Polymer Science 103 (2007): 380-385.
- [66] Xu, W., Karst, D., Yang, W., and Yang, Y. Novel zein-based electrospun fibers with the water stability and strength necessary for various applications. Polymer International 57 (2008): 1110-1117.
- [67] Suwantong, O., Pavasant, P., and Supaphol, P. Electrospun zein fibrous membranes using glyoxal as cross-linking agent: preparation, characterization and potential for use in biomedical applications. Chiang Mai Journal of Science 38 (2011): 56-70.
- [68] Sareen, D., Kaur, P., and Singh, K. Strategies in detection of metal ions using dyes. Coordination Chemistry Reviews 265 (2014): 125-154.
- [69] Gupta, V.K. and Suhas. Application of low-cost adsorbents for dye removal-a review. Journal of Environmental Management 90 (2009): 2313-2342.

- [70] Bernabé-Pineda, M., Ramírez-Silva, M.T., Romero-Romo, M., González-Vergara, E., and Rojas-Hernández, A. Determination of acidity constants of curcumin in aqueous solution and apparent rate constant of its decomposition. Spectrochimica Acta Part A: Molecular and Biomolecular Spectroscopy 60 (2004): 1091-1097.
- [71] Wang, Y.-J., Pan, M.-H., Cheng, A.-L., Lin, L.-I., Ho, Y.-S., and Lin, J.-K. Stability of curcumin in buffer solutions and characterization of its degradation products. Journal of Pharmaceutical and Biomedical Analysis 15 (1997): 1867-1876.
- [72] Brahatheeswaran, D., Mathew, A., Aswathy, R.G., Nagaoka, Y., Venugopal, K., Yoshida, Y., Maekawa, T., and Sakthikumar, D. Hybrid fluorescent curcumin loaded zein electrospun nanofibrous scaffold for biomedical applications. Biomedical Materials 7 (2012): 45001-45009.
- [73] Jovanovic, S.V., Steenken, S., Boone, C.W., and Simic, M.G. H-atom transfer is a preferred antioxidant mechanism of curcumin. Journal of the American Chemical Society 121 (1999): 9677-9681.
- [74] Kim, H.-J., Kim, D.-J., Karthick, S.N., Hemalatha, K.V., Raj, C.J., Ok, S., and Choe, Y. Curcumin dye extracted from *Curcuma longa* L. used as sensitizers for efficient dye-sensitized solar cells. International Journal of Electrochemical Science 8 (2013): 8320-8328.
- [75] Picciano, A.L., and Vaden, T.D. Complexation between Cu(II) and curcumin in the presence of two different segments of amyloid beta. Biophysical Chemistry 184 (2013): 62-67.
- [76] Borsari, M., Ferrari, E., Grandi, R., and Saladini, M. Curcuminoids as potential new iron-chelating agents: spectroscopic, polarographic and potentiometric study on their Fe(III) complexing ability. Inorganica Chimica Acta 328 (2002): 61-68.
- [77] Bernabé-Pineda, M., Ramírez-Silva, M.T., Romero-Romo, M.A., González-Vergara, E., and Rojas-Hernández, A. Spectrophotometric and electrochemical determination of the formation constants of the complexes curcumin-Fe(III)-

- water and curcumin–Fe(II)–water. Spectrochimica Acta Part A: Molecular and Biomolecular Spectroscopy 60 (2004): 1105-1113.
- [78] Huh, J.O., Do, Y., and Lee M.H. A BODIPY-borane dyad for the selective complexation of cyanide ion. Organometallics 27 (2008): 1022-1025.
- [79] Jamkratoke, M., Ruangpornvisuti, V., Tumcharern, G., Tuntulani, T., and Tomapatanaget, B. A-D-A sensors based on naphthoimidazoledione and boronic acid as turn-on cyanide probes in water. The Journal of Organic Chemistry 74 (2009): 3919-3922.
- [80] Xu, Z., Xiao, Y., Qian, X., Cui, J., and Cui, D. Ratiometric and selective fluorescent sensor for cull based on internal charge transfer (ICT). Organic Letters 7 (2005): 889-892.
- [81] Chung, S.K., Tseng, Y.R., Chen, C.Y., and Sun, S.S. A selective colorimetric Hg²⁺ probe featuring a styryl dithiaazacrown containing platinum (II) terpyridine complex through modulation of the relative strength of ICT and MLCT transitions. Inorganic Chemistry 50 (2011): 2711-2713.
- [82] Galievsky, V.A., Druzhinin, S.I., Demeter, A., Mayer, P., Kovalenko, S.A., Senyushkina, T.A., and Zachariasse, K.A. Ultrafast Intramolecular charge transfer with *N*-(4-cyanophenyl) carbazole. evidence for a LE precursor and dual LE + ICT fluorescence. The journal of Physical Chemistry A 114 (2010): 12622–12638.
- [83] Li, G., Zhang, L., Li, Z., and Zhang, W. PAR immobilized colorimetric fiber for heavy metal ion detection and adsorption. Journal of Hazardous Materials 177 (2010): 983-989.
- [84] Wang, X., Drew, C., Lee, S.-H., Senecal, K.J., Kumar, J., and Samuelson, L.A. Electrospun nanofibrous membranes for highly sensitive optical sensors. Nano Letters 11 (2002): 1273-1275.
- [85] Adewuyi, S., Ondigo, D.A., Zugle, R., Tshentu, Z., Nyokong, T., and Torto, N. A highly selective and sensitive pyridylazo-2-naphthol-poly(acrylic acid) functionalized electrospun nanofiber fluorescence “turn-off” chemosensory system for Ni²⁺. Analytical Methods 4 (2012): 1729-1735.

- [86] Li, Y., Si, Y., Wang, X., Ding, B., Sun, G., Zheng, G., Luo, W., and Yu, J. Colorimetric sensor strips for lead (II) assay utilizing nanogold probes immobilized polyamide-6/nitrocellulose nano-fibers/nets. Biosensors and Bioelectronics 48 (2013): 244-250.
- [87] Ondigo, D.A., Tshentu, Z.R., and Torto, N. Electrospun nanofiber based colorimetric probe for rapid detection of Fe²⁺ in water. Analytical Chimica Acta 804 (2013): 228-234.
- [88] Lv, Y.-Y., Wu, J., and Xu, Z.-K. Colorimetric and fluorescent sensor constructing from the nanofibrous membrane of porphyrinated polyimide for the detection of hydrogen chloride gas. Sensors and Actuators B: Chemical 148 (2010): 233-239.
- [89] Schueren, L.V., Mollet, T., Ceylan, O., and Clerck, K.D. The development of polyamide 6.6 nanofibres with a pH-sensitive function by electrospinning. European Polymer Journal 46 (2010): 2229-2239.
- [90] Chaicham, A. Sensor based on curcumin borondifluoride for naked-eye detection of cyanide. Master of Science Program in Chemistry, Chemistry Chulalongkorn, 2009.
- [91] Khumsri, A. Cyanide fluorescent sensors from diphenylacetylene derivatives. Master of Science Program in Chemistry, Chemistry Chulalongkorn, 2011.
- [92] Reddy, N., Li, Y., and Yang, Y. Wet cross-linking gliadin fibers with citric acid and a quantitative relationship between cross-linking conditions and mechanical properties. Journal of Agricultural and Food Chemistry 57 (2009): 90-98.
- [93] Weckhuysen, B.M. Ultraviolet-visible spectroscopy. United States of America: American Scientific Publishers, 2004.
- [94] Simonet, B.M. Quality control in qualitative analysis. TrAC Trends in Analytical Chemistry 24 (2005): 525-531.
- [95] Bualom, C., Ngeontae, W., Nitiyanontakit, S., Ngamukot, P., Imyim, A., Tuntulani, T., and Aeungmaitrepirom, W. Bulk optode sensors for batch and flow-through determinations of lead ion in water samples. Talanta 82 (2010): 660-667.

- [96] Zebib, B., Mouloungui, Z., and Noirot, V. Stabilization of curcumin by complexation with divalent cations in glycerol/water system. Bioinorganic Chemistry and Applications (2010): 292760-292768.
- [97] Kim, H.-L., Kim, D.-J., Karthick, S.N., Hemalatha, K.V., Raj, C.J., Ok, S., and Choe, Y. Curcumin dye extracted from *Curcuma longa* L. used as sensitizers for efficient dye-sensitized solar cells. International Journal of Electrochemical Science 8 (2013): 8320 - 8328.
- [98] Suwantong, O., Opanasopit, P., Ruktanonchai, U., and Supaphol, P. Electrospun cellulose acetate fiber mats containing curcumin and release characteristic of the herbal substance. Polymer 48 (2007): 7546-7557.
- [99] Gao, J., Y.L., and Yang, L. Thermal stability of boron-containing phenol formaldehyde resin. Polymer Degradation and Stability 63 (1999): 19-22.
- [100] Li, D., and Xia, Y. Electrospinning of nanofibers: reinventing the wheel? Advanced Materials 16 (2004): 1151-1168.
- [101] Ghosh, M., Singh, A.T., Xu, W., Sulchek, T., Gordon, L.I., and Ryan, R.O. Curcumin nanodisks: formulation and characterization. Nanomedicine 7 (2011): 162-167.
- [102] Dyrssen, D.W., Novikov, Y.P., and Uppstrom, L.R. Studies on the chemistry of the determination of boron with curcumin. Analytica Chimica Acta 60 (1972): 139-151.
- [103] Banerjee, R. Effect of curcumin on the metal ion induced fibrillization of amyloid-beta peptide. Spectrochimica Acta Part A: Molecular and Biomolecular Spectroscopy 117 (2014): 798-800.
- [104] Tennesen, H.H., and Greenhill, J.V. Studies on curcumin and curcuminoids. XXII: curcumin as a reducing agent and as a radical scavenger. International Journal of Pharmaceutics 87 (1992): 79-87.
- [105] Pollution Control Department, Water quality standards.
- [106] ISO 11885 Water quality. In *determination of selected elements by inductively coupled plasma optical emission spectrometry (ICP-OES)*. 2007: Switzerland.

- [107] Goebes, M.D., Strader, R., and Davidson, C. An ammonia emission inventory for fertilizer application in the united states. Atmospheric Environment 37 (2003): 2539-2550.
- [108] Xu, P., Zhang, Y., Gong, W., Hou, X., Kroeze, C., Gao, W., and Luan, S. An inventory of the emission of ammonia from agricultural fertilizer application in china for 2010 and its high-resolution spatial distribution. Atmospheric Environment 115 (2015): 141-148.
- [109] Huh, J.O., Do, Y., and Lee, M.H. A BODIPY-borane dyad for the selective complexation of cyanide ion. Organometallics 27 (2008): 1022-1025.
- [110] Ye, J.-H., Liu, J., Wang, Z., Bai, Y., Zhang, W., and He, W. A new Fe³⁺ fluorescent chemosensor based on aggregation-induced emission. Tetrahedron Letters 55 (2014): 3688-3692.
- [111] Buss, J.L., Arduini, E., Shephard, K.C., and Ponka, P. Lipophilicity of analogs of pyridoxal isonicotinoyl hydrazone (PIH) determines the efflux of iron complexes and toxicity in K562 cells. Biochemical Pharmacology 65 (2003): 349-360.
- [112] Aydin, Z., Wei, Y., and Guo, M. A highly selective rhodamine based turn-on optical sensor for Fe³⁺. Inorganic Chemistry Communications 20 (2012): 93-96.

VITA

Miss Amornrat Saithongdee was born on December 18, 1984 in Prachuapkhirikhan, Thailand. She received a Bachelor's degree of Science in Chemistry from Srinakharinwirot University in 2007 and a Master's degree of Science Program in Petrochemistry and Polymer Science. After that, she finished her Doctor of Philosophy (Petrochemistry) in Academic Year 2015. Her present address is 125/1183, Kao-Noi, Pranburi, Prachuapkhirikhan, Thailand, 77160. E-mail: fah_amorn@hotmail.com

Publication

1. A. Saithongdee, P. Varanusupakul, A. Imyim, Preparation of hydrogel film and characterization by infrared and nuclear magnetic resonance spectroscopy, *Journal of Scientific and Technological Research Equipment Centre*, 17 (2009): 54-63.
2. A. Saithongdee, P. Varanusupakul, A. Imyim, Preparation of thermally sensitive poly[N-isopropylacrylamide-co-(maleic acid)] hydrogel membrane by electrospinning using a green solvent, *Green Chemistry Letters and Reviews*, 7 (2014): 220-227.
3. A. Saithongdee, N. Praphairaksit, A. Imyim, Electrospun curcumin-loaded zein membrane for iron(III) ions sensing, *Sensors and Actuator B: Chemical*, 202 (2014): 935-940.